

Human-Robot Collaborative Disassembly in A Cyber-Physical Remanufacturing System

Youxi Hu
Doctor of Philosophy

Aston University
April 2024

©YOUXI HU, 2024

Youxi Hu asserts his moral right to be identified as the author of this thesis.

This copy of the thesis has been supplied on condition that anyone who consults it is understood to recognise that its copyright belongs to its author and that no quotation from the thesis and no information derived from it may be published without appropriate permission or acknowledgement.

Abstract

Remanufacturing is increasingly recognised as a pivotal technology for enhancing the lifespan and residual value of end-of-life (EoL) products. Contrasting with conventional manufacturing systems, which are highly integrated and automated, remanufacturing processes must navigate a multitude of uncertainties, including small-batch and customised production demands. Presently, the intelligence and autonomy levels within remanufacturing systems are rudimentary, offering limited support for autonomous decision-making and optimisation of production strategies. Thus, this dissertation aims to elevate the intelligence and dependability of the remanufacturing system, with a particular emphasis on the disassembly process as the primary area of study.

Initially, drawing inspiration from the broad application of Digital Twins (DT) and Cyber-Physical Systems (CPS) within the realm of intelligent manufacturing, this work proposes a systemic conceptual framework for a Cyber-Physical Remanufacturing System (CPRS). This framework seeks to enhance the automation, intelligence, and operational capabilities of remanufacturing systems. Subsequently, at the workshop level, to efficiently manage the

disassembly of vast quantities and diverse types of EoL products, disassembly lines are introduced to boost the cost-effectiveness and productivity of these operations. This thesis introduces a novel simulated annealing-based hyper-heuristic algorithm (HH) designed for the multi-objective optimisation of the stochastic parallel complete disassembly line balancing problem. Furthermore, human-robot collaborative disassembly (HRCd), an innovative semi-automatic disassembly approach, is explored to increase flexibility and efficiency by offering multiple disassembly methods. An individual-level general ontology model for modelling EoL products is proposed, along with a rule-based reasoning method to autonomously generate optimal disassembly sequences and schemes. In addition, an analysis of disassembly sequence reliability, leveraging a large-language model (LLM), is conducted to assess the efficacy of these disassembly sequences. The practical applicability of these case studies is demonstrated through experimental validation.

Key words: Remanufacturing, Cyber-Physical System, Human-Robot Collaborative Disassembly, Disassembly Line Balancing Problem, Large Language Model.

DEDICATION

Dedicated to my parents, Zubiao Hu and Shili Shen,
for their unwavering support and belief in my potential.

For my fiancée, Yachen Feng, my rock and harbour.

Your love, patience, and encouragement have been my sanctuary.

This journey would not have been possible without you by my side.

*Those who are outside want to get in,
and those who are inside want to get out.*

Zhongshu Qian, "Fortress Besieged"

Acknowledgements

First and foremost, I express my sincerest gratitude to my supervisor, Prof. Yuchun Xu, for giving me the great opportunity to undertake this PhD research, providing financial support, and offering unwavering guidance and expertise. His mentorship was invaluable in shaping the direction and completion of this research. I am deeply thankful for the patience, motivation, and immense knowledge he has provided throughout my academic journey.

I would also like to extend my thanks to my co-supervisor, Dr. Yu Jia, whose insights and suggestions have been invaluable throughout this research process. Moreover, I am deeply thankful for his financial support in covering international travel.

I would also like to give my greatest thanks to the other co-supervisor, Dr. Chao Liu, whose perspectives and rigorous feedback have significantly contributed to the quality of this thesis. His expertise and insights have been crucial in leading and enhancing the scope of this research. Moreover, I am also deeply thankful for his financial support through casual work.

To my friend and mentor, Dr. Ming Zhang, thank you for the constant

discussions, and for all the fun we have had in the last few years. Your camaraderie has made my PhD journey a memorable and enjoyable experience. To other teachers and colleagues, Dr. Xianghong Ma, Dr. Muftooh Siddiqi, Dr. Nasser Amaitik, Dr. Zezhong Wang, Dr. Jian Wan, Dr. Chonghui Wang, it is a great honour for me to work with you.

I must acknowledge the role of Aston University for providing the resources, facilities, and academic environment that served as the foundation for my research. Special thanks to the administrative and technical staff for their assistance and support.

I am deeply indebted to my family for their love, support, and sacrifice. To my parents, Zubiao Hu and Shili Shen, thank you for instilling in me the value of hard work and education; and to my love, Yachen Feng, for your understanding, patience, and unwavering support. Your encouragement when times got tough has been a driving force behind my perseverance.

This thesis stands as a milestone in my academic journey, made possible by the collective support and belief of everyone mentioned above, along with many others who, while unnamed, have contributed significantly to my personal and professional growth.

Thank you.

Youxi Hu

Youxi Hu

April 2024

Contents

1	Introduction	25
1.1	Research Background	25
1.1.1	Background of Smart Manufacturing	25
1.1.2	Introduction of Remanufacturing	32
1.1.3	Current Status of Remanufacturing	34
1.2	Research Challenges and Scopes	37
1.2.1	Research Challenges	37
1.2.2	Research Questions and Scope	40
1.3	Thesis Organisation	43
1.4	Chapter Summary	45
2	Literature Review	46
2.1	Cyber-Physical Production Systems	46
2.1.1	Cyber-Physical System (CPS)	46
2.1.2	Cloud-Based Manufacturing (CBM)	47
2.1.3	Cyber-Physical Production System (CPPS)	48

2.2	Disassembly Line Balancing Problem	49
2.2.1	Layout Type of Disassembly Line	49
2.2.2	Optimisation Algorithms for DLBP	51
2.2.3	The Categories of EoL Product in DLBP	53
2.3	Human-Robot Collaborative Disassembly	54
2.3.1	Background of HRCd	55
2.3.2	Ontology-Based Product Information Model	57
2.3.3	Rule-Based Reasoning for Disassembly Sequence Planning	60
2.4	Large-Language Model for Disassembly	62
2.4.1	Large-Language Model for Robot	62
2.4.2	Large-Language Model for Sequence Planning	67
2.5	Research Gaps and Challenges	69
2.5.1	CPRS	69
2.5.2	DLBP	71
2.5.3	HRCd	73
2.5.4	LLM in HRCd	74
2.6	Research Aim and Objectives	75
2.7	Chapter Summary	76

3 A Conceptual Framework of Cyber-Physical Remanufacturing System **78**

3.1	Introduction	78
-----	------------------------	----

3.2	The Concept and Process of CPRS	81
3.2.1	Definition of Smart Remanufacturing	81
3.2.2	The Process of CPRS	84
3.3	The Conceptual Framework of CPRS	89
3.3.1	Physical Layer	90
3.3.2	Edge Layer	95
3.3.3	Cloud Service Layer	99
3.4	Current Challenges and Future Perspectives of CPRS	100
3.4.1	EoL Product Modelling for CPRS	101
3.4.2	Process Planning and Scheduling in CPRS	101
3.4.3	Data Exchange and Communication	102
3.5	Chapter Summary	102
4	A Simulated Annealing-Based Hyper-Heuristic Algorithm for Stochastic Parallel Disassembly Line Balancing in CPRS	105
4.1	Introduction	105
4.2	Stochastic Parallel Disassembly Line Balancing Problem	109
4.2.1	Description of DLBP-SP	109
4.2.2	Notations and Assumptions of DLBP-SP	110
4.2.3	Mathematical Model of DLBP-SP	113
4.3	The Proposed Hyper-Heuristic Algorithm for DLBP-SP	120
4.3.1	Encoding Strategy	121

4.3.2	Procedure of Proposed Hyper-Heuristic Algorithm . . .	125
4.3.3	Simulated Annealing Based High-Level Heuristic Algorithm	129
4.3.4	Decoding Process	129
4.4	Computational Experiments	131
4.4.1	Comparison Experiment	131
4.4.2	Case Study	134
4.5	Chapter Summary	147

5 An ontology and rule-based method for human-robot collaborative disassembly planning in CPRS150

5.1	Introduction	150
5.2	HRCO Ontology and Product Semantic Model	154
5.2.1	The Proposed HRCO Ontology	155
5.2.2	Object and Data Properties of HRCO Ontology	159
5.2.3	An Illustrative Example	164
5.3	Rule-Based Reasoning for HRCO Sequence Planning	167
5.3.1	Rules for Reasoning Disassembly Precedence Constraints	168
5.3.2	Rules for Determining Disassembly Method	172
5.3.3	Auxiliary Rules	175
5.3.4	Process for Generating The Optional Disassembly Scheme	177
5.4	Case Study	182
5.4.1	HRCO Ontology Model of Gearbox	183

5.4.2	Precedence Constraints of The Gearbox	183
5.4.3	Optimal HRC D Scheme of The Gearbox	186
5.5	Chapter Summary	192
6	Large-language model for Human-Robot Collaborative Disassembly Sequence Planning and Analysis in CPRS	195
6.1	Introduction	195
6.2	Methodology	199
6.2.1	Problem Statement	199
6.2.2	Generated Disassembly Graph	201
6.2.3	Disassembly Graph-Based Bayesian Network	204
6.2.4	LLM-based sequence planning	205
6.2.5	GAN Based HRC D Sequence Planning	206
6.3	Case Study	209
6.3.1	Case Study I: belt roller	209
6.3.2	Case Study II: gearbox	213
6.4	Chapter Summary	219
7	Conclusions and Future Work	221
7.1	Recap of The Research	221
7.2	Research Contributions	223
7.3	Limitations and Future Research Directions	226
7.3.1	Disassembly Line Balancing Problem	226

7.3.2	Human-Robot Collaborative Disassembly	227
7.3.3	Large-Language Model for HRCd	228
7.4	Chapter Summary	230
8	Appendix	232
8.1	Appendix 8.1	233
8.2	Appendix 8.2	235
8.3	Link for The Illustrative Example and The Case Study	236

Acronyms

- **CPRS**: Cyber-Physical Remanufacturing System
- **HRC**: Human-Robot Collaborative Disassembly
- **CPPS**: Cyber-Physical Production System
- **LLM**: Large-Language Model
- **CPS**: Cyber-Physical System
- **CBM**: Cloud-Based Manufacturing
- **DLBP**: Disassembly Line Balancing Problem
- **EoL**: End-of-Life
- **DLBP-SP**: Stochastic Parallel Disassembly Line Balancing Problem
- **IIoT**: Industrial Internet of Things
- **SWRL**: Semantic Web Rule Language
- **BoM**: Bill of Material

- **cBDB**: canBeDisassembledBy
- **cBDI**: canBeDisassembledIn
- **cBDS**: canBeDisassembledSimultaneously
- **dC**: directCover
- **dF**: differentForm
- **dD**: disassemblyDirection
- **hC**: hasCost
- **hDA**: hasDisassemblyAction
- **hDD**: hasDisassemblyDirection
- **hDM**: hasDisassemblyMethod
- **hPO**: hasPartOf
- **hPT**: hasProcessTime
- **hTBDA**: hasToBeDisassembledAfter
- **hTBDDA**: hasToBeDirectDisassembledAfter
- **iDCB**: isDirectCoveredBy
- **iFB**: isFixedBy
- **iPO**: isPartOf

List of Figures

1.1	Fourth industrial revolution and Industry 5.0.	30
1.2	Energy consumption from renewable and waste sources in the manufacturing sector in the United Kingdom (UK) from 1990 to 2018. (Open source link in 8.3)	31
1.3	Circular economy of biological and technical. (Open source link in 8.3)	33
1.4	Remanufacturing processes.	35
1.5	The organisation and contents of this thesis.	44
2.1	Layout type of disassembly lines.	50
2.2	Goal with ChatGPT [115].	64
2.3	Conceptual framework of LLM-embedded HRCd.	65
2.4	The scheme of the learning from demonstration model [121].	67
3.1	The process of CPRS.	85
3.2	The structure of proposed CPRS.	91
3.3	Physical layer of CPRS.	92

3.4	Edge layer of CPRS.	96
4.1	Parallel disassembly lines.	110
4.2	The precedence graph and matrix of product.	123
4.3	Operation process of the partial mapped crossover.	128
4.4	Operation process of single-point insertion mutation.	128
4.5	Explosion diagram of splitter gearboxes.	138
4.6	Precedence relationship of splitter gearboxes.	138
4.7	The Gantt chart of optimal solution ($CT_1 = 50, CT_2 = 60$). . .	143
4.8	Box plots of hypervolume.	145
5.1	Overall workflow of this chapter.	154
5.2	The class hierarchy of the proposed HRCD ontology.	156
5.3	The class relationships of the proposed HRCD ontology.	160
5.4	An illustrative example.	166
5.5	Disassembly procedures and precedence constraints of the belt roller.	170
5.6	Workflow for generating precedence constraints of EoL product.	178
5.7	Workflow for generating optimal disassembly schemes.	181
5.8	Exploded view of the gearbox.	182
5.9	Screenshot of the human-robot disassembly ontology of gear- box in Protégé.	184
5.10	Precedence constraints of the gearbox.	187
6.1	Workflow of the Proposed LLM-based DiBN Model.	201

6.2 Disassembly graph of the satellite. 203

6.3 The querying process of the LLM. 207

6.4 Structure and precedence constraints of the belt roller. 210

6.5 Reward comparison between DiBN with and without LLM in
belt roller HRCDSP. 211

6.6 Training Loss comparison in belt roller HRCDSP. 211

6.7 Conditional probability of disassembly events in belt roller. . . 212

6.8 Cutting-edges methods comparison for belt roller HRCDSP. . 214

6.9 Precedence constraints graph of the gearbox. 215

6.10 Reward comparison between DiBN with and without LLM in
gearbox HRCDSP. 216

6.11 Conditional probability of disassembly events in gearbox. . . . 217

6.12 Condition probability with increase evidence in gearbox. . . . 217

6.13 Training Loss comparison in gearbox HRCDSP. 218

6.14 Cutting-edges methods comparison for gearbox HRCDSP. . . . 219

List of Tables

1.1	The comparison of manufacturing strategies.	27
1.2	The process of industrial revolution.	29
2.1	Definitions of cyber-physical systems.	47
2.2	Definitions of cloud-based manufacturing.	48
2.3	Definitions of cyber-physical production system.	49
2.4	Research topics in HRCD.	75
4.1	Definition and description of notations.	111
4.2	The information of product A on disassembly line 1.	119
4.3	The information of product B on disassembly line 2.	119
4.4	The modified information of product A and B on parallel disassembly lines.	119
4.5	A feasible disassembly sequence of the DLBP-SP.	120
4.6	Computational results (Part 1).	134
4.7	Computational results (Part 2).	135
4.8	Analysis of the computational results.	136
4.9	The combination of experiment parameters.	139

4.10	Multi-objective optimisation results and the number of non-dominated solutions.	140
4.11	One optimal sequence of the disassembly process ($CT_1 = 50, CT_2 = 60$).	141
4.12	One optimal sequence of the disassembly process ($CT_1 = CT_2 = 60$).	142
4.13	One optimal sequence of the disassembly process ($CT_1 = 90, CT_2 = 108$).	144
5.1	Object properties in the HRCd ontology.	163
5.2	Data properties in the HRCd ontology.	165
5.3	Rules for generating the precedence constrains of components.	169
5.4	Rules for determining disassembly method.	174
5.5	Auxiliary rules	175
5.6	Semantic assembly-relations of fasteners in the gearbox.	185
5.7	Semantic assembly-relations of accessory parts in the gearbox.	185
5.8	Semantic assembly-relations of functional parts in the gearbox.	186
5.9	Output of optional disassembly methods of components in the gearbox.	186
5.10	Optional HRCd sequence schemes.	187
5.11	Parameter settings for comparison experiments.	190
5.12	Comparison experiment results.	190
5.13	Comparison between our method and optimisation algorithms.	192

6.1	Component list of the belt roller.	209
8.1	Bill of materials of splitter gearboxes series 85000.	233
8.2	Bill of materials of splitter gearboxes series 90000.	234
8.3	Disassembly-related information of the gearbox.	235

Publications

Peer reviewed journal papers:

1. **Y. Hu**, C. Liu, M. Zhang, Y. Lu, Y. Jia, and Y. Xu, “An ontology and rule-based method for human–robot collaborative disassembly planning in smart remanufacturing,” *Robotics and Computer-Integrated Manufacturing*, vol. 89, p. 102766, 2024.
2. **Y. Hu**, C. Liu, M. Zhang, Y. Jia, and Y. Xu, “A Novel Simulated Annealing-Based Hyper-Heuristic Algorithm for Stochastic Parallel Disassembly Line Balancing in Smart Remanufacturing,” *Sensors-Basel*, vol. 23, no. 3, p. 1652, 2023.
3. M. Zhang, Y. Lu, **Y. Hu**, N. Amaitik, and Y. Xu, “Dynamic Scheduling Method for Job-Shop Manufacturing Systems by Deep Reinforcement Learning with Proximal Policy Optimization,” *Sustainability-Basel*, vol. 14, no. 9, p. 5177, 2022.

Work-in-Progress papers

1. **Y. Hu**, C. Liu, L. Xia, M. Zhang, Y. Jia and Y. Xu, “Large Language Models Embedded Human-Robot Collaborative Disassembly in Smart Remanufacturing,” *International Journal of Production Research*, 2024.
2. L. Xia, **Y. Hu**, C. Liu, and P. Zheng, “Leveraging Large Language Models to Empower Bayesian Networks for Reliable Human-Robot Collaborative Disassembly Sequence Planning in Remanufacturing,” *IEEE transactions on industrial informatics*, 2024.

Peer reviewed international conference papers:

1. **Y. Hu**, C. Liu, M. Zhang, Y. Laili, Y. Jia, and Y. Xu, “Ontology-Based Product Modeling for Disassembly Sequence Planning in Remanufacturing,” in 2023 28th International Conference on Automation and Computing (ICAC), 2023: IEEE, pp. 1-6.
2. **Y. Hu**, C. Liu, M. Zhang, Y. Lu, Y. Jia, and Y. Xu, “An Ontology-Based Product Modelling Method for Smart Remanufacturing,” in 2023 IEEE 19th International Conference on Automation Science and Engineering (CASE), 2023: IEEE, pp. 1-6.
3. **Y. Hu**, C. Liu, M. Zhang, Y. Jia, and Y. Xu, “A Conceptual Framework of Cyber-Physical Remanufacturing System,” in 2022 8th International Conference on Nanomanufacturing & 4th AET Symposium on

ACSM and Digital Manufacturing, 2022: IEEE, pp. 1-6.

4. **Y. Hu**, M. Zhang, C. Liu, Y. Xu, Z. Wang, and Y. Jia, “A simulated annealing hyper-heuristic algorithm for process planning and scheduling in remanufacturing,” in 2022 27th International Conference on Automation and Computing (ICAC), 2022: IEEE, pp. 1-6.
5. **Y. Hu**, Y. Xu, and Y. Jia, “Review of The Optimization Algorithms for Remanufacturing Disassembly Line,” in 2021 26th International Conference on Automation and Computing (ICAC), 2021: IEEE, pp. 1-6.

1

Introduction

1.1 Research Background

1.1.1 Background of Smart Manufacturing

Manufacturing involves the generation or fabrication of products through the utilisation of equipment, workforce, machinery, tools, and either chemical or biological techniques and processes [1]. The objective of manufacturing is to design and produce products that align with customer demands and ex-

pectations. Fundamental manufacturing procedures, including machining, forming, welding, casting, and assembling, are executed within factories or workshops. Over time, manufacturing techniques have progressed, aiming for efficiency, cost-effectiveness, and superior quality [2]. The manufacturing sector is in a perpetual state of evolution, marked by the emergence and adoption of novel technologies, methodologies, and materials, all geared towards enhancing efficiency, productivity, and quality standards. Serving as the cornerstone of the economy's secondary sector, the manufacturing industry plays a pivotal role in the global economic landscape, fostering employment opportunities and contributing substantial revenue streams for both businesses and governments [3].

Smart manufacturing has emerged as a pivotal element in the progression of societal development and economic infrastructure, marked by significant advancements in essential equipment, technology, manufacturing services, system control, micro-nano manufacturing, and intelligent robotics, among others [4]. Over the past decade, leading nations globally have rolled out an array of strategies related to smart manufacturing. Notable initiatives include the “Strategy for American Innovation [5]”, “Industry 4.0 [6]”, “High-Value Manufacturing [7]”, “New Robot Strategy [8]” and “Made-in-China 2025 [9]”. These strategic approaches, detailed in Table 1.1.

- “Strategy for American Innovation” emphasises the development of distributed and interconnected smart equipment to facilitate real-time control and volume-flexible production. It leverages advanced sensors

Table 1.1: The comparison of manufacturing strategies.

Strategies	Year	Country	Definition	Objectives
Strategy for American innovation	2012	American	Integration of smart devices and software and big data analysis	Establish smart manufacturing system
Industry 4.0	2013	Germany	Establish CPS	Establish a smart factory to realise smart production
New Robot Strategy	2014	Japan	Focus on industrial robots, 3D printing and new energy vehicles	Reshaping manufacturing method
High-Value Manufacturing	2015	UK	Integrate solve energy, digital revolution and economic life	Reinventing industry strength
Made-in-China 2025	2015	China	Integrate the information technology and manufacturing equipment	China's strength in manufacturing

and data management technologies throughout the product life cycle to achieve rapid innovation cycles, interoperability, and enhanced productivity within a fully digital manufacturing enterprise.

- “Industry 4.0” focuses on employing Internet of Things (IoT) technology for the real-time perception and monitoring of vast amounts of data generated during the production process. This strategy aims to realise intelligent analysis and decision-making within the production system by establishing a cyber-physical system that supports smart production, network collaborative manufacturing, and large-scale personalised manufacturing.
- “New Robot Strategy” is dedicated to the advancement of industrial collaborative robots and automated factories. It addresses productivity shortfalls through the use of innovation networks, software systems,

industrial robots, material networks, and other technologies, fostering a more efficient production landscape.

- “High-Value Manufacturing” seeks to respond more swiftly to market demands, advocates for sustainable development, fosters high-quality labour, and aims to realise the remanufacturing process within a production centric value chain. This approach is geared towards enhancing the industry’s ability to innovate and adapt to changing market needs.
- “Made-in-China 2025” is predicated on the integration of new generation information technologies such as IoT, big data, and edge computing across all facets of manufacturing activities. It encompasses product design, process management, and after-sales service, implementing advanced functions like in-depth self-perception of information, smart optimisation, automatic control, and dynamic self-executing manufacturing processes.

Strategies are various in their emphasis and objectives, reflecting the diverse priorities and policy orientations across different countries. However, ‘Industry 4.0’ is one of the highest recognition, acceptable and widest separated strategy around the world. The development and main characteristics of industrial revolution as shown in Table 1.2 and Figure 1.1. Since the dawn of the first industrial revolution, humanity has experienced three subsequent revolutions, leading us to the current era of Industry 4.0. The second revolution introduced the modern production line by Ford, significantly enhancing

the speed of manufacturing and realise the mass production. The third revolution was marked by the advent of industrial robots and advancements in computing and sensing technologies. Industry 4.0 has further developed advanced networking and big data analysis capabilities, incorporating artificial intelligence techniques such as cyber-physical systems and the Internet of Things (IoT). Looking ahead to Industry 5.0, a more human-centric approach is anticipated, emphasising technologies that enhance human-centric manufacturing and foster a synergistic human-machine interface, thereby amplifying human creativity [10]. As manufacturing technology has advanced, it has also led to improved working conditions, such as shorter working hours and reducing repetitive work. The focus on enhancing the working conditions of human labourers remains paramount as the industry transitions into the Industry 5.0 era.

Table 1.2: The process of industrial revolution.

Era	Time	Important event	Characteristic
Steam engine	1840-1870	<ul style="list-style-type: none"> ●Spinning machine (1765) ●Steam engine (1785) ●UK completed the first industrial revolution (1840) 	<ul style="list-style-type: none"> ●Development of industrial cities ●Development of the steel and textile industries ●Machines replace manual labour
Electrical	1871-1914	<ul style="list-style-type: none"> ●Power generator (1866) ●Assembly line (1913) ●Programmable logic controller (1969) 	<ul style="list-style-type: none"> ●New industrial expansion ●Massive production ●Analog electronic equipment
Information	1915-1999	<ul style="list-style-type: none"> ●Internet (1969) ●Big Data (2008) 	<ul style="list-style-type: none"> ●Personal computer ●Smart cell phone
Digital	2000-	<ul style="list-style-type: none"> ●Industry 4.0 (2014) ●Made in China 2025 (2015) 	<ul style="list-style-type: none"> ●Technology in Emerging Fields (IoT, Robotic, Biotechnology) ●Customized production

Moreover, in the landscape of modern smart manufacturing, the strategies of manufacturing are more focused on the sustainability, improving resource

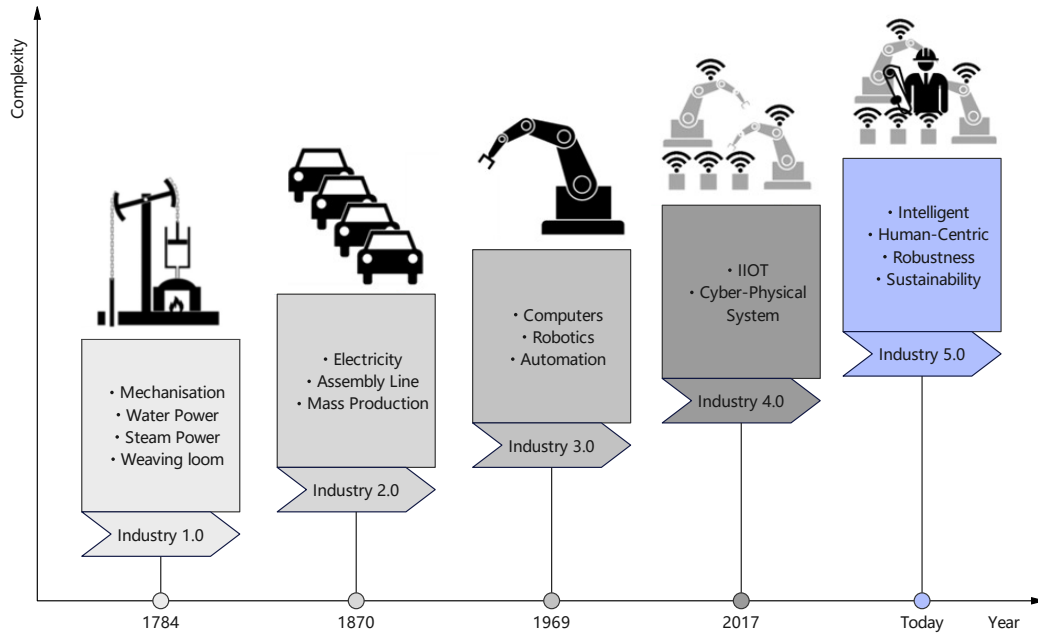


Figure 1.1: Fourth industrial revolution and Industry 5.0.

efficiency, reducing energy consumption and extending product life-cycles due to the recognition of the environmental, economic, and societal benefits. Figure 1.2 shows the energy consumption from renewable and waste sources in the manufacturing sector of the United Kingdom between 1990 and 2018. The bar chart intuitively demonstrates a progressive ascent in energy consumption within the manufacturing sector of the United Kingdom. Commencing at a consumption level of 537 tons in 1990, a marked escalation is observable, particularly from the year 2010 onwards. The apex of this upward trajectory was attained in 2018, with the sector consuming approximately 3,640 tons. To elucidate, the year 2018 witnessed the manufacturing sector’s consumption of renewable and waste energy sources reaching ap-

proximately 3.6 million metric tons of oil equivalent, the zenith within the evaluated time-frame. This represents an approximately seven-fold augmentation from the initial figures recorded in 1990.

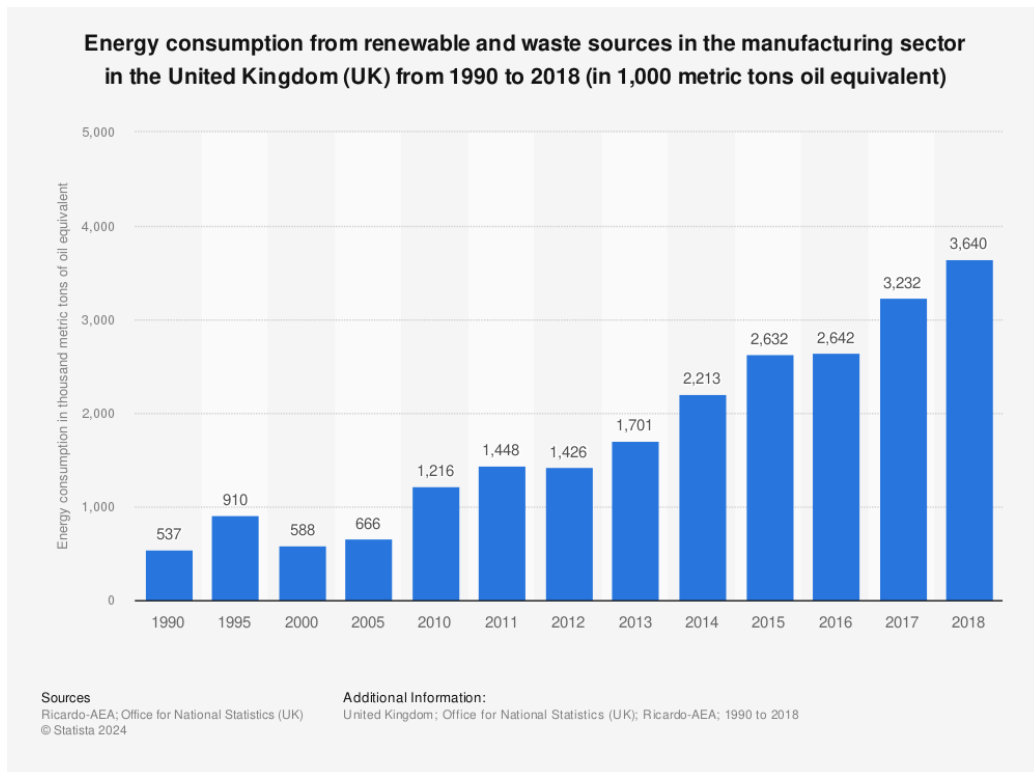


Figure 1.2: Energy consumption from renewable and waste sources in the manufacturing sector in the United Kingdom (UK) from 1990 to 2018. (Open source link in 8.3)

Introducing more effective methods to reduce energy, resource consumption, and extend the life-cycle of products is crucial for enhancing sustainability in manufacturing. Such approaches, as highlighted in recent analyses, encompass a broad spectrum of strategies including optimising product design for material efficiency, leveraging low-carbon materials, and ensuring

products are recyclable or reusable at their end of life. The integration of lean manufacturing principles with sustainability-specific concepts, such as energy recovery and waste-material reuse, signifies a critical shift towards resource productivity optimisation (RPO). This shift not only aids in the significant reduction of environmental impact but also aligns with economic benefits by improving process efficiency and reducing waste. These strategies underscore the importance of a comprehensive approach to manufacturing that marries profitability with environmental stewardship, thereby meeting the growing regulatory and consumer demand for more sustainable products while ensuring competitive advantage in the market.

1.1.2 Introduction of Remanufacturing

As a novel and advance technology, remanufacturing not only contributes to the sustainability of manufacturing practices but also propels the economy towards a more sustainable and resilient future. Remanufacturing is a comprehensive and rigorous industrial process by which an EoL product is restored to an original-produced or better-than-new condition and is warranted in terms of performance level and quality [11].

As shown in Figure 1.3, remanufacturing supports the circular economy by extending the lifespan of products and significantly reducing waste and the need for raw materials. Unlike recycling, which destroys the original shape of the product to recover materials, remanufacturing preserves the product's form and retains much of the value added during its initial manufacture.

This process is also distinct from other product recovery processes due to its potential to conserve more energy and resources, which contributes to the reduction of environmental impacts. According to prior literature, remanufacturing saves 80% resources, 80% costs and reduces 85% the air emission comparing to producing new products.

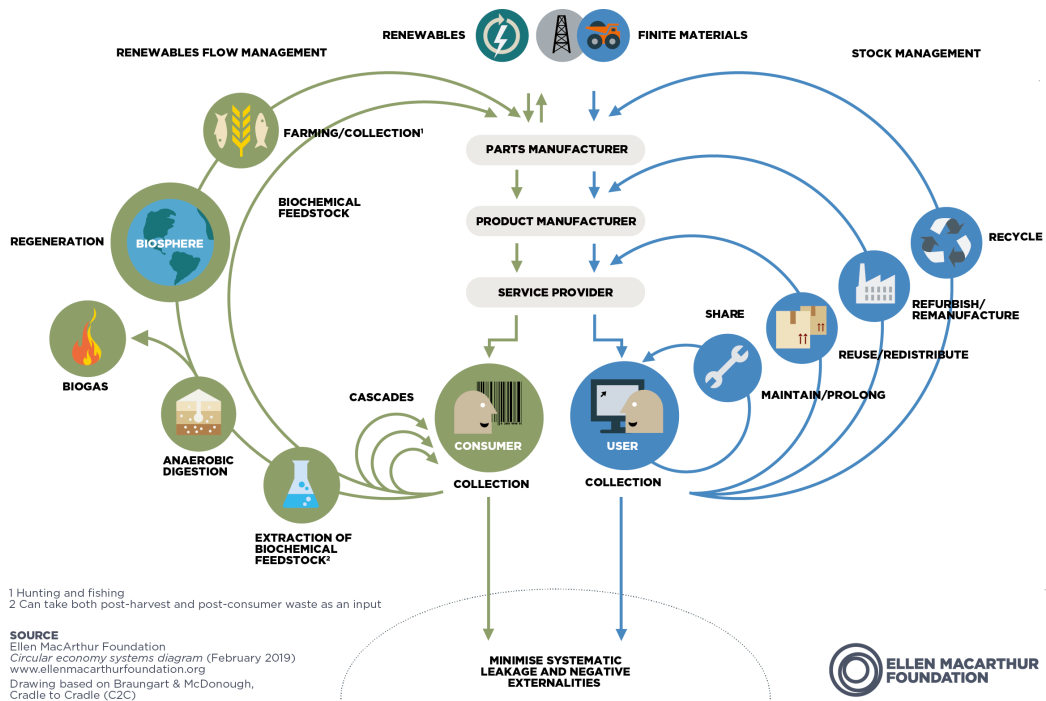


Figure 1.3: Circular economy of biological and technical. (Open source link in 8.3)

From the economic aspect, it was reported that the remanufactured automotive products can be sold at a price of 40% lower than the new products and the profit is 20%. Remanufacturing, as an industry, also helps to create jobs such as disassembly, testing operators. Remanufacturing, as a newly

emerging technique, it also helps the sustainability development in the developing countries due to the modern techniques used in remanufacturing, such as, IoT, has minimised the technique gap between developing countries and developed countries. Since developing countries consume over two-thirds of industrial goods, the contribution of remanufacturing is unbelievably valuable. The evidence above shows that remanufacturing can be beneficial for all three pillars of sustainability: environmentally friendly, economic, and societal beneficial. Therefore, it is a sustainable choice for the EoL products for the manufacturers, which can lead to a positive impact to the society and environment.

1.1.3 Current Status of Remanufacturing

There has been significant progress in the field of remanufacturing over the past decade, positioning it as a critical element of the circular economy. A typical remanufacturing process is presented in Figure 1.4. Remanufacturing offers a pathway to sustainable manufacturing by refurbishing used products to a condition akin to new, resulting in substantial economic and environmental benefits. However, despite its advantages, remanufacturing encounters distinct challenges that may impede its adoption and efficacy. From a macro-level perspective, logistical, and marketing issues emerge as primary obstacles affecting the recognition and fulfilment of remanufacturing practices.

- Collection and logistics: effective remanufacturing requires a reliable

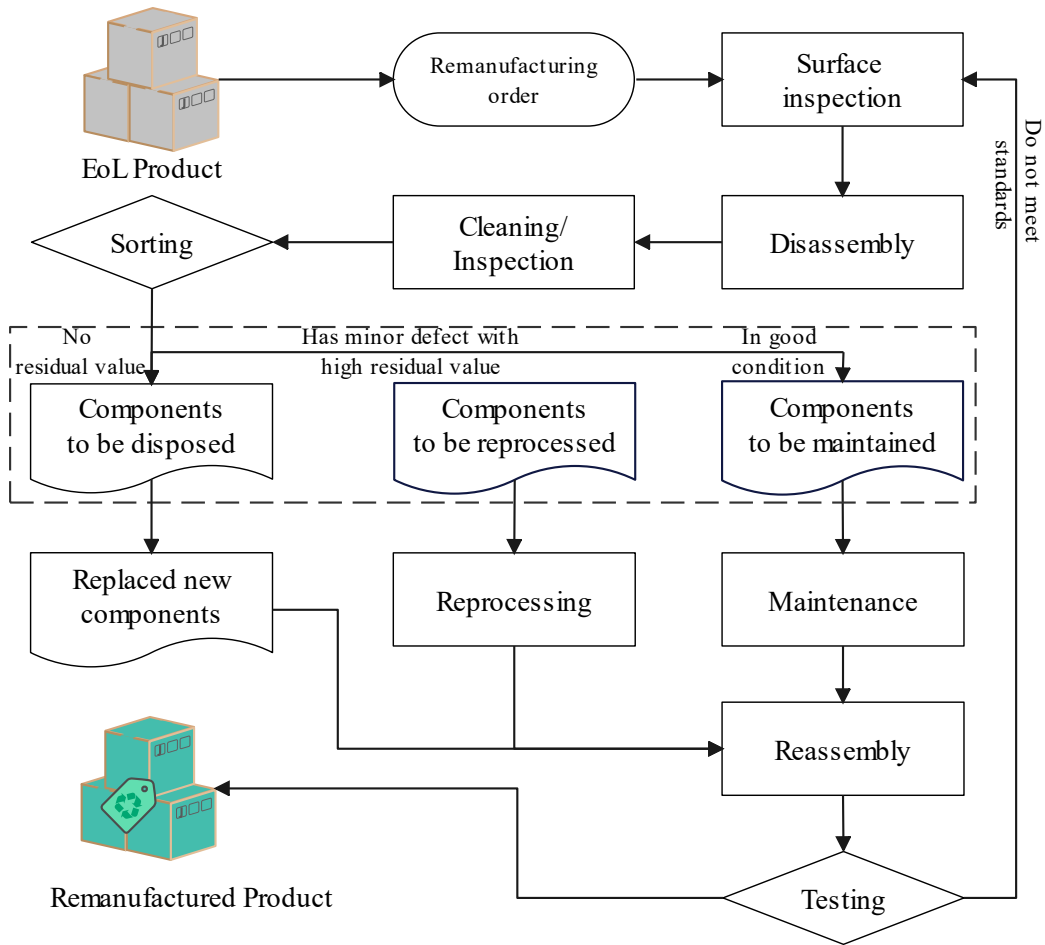


Figure 1.4: Remanufacturing processes.

supply of used products. However, collecting these products can be logistically challenging and costly, affecting the overall efficiency of the remanufacturing process [12].

- Quality assurance and market acceptance: ensuring and conveying the quality of remanufactured products is crucial for consumer acceptance. Misconceptions about remanufactured products being inferior to new

ones pose a significant challenge [13].

- Regulatory and policy frameworks: the lack of standardised regulations and policies for remanufactured products can create market uncertainties, hindering the growth of remanufacturing industries [14].

At the technical level, numerous fundamental research challenges persist regarding remanufacturing from both a systemic and procedural standpoint.

- From the point of view of products, there has no set list of products which can be remanufactured, and the condition of retrieved products are various. As the specialised technology and craftsmanship with high and advanced technology, the operating cost of remanufacturing process needs to consider the economics and feasibility of remanufactured products [15]. Apart from the investment cost of remanufacturing technology, the condition monitoring and component relationship modelling for the remanufacturing products are also well worth for further research.
- From the remanufacturing process view, the physical model of remanufactured products is highly uncertain, and the complexity of the remanufacturing process is also hard to define. Different from the highly integrated and automated smart manufacturing process, the condition and processing time of remanufacturing products are various, lacking the cooperation mechanism and track management to implement collaborative remanufacturing process [16]. The smart, flexible and autonomous

remanufacturing process has not yet been realised in large-scale industrial remanufacturing operations and it is insensitive to the dynamic response to the disturbance of the remanufacturing process [17].

1.2 Research Challenges and Scopes

1.2.1 Research Challenges

Drawing upon the current foundational research goals and objectives in remanufacturing, this study seeks to develop a Cyber-Physical Remanufacturing System (CPRS) aimed at facilitating adaptive, cooperative, and autonomous process planning and scheduling. This initiative takes into account the uncertain and variable conditions prevalent within remanufacturing systems. To manage the research plan effectively, several research challenges must be addressed:

Firstly, a comprehensive literature review has established that there is no CPS designed specifically for the complete remanufacturing process. Unlike CPPS, the remanufacturing process involves factors such as the diversity and uncertainty of EoL products, which complicate the cost-profit analysis [18]. The remanufacturing process typically undergoes a series of steps and involves various mechanical equipment, making the communication and data exchange between different pieces of equipment challenging. At the same time, there is a notable deficiency in system-level equipment integration, and the intelligence and autonomy of existing remanufacturing systems are rel-

atively low [19]. From the perspective of smart manufacturing, theoretical models have not effectively integrated advanced technologies associated with the ‘Industry 4.0’ era in actual production scenarios, leading to issues such as rigidity in theoretical models, insufficient modelling accuracy, and significant delays, thus failing to achieve smart and effective production and operations [20]. Additionally, current remanufacturing systems cannot meet the production demands of small batches and customisation, nor can they adapt to the dynamic factors encountered in actual production environments. Therefore, proposing a CPS for remanufacturing that embodies a higher degree of intelligence and autonomy presents a challenging yet worthwhile endeavour [21].

Secondly, the disassembly process in remanufacturing is inherently divergent, potentially following multiple disassembly routes. Furthermore, as previously noted, the distinctive features of small-batch and customised production emphasise the critical role of planning and scheduling in determining the efficiency of remanufacturing systems [22]. The production process is fraught with inherent uncertainty [23]. Traditional stochastic programming methods, such as the scene tree method, struggle to exhaustively describe these continuous uncertain parameters due to their large-scale intractability, issues with scenario decomposition, and the complexities of chance-constrained programming, which relies heavily on joint probability information [24]. Thus, the challenge lies in comprehensively considering uncertain parameters and model complexity to develop advanced algorithms that can integrate process

planning and scheduling optimisation while analysing system robustness and the optimisation modelling process.

Thirdly, the disassembly of EoL products involves a divergent process with potential for multiple routes. Given the uncertain characteristics and conditions of EoL products, it is impractical to apply a uniform standard process to the remanufacturing of various EoL items [25]. Furthermore, the vast and often unbounded information related to EoL products typically includes a significant amount of redundant data, which is not very useful or relevant for remanufacturing purposes. Therefore, defining an effective information scope and modelling the EoL products represent significant challenges in the field [26].

The technology related to human-robot collaborative disassembly processes is still in its infancy. Initially, planning the disassembly sequence and optimising task allocation to adapt to the capabilities and efficiencies of human and robotic participants presents a significant challenge. The proposed optimisation algorithms must consider various factors, including the time required to complete tasks, task complexity, and the respective capabilities of human workers and robots [27]. Additionally, it is also important to improve the precision and flexibility of collaborative robots for achieving a more efficient cooperation model. Currently, artificial intelligence technologies such as large language models and machine learning are rapidly advancing. By effectively integrating these AI technologies, not only can the intelligence level of collaborative robots be enhanced, but the efficiency of the overall

human-robot collaborative disassembly process can also be improved [28].

Furthermore, the effectiveness of human-robot collaboration hinges on the ability to facilitate seamless communication between human operators and robotic systems. Overcoming this challenge involves the development of interfaces that enable humans to effortlessly communicate instructions to robots and comprehend their actions. The creation of intuitive communication methods, which may encompass voice commands, gestures, or even direct physical interaction with robots, is essential for fostering efficient and cohesive teamwork.

1.2.2 Research Questions and Scope

The research scope of this study is designed to address the multifaceted challenges associated with the development and implementation of advanced Cyber-Physical Remanufacturing Systems (CPRS). By focusing on these key areas, the research aims to enhance the efficiency, intelligence, and adaptability of remanufacturing systems in the face of uncertain and variable conditions. The research questions, scope and objectives are mainly summarised as follow:

- What is the significance of CPRS? Why is it well worth to research on and how to validate it?

The conceptual framework for the CPRS is proposed in this thesis to explore the integration of advanced optimisation algorithms, robotics, and information technology to create a seamlessly connected and au-

tomated environment for remanufacturing operations. This research objective is an initial attempt to establish a complete CPRS to cover overall remanufacturing steps and will focus on the interaction between human operators and robots, leveraging real-time data analytics for decision support and dynamic task allocation. The proposed conceptual framework is validated through the case studies focus on disassembly process.

- What kind of method has been proposed and applied for solving DLBP? What kind of advantages does this method have?

To solve this research question, this thesis primarily proposes an innovative optimisation algorithm called hyper-heuristic algorithm that enhances rapid decision-making and efficiency in solving the disassembly line balancing problem under uncertainty. The proposed algorithm can dynamically allocate tasks, manage resources efficiently, and has the ability to handle multiple uncertainties, thereby reducing bottlenecks quickly and stably.

- How to model the EoL product in a standard and effective manner?

This thesis proposes an ontology model for modelling EoL products to improve the efficiency and effectiveness of information management. The proposed ontology model is standard and universal, making it easy to store and reuse, specifically for those complex EoL products with various and complex components.

- How to allocate disassembly tasks between human and robot? How to determine the optimal HRCD sequence effectively?

The disassembly ontology model will provide a structured database to represent knowledge about the components, tools, tasks, and human-robot interactions necessary for effective disassembly. The rule-based method will leverage this ontology to devise efficient sequencing strategies that optimise task allocation and workflow, thereby enhancing productivity and safety. The combination of proposed methods can effectively plan and determine the optimal disassembly scheme of HRCD.

- How to quantitatively evaluate the optional disassembly sequence of HRCD?

This thesis proposes the integration of large-language models into HRCD to enhance communication and decision-making processes between humans and robots. The use of a large-language model aims to quantitatively evaluate optional disassembly sequences, facilitating more reliable and efficient human-robot interactions during disassembly tasks.

There are some elements out of scope of this project:

- Other processes in remanufacturing: The proposed CPRS is a conceptual framework which covers all processes in remanufacturing. However, the research scope of implementation all processes is too large.

Therefore, this research only considers disassembly as case study to validate the proposed framework of CPRS.

- Trust and explainability: In this study, new methods and experimental techniques for evaluating the reverse logistic and close loop supply chain logistics explanations are not considered.

1.3 Thesis Organisation

The organisation and depicting flowchart of this thesis is presented in Figure 1.5. In detail:

- Chapter 1 introduces the background of this thesis by detailing the research background, challenges, questions and scope.
- Chapter 2 provides a literature review on cyber-physical production systems (CPPS), disassembly line balancing problem, human-robot collaborative disassembly and large-language model in human-robot collaborative disassembly.
- Chapter 3 conceptualises a framework for cyber-physical remanufacturing systems (CPRS), delineating the process, definition, connections, current challenges, and future perspectives.
- Chapter 4 proposes a novel simulated annealing-based hyper-heuristic algorithm for parallel disassembly line balancing problem (DLBP-SP), including computational experiments and conclusions.

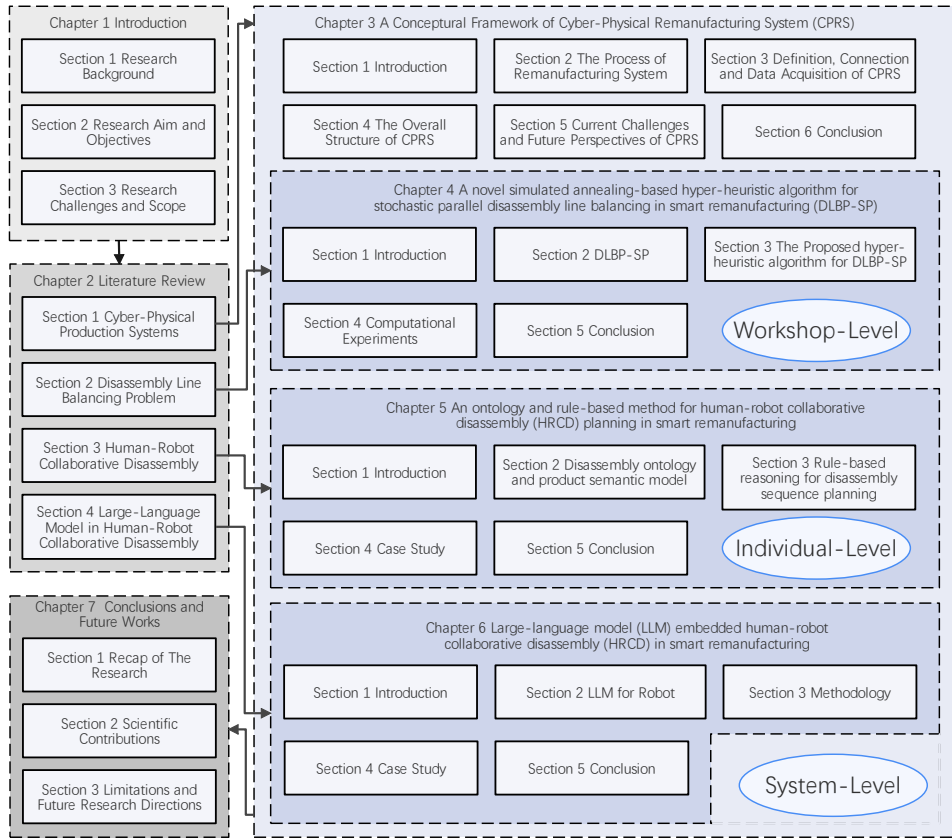


Figure 1.5: The organisation and contents of this thesis.

- Chapter 5 advances an ontology and rule-based method for human-robot collaborative disassembly planning in remanufacturing, with a case study and conclusion.
- Chapter 6 integrates a large-language model (LLM) into human-robot collaborative disassembly (HRCD) in remanufacturing, covering the LLM for robots, methodology, and case study.

- Chapter 7 recaps this thesis and summarises the research contributions in this thesis. Moreover, indicating several future research directions of based on this research.

Each chapter is systematically divided into sections, providing a comprehensive approach to addressing the complexities and innovations in the field of remanufacturing and human-robot collaborative disassembly.

1.4 Chapter Summary

The introduction chapter sets the stage for an in-depth exploration of the smart manufacturing with a focus on remanufacturing. It begins by outlining the background of smart manufacturing, introducing remanufacturing, and discussing the state-of-the-art of remanufacturing practices. It further delves into the research challenges and scope, where it identifies specific obstacles and delineates the boundaries of the research. Additionally, the organisation of the thesis is presented, providing a road-map for the reader. Finally, the chapter concludes with a summary, encapsulating the key points discussed and setting the foundation for the subsequent chapters.

This introduction is crucial for establishing the context and significance of the research, as well as highlighting the contribution it seeks to make in the fields of smart manufacturing and remanufacturing.

2

Literature Review

2.1 Cyber-Physical Production Systems

2.1.1 Cyber-Physical System (CPS)

CPS is a multi-dimensional complex system that integrates the information network world and the dynamic physical world. Through the integration and collaboration of computing, communication and control (3C), CPS provides services such as real-time sensing, information feedback, and dynamic con-

trol [29]. Through connections and feedback loops, the virtual information exchange and physical processes are integrated and interacted in real-time to monitor the physical entities. There are some basic definitions of CPS as shown in Table 2.1.

Table 2.1: Definitions of cyber-physical systems.

CPS	Definition	Reference
1	‘Cyber-physical systems are integrations of computation and physical processes. Embedded computers and networks monitor and control the physical processes, usually with feedback loops where physical processes affect computations and vice versa.’	[30]
2	‘Cyber-physical systems (CPS) are systems of collaborating computational entities which are in intensive connection with the surrounding physical world and its on-going processes, providing and using, at the same time, data-accessing and data-processing services available on the Internet’	[31]
3	‘A cyber-physical system (CPS) or intelligent system is a computer system in which a mechanism is controlled or monitored by computer-based algorithms. In cyber-physical systems, physical and software components are deeply intertwined, able to operate on different spatial and temporal scales, exhibit multiple and distinct behavioural modalities, and interact with each other in ways that change with context’	US National Science Foundation

2.1.2 Cloud-Based Manufacturing (CBM)

CBM is an advanced technology that integrated advanced information technology, manufacturing technology and emerging Internet of Things technology. CBM can improve the autonomous and innovation capability of the manufacturing industry through integrating the manufacturing resources and providing high-value-added and low-cost manufacturing services [32]. There are several definitions of CBM as shown in Table 2.2.

Table 2.2: Definitions of cloud-based manufacturing.

CPS	Definition	Reference
1	‘Cloud manufacturing is a computing and service-oriented manufacturing model developed from existing advanced manufacturing models (e.g., application service providers, agile manufacturing, networked manufacturing, manufacturing grids) and enterprise information technologies under the support of cloud computing, the Internet of things (IoT), virtualisation and service-oriented technologies, and advanced computing technologies’	[32]
2	‘Cloud manufacturing is a model for enabling ubiquitous, convenient, on-demand network access to a shared pool of configurable manufacturing resources (e.g., manufacturing software tools, manufacturing equipment, and manufacturing capabilities) that can be rapidly provisioned and released with minimal management effort or service provider interaction’	[33]
3	‘Cloud-Based Manufacturing (CBM) refers to a networked manufacturing model that exploits on-demand access to a shared collection of diversified and distributed manufacturing resources to form temporary, reconfigurable production lines which enhance efficiency, reduce product life-cycle costs, and allow for optimal resource allocation in response to variable-demand customer generated tasking.’	[34]

2.1.3 Cyber-Physical Production System (CPPS)

To deal with the variable environment, the manufacturing mode is changing from large-scale centralised rigorous structure to distributed flexible structure. Through integrating the advanced technologies, CPPS is proposed from the integration of CPS and manufacturing systems. CPPS can realise functions such as heterogeneous integration, ubiquitous connection and virtual-reality mapping through dynamic hybrid organisational structure, which has the characteristics of smartness, connectedness and responsiveness [31]. There are two definitions of CPPS as shown in Table 2.3.

Table 2.3: Definitions of cyber-physical production system.

CPS	Definition	Reference
1	‘Cyber-Physical Production Systems (CPPS) consist of autonomous and cooperative elements and subsystems that are connected based on the context within and across all levels of production, from processes through machines up to production and logistics networks (Three main characteristic: Smartness, Connectedness, Responsiveness)’	[31]
2	‘Cyber-Physical Production Systems are systems of systems of autonomous and cooperative elements connecting with each other in situation dependent ways, on and across all levels of production, from processes through machines up to production and logistics networks, enhancing decision-making processes in real-time, response to unforeseen conditions and evolution along time’	[35]

2.2 Disassembly Line Balancing Problem

This section covers three aspects, including layout types for disassembly lines, optimisation algorithms, and the studied disassembly products of DLBP. These three aspects are the foundation for the research backgrounds, methods and objects of DLBP. The research gaps and challenges of DLBP are discussed and summarised.

2.2.1 Layout Type of Disassembly Line

The layout type of the disassembly line is decided at the design stage for determining the function and capability of the disassembly line, in which the number of workstations and cycle time are two key factors that affect the overall efficiency of the disassembly line. Workstations refer to any point on the disassembly line where operators execute a disassembly task on EoL products. Cycle time is the time it takes to complete each workstation task,

which includes working time and idle time. The overall efficiency of the disassembly line can be improved by minimising the idle time of each workstation. Different disassembly line layouts represent different implementation modalities of EoL products disassembled by workstations. According to the literature review, there are four main layout types of disassembly lines, including straight, U-type, two-sided, and parallel, as shown in Figure 2.1.

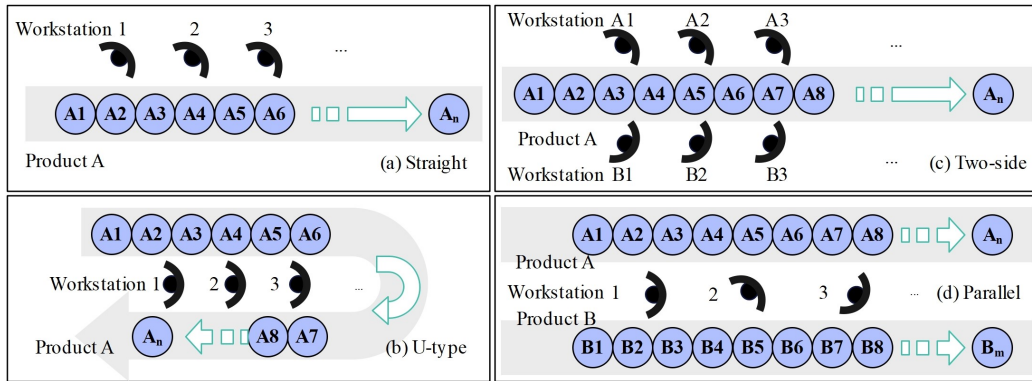


Figure 2.1: Layout type of disassembly lines.

The straight type is the most commonly used layout type for disassembly lines. The workstations are sequentially organised in a line array, as shown in Figure 2.1 [36]. The structure of the straight disassembly line is simple, making it easy to construct the mathematical model for DLBP. On this basis, several studies have incorporated different scenarios for further research, such as partial disassembly [37], and automatic robotic disassembly [38]. However, the straight disassembly system has a relatively low dynamic range and is only suitable for processing a single type of EoL product. The U-type disassembly line was first proposed by Agrawal and Tiwari [39]. Compared to

the straight type, the U-type has the advantages of relatively high operation flexibility, high efficiency and short setup times [40]. The two-sided disassembly line was introduced by Wang et al. [41] and Kucukkoc [42], which is designed specifically for processing the disassembly of large-sized equipment. Both U-type and two-sided layouts cannot be used for disassembling multi-type EoL products [43]. Therefore, the parallel disassembly line was first proposed by Karadag and Turkbey [44] for dealing with the disassembly process of multi-type EoL products simultaneously. Wang et al. proposed the genetic simulated annealing algorithms for solving parallel DLBP under uncertainty [45]. The parallel disassembly line achieves high flexibility and can disassemble multiple types of EoL products. Given the increasing quantity and variety of EoL products, the parallel disassembly line is more suitable and advantageous for practical applications in real-world scenarios [46].

2.2.2 Optimisation Algorithms for DLBP

The optimisation of DLBP is a typical non-deterministic polynomial (NP) complete linear programming problem [47], which cannot determine the optimal solution. According to the characteristics of DLBP, there are three main types of optimisation methods in DLBP: exact methods, heuristic algorithms and meta-heuristic algorithms. At the initial stage, the exact methods are considered and applied in DLBP. Altekin et al. [48] proposed the linear programming methods and developed the mixed integer programming for-

mulation for solving the profit-oriented partial DLBP [49]. Igarashi et al. [50] proposed integer programming to design the disassembly system and achieve the multi-objective optimisation goals in a closed-loop supply chain. Ozceylan and Paksoy [51] developed a nonlinear programming model for assigning disassembly tasks to optimise the reverse supply chain. With the development of global and intelligent optimisation algorithms, an increasing number of heuristic and meta-heuristic algorithms are introduced and applied in DLBP. The heuristic algorithms are generated and developed by imitating natural behaviours, including greedy algorithm, hill climbing algorithm, simulated annealing algorithm, ant colony algorithm, etc. McGovern and Gupta developed the mixed hill-climbing [52] and greedy algorithm [53] to generate the disassembly sequence and solve the DLBP. Kalayci and Gupta published a series of research for solving sequence-dependent DLBP, which took simulated annealing (SA) algorithm [54], and ant colony optimisation (ACO) algorithm [55]. All the heuristic algorithms are formulated and programmed with regulations for solving specific optimisation problems. Nowadays, meta-heuristic algorithms are becoming the most popular optimisation algorithm in DLBP. The meta-heuristic algorithm is derived from the heuristic algorithm, which combines the stochastic process and the local search algorithm. There are several heuristic algorithms that are also implemented to optimise the DLBP, such as the hybrid genetic algorithm (GA) [56], particle swarm optimisation (PSO) algorithm [57], artificial bee colony algorithm [58] and Tabu algorithm [59] for solving the optimisation process of

DLBP. Zhang et al. [60] proposed the artificial fish swarm algorithm for solving multi-objective DLBP under uncertain disassembly time. Zhu et al. [61] constructed the firefly algorithm for solving the discrete DLBP and taking hazardous disassembly operations into account.

In summary, the exact method may obtain the optimal solution, but it has limitations and is not suitable for solving the large-scale and multi-objective optimisation of DLBP. The exact method consumes high computing resources and time dealing with large-scale optimisation of DLBP [62]. According to the characteristic of heuristic algorithms, the proposed heuristic algorithms cannot obtain the optimal solution of NP problems and easily obtain the local optimal solutions [63]. The heuristic algorithms are not suitable for solving high-complexity DLBP. Meta-heuristic algorithms are able to provide more optimal solutions with limited resources, and they are suitable for dealing with large-scale and multidimensional optimisation problems. However, the model and computational complexity of the meta-heuristic algorithm are higher than exact methods and heuristic algorithms.

2.2.3 The Categories of EoL Product in DLBP

Traditionally, research on DLBP is focused on constructing a mathematical model and proposing an optimisation algorithm. Most case studies are implemented based on benchmark test datasets without considering actual EoL products [64]. The benchmark test datasets are commonly generated from software modelling, mainly applied for verifying and validating the perfor-

mance of the proposed algorithms.

In order to promote and enrich the application of automation disassembly in the real-world, the disassembly of actual EoL products is gradually introduced in DLBP. The majority of actual EoL products are focused on waste electric and electronic equipment (WEEE), such as personal computers (PC) [65], mobile phones [66], laptops [67], etc. These WEEE products are suitable for conducting experiments due to their variety and simple physical structure. However, the resource recycling and economic benefits from the disassembly process of electronic products are limited [4]. Industrial equipment disassembly has more significant social benefits as a result of its large scale and high added value. However, only a few studies consider industrial equipment as a case study, including hammer drills [68], corn harvester cutting tables [69] and automobile engines [70].

2.3 Human-Robot Collaborative Disassembly

This section is reviewed and summarised from three aspects: human-robot collaborative disassembly, ontology-based product information models, and rule-based reasoning for disassembly planning. These three aspects cover the background and methodologies related to HRCD. At the end of this section, the research gaps and challenges associated with implementing human-robot collaborative disassembly are discussed.

2.3.1 Background of HRCD

In line with definitions from smart manufacturing, human-robot collaboration in smart remanufacturing is defined as an interactive environment where humans and industrial robots coexist, sharing the same workspace, resources, and remanufacturing tasks [71]. While humans primarily control and monitor the remanufacturing processes, industrial robots, endowed with environmental sensing, cognitive capabilities, and relevant knowledge, are positioned to closely assist humans in accomplishing the remanufacturing tasks, or operate autonomously [72]. The advantage of human-robot collaboration lies in the ability of these robots to handle high-load, repetitive, and hazardous tasks while ensuring human safety [73]. This not only improves overall production efficiency but also substantially reduces the workload and stress on humans. Compared to the traditional human disassembly process, human-robot collaboration in disassembly can improve overall efficiency by combining the automation and intelligence with the human's knowledge and expertise [74, 75].

Liu et al. [76] integrated advanced technologies such as cyber-physical production systems (CPPS) and Artificial Intelligence (AI) to establish a comprehensive HRCD system framework. They validated the feasibility and efficiency of the system through case studies involving HRCD task planning, distance-based safety strategies, and motion-driven control methods. Huang et al. [77] introduced an active compliance control method for the HRCD of press-fit components. They demonstrated the feasibility of their approach

with a case study in which a human and robot collaboratively disassembled an automotive water pump. In their follow-up study, they designed a human-robot collaboration paradigm comprising two collaborative robots and an operator, and validated it using the same method [78]. Lee et al. [79] proposed a disassembly sequence planning algorithm for the HRC environment. Considering constraints such as limited resources and worker safety, the proposed algorithm aims to reduce the overall disassembly time. The effectiveness of the proposed method was validated through a case study involving the disassembly of a disposed hard disk drive. Xu et al. [80] introduced the Pareto-based modified discrete bees algorithm (MDBA-Pareto) to address the disassembly sequence planning problem in human-robot collaborative settings. This method considers multiple optimisation objectives, including disassembly time, cost, and difficulty. By employing computer disassembly as a case study and comparing their method with other relevant algorithms, they demonstrated the effectiveness of their proposed approach. Parsa and Saadat [81] classified human-robot collaboration tasks by evaluating the remanufacturing capability of EoL product components. This enriched the definitions of collaboration categories within human-robot collaboration. Subsequently, they generated a near-optimal disassembly sequence using an enhanced genetic algorithm. The efficiency of their approach was validated by comparing it to the particle swarm optimisation algorithm. Aguinaco et al. [82] introduced a goal-conditioned reinforcement learning approach to ensure real-time collision avoidance, facilitating safe interactions

in the human-robot disassembly process. Chu and Chen [83] proposed a hybrid particle swarm optimisation algorithm based on Q-learning to address HRCDC challenges of power batteries. By comparing their proposed algorithm with other related meta-heuristic approaches, they affirmed its effectiveness. Guo et al. [84] developed a method for human-robot collaborative partial-destructive disassembly sequence planning, considering multiple failure modes of EoL products. They employed a multi-layer chromosome encoding technique with the aim of determining the optimal disassembly sequence.

The majority of papers addressing the HRCDC issue focus on developing optimisation algorithms for disassembly sequence planning, aiming to identify the optimal disassembly sequence [85]. However, given that disassembly sequence planning is inherently an NP-hard problem, it becomes theoretically impossible to determine the optimal disassembly sequence through those optimisation algorithms [86]. Consequently, there is a need to consider incorporating alternative methods, such as graph theory, and knowledge reasoning, to plan and determine the optimal human-robot collaborative disassembly sequences.

2.3.2 Ontology-Based Product Information Model

The product information model, which represents products and associated disassembly data in a structured format, serves as the premise for disassembly sequence planning [87]. For effective disassembly sequence planning, it is es-

sential to construct a well-defined, comprehensive product information model for EoL products. This model should be able to offer a shared, scalable, and organised information structure in a designated format [88]. Two primary models are predominantly used at the current stage: matrix-based models and graph-based models. Both models can properly represent the connection relationships and precedence constraints among components in EoL products [89], intuitively generating disassembly sequences. However, these two models are not suitable for storing and transferring other disassembly-related knowledge, such as the required direction, action, or tool for each component's disassembly. This drawback significantly hampers the expansion of disassembly knowledge and reduces the quality of disassembly planning solutions. To compensate for this limitation, the product information model requires a more standardised, structured, and intelligent method to build upon.

Knowledge engineering has been widely employed for knowledge acquisition and sharing in manufacturing [90]. It stores and shares knowledge in the form of ontologies. Ontologies, serving as tools for building conceptual models and expressing semantic knowledge, have been widely deployed in fields like artificial intelligence and systems engineering [91]. The ontology-based product information model is capable of representing knowledge in a more standardised and structured manner [92]. It facilitates the easy storage and access of various disassembly-related knowledge, including product hierarchical structures, connection constraints, disassembly rules, and selection

criteria for disassembly directions, actions, tools, etc.

Over the past few years, ontology-based models for assembly have garnered significant attention for their potential in enhancing the assembly process's efficiency and intelligence. According to Qiao et al. [93] and Zhong et al. [94], ontologies can capture complex interrelationships among components and assembly processes, thereby facilitating more effective and automated assembly sequence planning. This sentiment is further demonstrated by Gong et al. [95], who emphasised the importance of semantic representations in reducing assembly errors and reusing both process knowledge and assembly sequence planning experience.

Moreover, it possesses good scalability, allowing timely adjustments to meet different scenarios in disassembly. Zhu and Roy [96, 97] developed a disassembly information model that includes various types of knowledge related to EoL products, such as product hierarchical structure, feasible disassembly sequences, component uncertainties, and degradation information. Building on this, they aimed to generate more reasonable disassembly sequences. Foo et al. [98, 99] proposed an ontology-based structural model to manage the disassembly-related knowledge of EoL products. They employed an artificial learning method for component recognition during disassembly and validated its efficacy using the disassembly of LCD monitors as a case study.

The consensus in the literature indicates a promising future for ontology-based assembly models, as they pave the way for more intelligent, adapt-

able, and efficient manufacturing processes. However, existing disassembly information models have not been designed for human-robot collaborative disassembly scenarios. Moreover, these models are relatively simplistic and unsuitable for the disassembly process in remanufacturing. Therefore, there is a need to develop a more comprehensive ontology-based model for EoL products, specifically tailored to human-robot collaborative disassembly in remanufacturing.

2.3.3 Rule-Based Reasoning for Disassembly Sequence Planning

Rule-based reasoning inherently operates by constructing pertinent semantic rules or processing mechanisms to extract tacit knowledge hidden within explicit knowledge [100]. Furthermore, knowledge reasoning can resolve inconsistencies within the product information model and detect contradictions present within the existing knowledge [101].

Veerakamolmal and Gupta [102] proposed a case-based reasoning method to automatically plan and generate the disassembly sequence. Giudice [103] proposed a rule-based approach to reason the difficulty of spatial and junction constraints of components. Consequently, this approach supports determining the optimal disassembly depth and enhances the disassemble ability of EoL products. Chen et al. [104] proposed a system based on ontology and case-based reasoning method to realise the automatic disassembly decision-making and reduce costs. Yu et al. [105] developed an ontology and partial

destructive rule-based method, which automated planning the disassembly sequence of disposed automotive traction batteries (ATB).

The rule-based reasoning method offers a range of distinct advantages, especially its structured approach to problem-solving. Tor et al. [106] proposed a rule-based representation approach for the functional design of mechanical products. Its deterministic nature ensures that, given a specific input, the output remains consistent, thereby reducing uncertainty in decision-making processes related to physical behaviours. Such consistency leads to more straightforward debugging and validation of processes. Zheng et al. [107] introduced a knowledge-based engineering method for designing the architectures of robotic manufacturing systems. Within this method, a rule-based reasoning process is outlined to describe the explicit semantic information of the components of robotic manufacturing systems [108]. Integrating expert knowledge in the form of predefined rules guarantees that the system operates based on tried and tested expertise, Reddy and Fields [109] laying a foundation for reliability. Additionally, highlighted two other advantages of the rule-based reasoning method through his review paper:

1. The transparency of rule-based systems means that decisions can be traced back to specific rules, offering enhanced interpretability and understandability. This feature is especially vital in complex systems where grasping the logic behind decisions is essential.
2. Rule-based reasoning can be effortlessly expanded by adding new rules

without necessarily modifying existing ones, which supports scalability and adaptability.

In summary, the rule-based reasoning method presents a clear, scalable, and reliable approach to automated reasoning and decision-making. It is evident that rule-based reasoning for disassembly planning primarily relies on pre-established product information semantic models. Therefore, the existing rules are non-transferable and unsuitable for contexts involving human-robot collaborative disassembly.

2.4 Large-Language Model for Disassembly

In the realm of advanced manufacturing and sustainable industrial processes, the fusion of artificial intelligence (AI), particularly through Large Language Models (LLMs), with robotic systems has emerged as a frontier of innovation. This integration promises to revolutionise the efficiency and effectiveness of human-robot collaborative disassembly, a critical component in addressing global challenges of waste reduction, recycling, and remanufacturing. These works collectively illuminate the trajectory of embedding LLMs in robotic systems to enhance human-robot interaction, decision-making processes, and the execution of complex disassembly tasks.

2.4.1 Large-Language Model for Robot

Li et al. [110] and Li et al. [111] offer complementary perspectives on the integration of LLMs for task-oriented dialogues and interactive decision-making

in industrial settings. These contributions highlight the role of pre-trained language models in facilitating nuanced interactions between humans and robots, enabling machines to participate in planning and decision-making processes based on natural language input. The emphasis on humanised dialogue systems and decision-making algorithms suggests a move towards more intuitive and accessible robotic systems for non-expert users.

The pioneering work by Benjdira et al. [112] on ROSGPT_Vision introduces a novel approach to commanding robots using language model prompts, bridging the communication gap between humans and robots. This advancement underscores the potential of LLMs to interpret human commands into actionable tasks, a critical capability for collaborative disassembly environments where adaptability and precision are paramount. Similarly, Brohan et al. [113] delves into the grounding of language in robotic affordances, suggesting that robots can understand and act upon commands based on their physical capabilities and the context of their environment, further enhancing the fluidity of human-robot collaboration.

Pan et al. [114] provides a road-map for unifying LLMs with knowledge graphs, proposing a framework that could enhance the contextual understanding of robots in disassembly tasks. This integration is crucial for enabling robots to access and leverage vast amounts of structured knowledge, improving their ability to make informed decisions and execute tasks with a higher degree of autonomy. Vemprala et al. [115] discusses the design principles and model abilities necessary for embedding ChatGPT in robotics,

offering insights into the practical considerations for implementing LLMs in robotic systems.

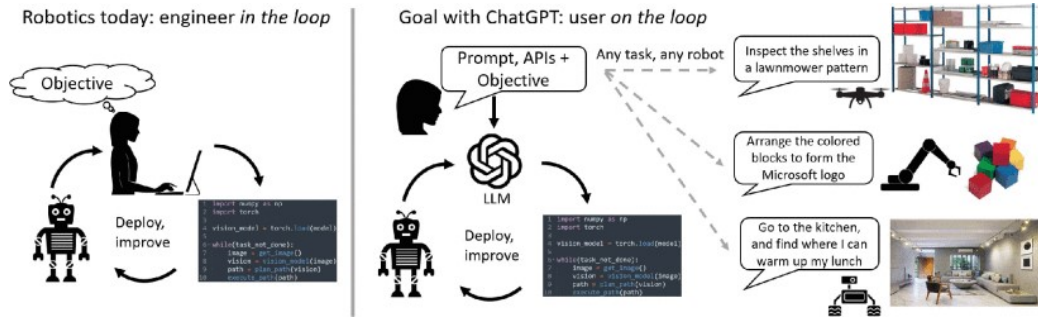


Figure 2.2: Goal with ChatGPT [115].

Figure 2.2 from paper [115] presented appears to be an illustrative comparison between the traditional model of robotics, which is “Robotics today: engineer in the loop,” and an envisioned model involving ChatGPT, titled “Goal with ChatGPT: user on the loop.” In the traditional model, the engineer is depicted as central to the process, with a feedback loop that includes setting objectives, programming the robot, and deploying and improving its functions, as suggested by the code snippet and the illustration of an engineer working on a computer while a robot seems to be waiting for commands. On the other hand, the “Goal with ChatGPT” model proposes a shift where the user directly interacts with a language model (LLM) through prompts and application programming interfaces to command any robot to perform various tasks. This is visually represented by a user silhouette with arrows indicating a more direct loop between the user’s objectives and the deployment and improvement of the robot’s tasks without the need for in-depth

programming. Supporting this model, the figure provides examples of tasks such as inspecting shelves in a specific pattern, arranging coloured blocks to create the Microsoft logo, and navigating a kitchen environment to warm up lunch, illustrating the versatility and user-friendly approach of the proposed ChatGPT-enhanced robotics system.

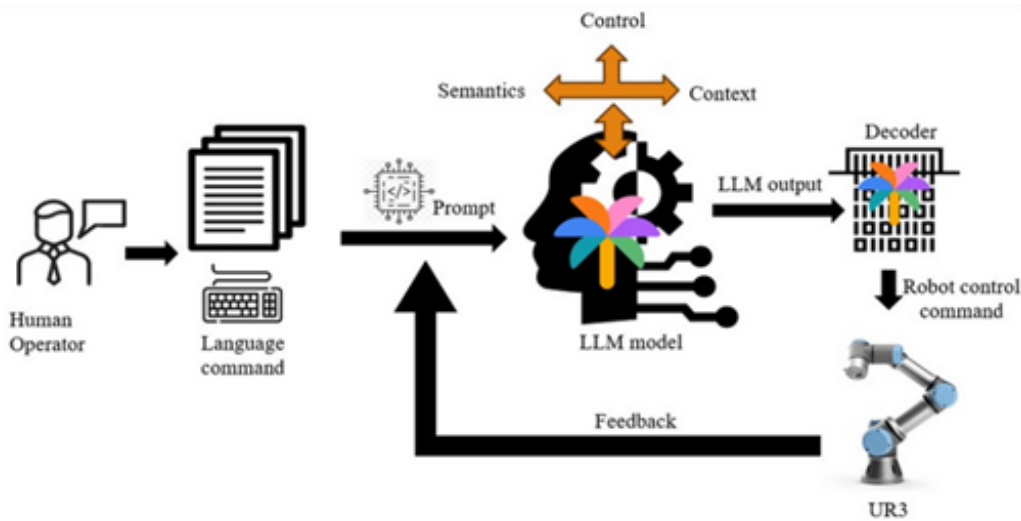


Figure 2.3: Conceptual framework of LLM-embedded HRC.

Figure 2.3 provides a schematic representation of a process where a human operator interfaces with a robot through a language model, indicative of a natural language processing (NLP) application in robotics control. The flow begins with the human operator issuing a language command, which is presumably translated into a written prompt. This prompt is then processed by a large language model (LLM), which incorporates semantics and context to understand and respond to the prompt appropriately. The output from the LLM is passed through a decoder, which is responsible for translating

the language output into a robot control command. The depiction of the control flow suggests a feedback loop, implying that the robot's performance or status can influence subsequent interactions with the LLM model. At the end of the sequence, the UR3 robot, a specific model known for its precision and versatility in automation, acts on the decoded commands. This diagram illustrates the integration of advanced language understanding within the control systems of robotics, showcasing the potential for more intuitive and flexible human-robot interactions in complex tasks.

The surveyed documents also explore the challenges and opportunities in enhancing LLMs' capabilities for specific tasks such as planning goals translation [116], generative information extraction [117], and foundation models for decision-making [118]. Each of these contributions addresses different facets of the problem space, from the translation of natural language into planning goals to the extraction of relevant information for task execution, highlighting the versatility and potential of LLMs to transform robotic disassembly.

Further, the review and survey papers by Zhang et al. and Zhao et al. [119, 120] offer comprehensive overviews of the current state of research in LLMs for human-robot interaction, knowledge graph completion, and commonsense knowledge for task planning, respectively. These works synthesise the collective progress in the field, identifying gaps in current methodologies and proposing directions for future research.

2.4.2 Large-Language Model for Sequence Planning

LLM has been increased popular, while the application of LLM in sequence planning is still limited.

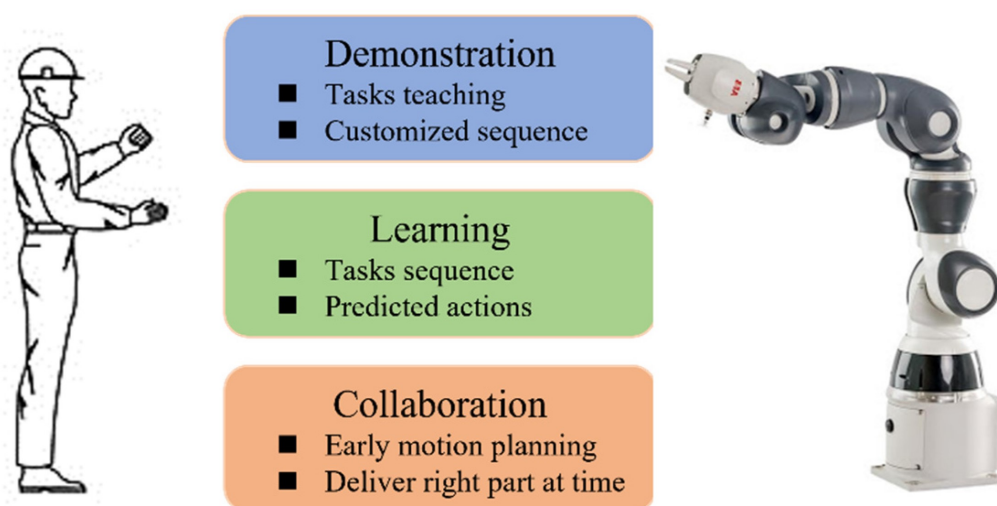


Figure 2.4: The scheme of the learning from demonstration model [121].

Figure 2.4 from Zhang et al. [121] appears to conceptualise a human-robot interaction framework for industrial automation, segmented into three main processes: Demonstration, Learning, and Collaboration. The human operator is depicted providing a demonstration, which involves tasks teaching and establishing a customised sequence of operations. This is graphically connected to an industrial robotic arm on the right, suggesting the transfer of knowledge or instructions from human to machine. The central part of the image is organised into three coloured blocks, each describing a different aspect of the interaction. The blue block corresponds to the “Demonstration”

phase, where the operator’s actions serve as a template for the robot’s tasks. The green block, labelled “Learning” implies that the robot is designed to understand and internalise the task sequence and predict subsequent actions autonomously. The final orange block, “Collaboration” suggests an advanced phase where the robot is capable of early motion planning and delivering the right part at the correct time, indicating a real-time, responsive interaction with the human operator. Collectively, the figure encapsulates a sophisticated model where human expertise is leveraged through demonstration and subsequently refined through machine learning, culminating in a collaborative interaction that enhances efficiency and precision in automated tasks.

Straightforwardly, the semantic information involved in sequence planning can be queried through LLM to obtain feasible solutions. Ruan et al. [122] introduce two different agents to understand different situations based on their domain angle, where the integration of two agents’ suggestions can serve as the inference process. Besides, knowledge graph can be utilised as a rule-based model to guide the sequence planning process with LLM [123]. Furthermore, reinforcement learning can be utilised to generate a graphical representation of sub-goals, which improves its explainability [124].

Another typical application scenario is robotic planning, where most of their input is in image format. A tailored prompt can help robot to perceive current situation and understand the requirements better [125]. Besides, Dagan et al. [126] applied LLM to analyse the dynamic image in the robotic planning, where the LLM enables to keep track of the world state to adapt

to changes and make informed decisions. Furthermore, Song et al. [127] proposed a visual-based few shot learning method in embodied agents and adjusted the sequence policy based on evidence.

However, the disassembly sequence planning always has prior knowledge as constriction. The response from LLM may not consider such prior constriction. Meanwhile, the LLM is more like a black box, where the uncertainty issue may introduce to the sequence planning task.

1. Engineers often face a plethora of choices during the disassembly process, each linked to uncertain outcomes, leading to substantial challenges.
2. The challenge lies in harnessing the knowledge embedded in LLM to aid disassembly sequence planning, which remains an unresolved task.

2.5 Research Gaps and Challenges

2.5.1 CPRS

In recent years, the evolution of smart remanufacturing has seen significant progress through integration with digital technologies, marking a period of rapid expansion. Nevertheless, the level of intelligence and autonomy within remanufacturing systems remains nascent, exposing several research gaps and challenges:

1. Equipment and System Integration: Modern remanufacturing systems commonly do not achieve fully intelligent production and operations.

Although there have been significant theoretical developments, the implementation of these frameworks in real-world production environments often does not meet expected outcomes. This issue primarily arises due to the inflexibility of theoretical models, errors in model accuracy, substantial delays, and insufficient responsiveness to changing production variables [128].

2. Cyber-Physical System Modelling and Reliability Analysis: When accounting for uncertainties in systematic production scheduling, the diversity of uncertainty sources and system configurations necessitates varied dynamic scheduling strategies, both passive and active [129]. The primary challenge lies in applying advanced optimisation algorithms to mitigate risks and minimising the impact of equipment failures within smart manufacturing strategies.
3. EoL Products Modelling: In the context of remanufacturing, it is impractical to extract constraint and fastener information directly from CAD, CAM, and BOM files owing to the unpredictable conditions of EoL products [130]. Consequently, it is essential to employ advanced methodologies and delineate the extent of information necessary to enhance the effectiveness and unearth the implicit information contained within EoL products.
4. Optimisation Modelling under Uncertainty: Traditional stochastic programming methods, such as the scenario tree approach, struggle to

comprehensively address the continuous uncertain parameters inherent in production processes due to the vast scale and complexity of the models. The challenges include the intractability of large-scale stochastic programming, issues with scenario decomposition, and the complexities introduced by chance-constrained programming, which relies on joint probability data.

These challenges underscore the significant theoretical and practical gaps in key technological areas within the field. Research into the modelling of EoL products and the optimisation of process planning and scheduling in cyber-physical remanufacturing systems could facilitate transformative advancements in enterprise operations. This thesis will tackle on this research challenge and propose the conceptual framework of CPRS. The proposed CPRS offers demonstrative and referential insights for key technology research and other decision-making processes.

2.5.2 DLBP

In summary, there are three major research gaps and challenges according to the literature review:

1. The majority of disassembly line layout types are straight with a determined environment [131], which cannot fully model the actual disassembly scenario. Straight disassembly lines are incapable of disassembling multi-type EoL products simultaneously [132]. The mathematical

model of the predetermined scenario cannot reflect the actual characteristics of both disassembly lines and EoL products.

2. The increasing complexity of the mathematical model and the uncertain conditions of DLBP limit the performance of existing optimisation algorithms. The single-objective optimisation of DLBP is linear. However, the multi-objective optimisation of DLBP-SP becomes a nonlinear and NP problem with higher computational complexity than DLBP. With the development of artificial intelligence methods, novel optimisation algorithms need to be proposed to deal with multi-objective optimisation with uncertain conditions and obtain better optimisation performance.
3. The disassembly process is inherently divergent, which introduces optional and variable methods and sequences. Additionally, the uncertain characteristics of EoL products contribute to variability in the time required for disassembly tasks. These uncertainties complicate the planning of disassembly sequences and make it challenging to determine the optimal disassembly sequence as well. Furthermore, most EoL products used in DLBP are derived from benchmark test datasets or WEEE . These products typically feature a limited number of disassembly tasks and relatively straightforward precedence constraints. Conversely, more complex industrial equipment represents a category with significant potential value for remanufacturing [4].

In accordance with the three aspects listed above, this research explores a more realistic and complex scenario of parallel assembly lines and proposes a novel optimisation model to solve multi-objective optimisation of the DLBP-SP. Furthermore, this research also introduces a new type of industrial equipment (gearbox) as a case study to enrich the disassembly research of industrial equipment.

2.5.3 HRC D

In this thesis, one of the primary research objectives focus on how to efficiently model and manage EoL products in HRC D. According to the previous literature review, ontology-based modelling is a common and effective method which is also applied in this thesis.

However, the existing ontology model has two limitations that makes it unsuitable and challenging for human-robot collaborative disassembly in remanufacturing:

1. Current disassembly ontology models are relatively simple, suggesting only two types of components in EoL products [104, 105]. This limited scope fails to effectively differentiate among various components, thereby impeding the decision-making process in disassembly sequence planning.
2. Moreover, current disassembly ontology models do not consider or establish a human-robot collaborative working environment and lack a

related knowledge base for robots. Based on the human-robot collaborative disassembly ontology model, there is also a need to formulate corresponding rules to reason and generate the optimal disassembly sequence scheme.

2.5.4 LLM in HRC

In conclusion, the integration of Large Language Models into human-robot collaborative disassembly represents a significant leap forward in the quest for more efficient, sustainable, and intelligent manufacturing processes. The reviewed body of literature delineates a multifaceted research landscape where LLMs serve as a bridge between human intuitive understanding and robotic precision. As this field continues to evolve, the foundational work discussed herein provides a road-map for future innovations. There are two challenges to overcome and highlighting the vast potential for LLMs to redefine human-robot collaboration disassembly in industrial settings.

Based on the previous literature review and review article [133], the main subjects of related research on HRC are summarised in Table 2.4. The research topics cover two major aspects, including disassembly and interaction. In disassembly, collaboration modes, disassembly levels and efficiency optimisation are three main research topics. In interaction, robustness and safety measures are considered. All the research topics aim at enhancing the overall performance and safety of the HRC. This thesis primarily focuses on efficiency optimisation and robustness enhancement of human-machine

collaboration in a collaborative, complete disassembly mode.

Table 2.4: Research topics in HRCD.

	Topics	Strategies	Description
Disassembly	Collaboration Mode	Sequential	Disassembly tasks are performed one after another by the human or robot.
		Parallel	Disassembly tasks can be dismantled simultaneously by the human and robot.
		Collaborate	Human and robot work actively interacting and assisting each other to implement disassembly tasks.
	Disassembly Level	Complete	The EoL product is disassembled to the lowest component level.
		Partially	Only specific components or target parts of the EoL product are disassembled.
	Efficiency Optimisation	Task Allocation	Strategies for distributing tasks between human and robot to maximise efficiency.
Sequence Planning		Optimising the disassembly sequence of the EoL product to minimise the idle time of human and robot.	
Path Planning		Optimising the movement paths of robots to reduce time and energy consumption.	
Interaction	Robustness	Flexibility	HRCD can adapt to different disassembly tasks and environments.
		Evaluability	HRCD requires efficiently assess through a quantitative metric.
		Trust Building	Strategies to enhance trust between human and robot to improve collaboration.
	Safety Measure	Proactive	HRCD designed to prevent accidents through anticipation and avoidance of risks.
		Reactive	Mechanisms that respond to incidents or errors to minimize harm and damage.

2.6 Research Aim and Objectives

The research endeavours to introduce a comprehensive conceptual framework for the cyber-physical remanufacturing system (CPRS), aimed at enhancing the intelligence and autonomy of the remanufacturing process. Specifically, the EoL products modelling, disassembly sequence planning, disassembly line balancing, and human-robot collaborative disassembly (HRCD) are developed and validated within the CPRS framework.

The research objectives of this research are based on the research aim and formulated after reviewing the status of remanufacturing, according to the potential research direction. The specific breakdown research objectives of this project are as follows:

- Objective 1: Define, design and propose **the conceptual framework of cyber-physical remanufacturing system (CPRS)** for managing the processes and improving the intelligence and autonomy of the remanufacturing system (System-level, overall scope).

- Propose **the hyper-heuristic algorithm for optimising the integrated process planning and scheduling** in CPRS (Workshop-level, performance indicator).
- Propose **the ontology and rule-based method for human-robot collaborative disassembly planning** in CPRS (Individual-level, procedure input).
- Develop the **large language model embedded human-robot collaborative disassembly** in CPRS (Improving the intelligence of collaborative robot).

2.7 Chapter Summary

Chapter 2 provides a comprehensive literature review that lays the groundwork for understanding the integration of cyber-physical systems in production, the complexities of disassembly line balancing, and the innovative approaches in human-robot collaborative disassembly, culminating in the exploration of the application of large language models for disassembly processes. It begins with an in-depth examination of Cyber-Physical Production Systems (CPPS), starting from the basics of Cyber-Physical Systems (CPS) and Cloud-Based Manufacturing (CBM) to the more integrated concept of CPPS. This foundation underscores the evolution of manufacturing systems into more interconnected, intelligent, and efficient entities capable of responding to dynamic production demands. The review then transitions

into the Disassembly Line Balancing Problem (DLBP), discussing various layout types, optimisation algorithms, and categories of End-of-Life (EoL) products. This segment highlights the challenges in achieving optimal disassembly line efficiency and the critical role of sophisticated optimisation techniques in managing the variability and complexity of EoL products.

Subsequently, the chapter shifts focus to Human-Robot Collaborative Disassembly, emphasising the background and potential of synergizing human flexibility and decision-making with robotic precision in disassembly tasks. It explores ontology-based product information models and rule-based reasoning for disassembly sequence planning as vital components for enhancing collaboration and efficiency. The exploration of research gaps reveals the need for advanced communication interfaces, improved safety measures, and more intuitive collaboration frameworks. The final section delves into the role of Large Language Models (LLMs) in disassembly, discussing their application in robotic comprehension and sequence planning. This innovative approach promises to revolutionise disassembly processes by enabling more natural and effective communication between humans and robots, although it also highlights significant research gaps, including the need for improved model understanding of technical language and the integration of LLMs with physical disassembly systems.

Through this literature review, Chapter 2 articulates the current state of research and identifies pivotal areas for future investigation, setting the stage for significant advancements in the field of CPRS.

3

A Conceptual Framework of Cyber-Physical Remanufacturing System

3.1 Introduction

Although traditional remanufacturing systems hold considerable promise, they encounter significant challenges. Establishing such systems comes with

several intractable issues, primarily due to the complexity of the processes involved, such as disassembly, cleaning, inspection, repair, reassembly, and testing [134]. As noted by Wang et al. [135], these remanufacturing processes have traditionally been labor-intensive and heavily dependent on the implicit knowledge and skills of experienced workers. This reliance often results in variability in both the quality and quantity of the remanufactured products [136]. Moreover, remanufacturing operations frequently face uncertainties concerning the timing, quantity, and quality of returned EoL products. These uncertainties introduce substantial remanufacturing process, logistical and inventory challenges, as discussed by Chen et al. [137].

Furthermore, traditional remanufacturing systems are often plagued by insufficient information flows, leading to inefficiencies throughout the remanufacturing processes. For example, the absence of detailed data regarding the condition of returned EoL products can lead to sub-optimal decisions within the remanufacturing process, as indicated by Xiao et al. [138]. Moreover, despite having a lower environmental impact compared to original manufacturers, remanufacturing still poses significant environmental concerns due to the reliance on non-renewable energy sources and solvents in some of its processes [15].

An additional drawback of existing remanufacturing systems is their inefficacy in managing and processing returned EoL products. According to research by Ferraro et al. [139], traditional remanufacturing systems frequently fall short in predicting and managing EoL product returns effectively, result-

ing in inventory and production inefficiencies. This challenge is exacerbated by a lack of standardised processes, which hinders scalability and elevates operational costs.

Addressing these challenges, the advent of "Industry 4.0" and "Smart Manufacturing" introduces a range of advanced technologies that enhance connectivity among infrastructures and increase the automation level in remanufacturing systems. Notable among these are the Internet of Things (IoT), Digital Twins (DTs), Cyber-Physical Systems (CPS), and Cloud Computing [140]. Specifically, IoT facilitates the connection and communication among different physical entities through technologies like radio-frequency identification (RFID) and smart sensors [141]. CPS and DTs significantly enhance the intelligence and efficiency of manufacturing systems by enabling iterative optimisation processes in a virtual environment, offering solutions that are both cost-effective and superior [142]. Furthermore, cloud computing provides the capability to tackle more complex manufacturing challenges [143].

The aforementioned technologies are integral to the advancement of smart manufacturing. Nonetheless, there remains a significant shortfall in the integration of modern technology within remanufacturing processes. Although some progress has been observed, the adoption of digital technologies that support digitalisation and intellectualisation remains limited. This gap in technology adoption impedes the optimisation of resource utilisation and process efficiency, both of which are essential for sustainably scaling reman-

ufacturing practices.

To promote the incorporation of the aforementioned advanced technologies in remanufacturing, this chapter introduces a conceptual framework for the Cyber-Physical Remanufacturing System (CPRS). This framework aims to address existing limitations by synergizing physical operations with networked digital technologies, thereby enhancing information accuracy, process efficiency, and resource optimisation. According to Chao et al. [75], the implementation of CPS within remanufacturing significantly boosts the adaptability and responsiveness of these systems. By providing real-time data and feedback loops throughout the product life-cycle, CPS enables improved forecasting, planning, and control—key elements in managing the variability and uncertainties typical of remanufacturing environments.

The structure of this chapter is organised as follows. Section 3.2 introduces the primary processes involved in the CPRS. Section 3.3 discusses the proposed overall conceptual framework for the CPRS. Section 3.4 explores the research challenges and key issues associated with the CPRS. The chapter concludes with a summary in Section 3.5.

3.2 The Concept and Process of CPRS

3.2.1 Definition of Smart Remanufacturing

Essentially, smart remanufacturing represents an evolving research area that signifies a major shift towards more interconnected, efficient, and sustainable

manufacturing practices. This provides a robust framework for handling EoL products in alignment with modern technological capabilities and environmental objectives [144]. From the perspective of long-term circular economy and green sustainability strategies, remanufacturing benefits society, industry, and the environment, creating a win-win-win situation.

However, smart remanufacturing is a relatively new field in the literature, with few definitions available. At present, one widely accepted definition proposed by Kerin et al. is:

“Smart remanufacturing uses Industry 4.0 technologies on products to be remanufactured, as well as on remanufacturing processing equipment and business management systems, primarily including Cyber-Physical Systems (CPS), Internet of Things (IoT), Artificial Intelligence (AI), and Big Data Analytics (BDA).” [145]

This definition, by integrating Industry 4.0 technologies, allows the smart remanufacturing system to identify, locate, and determine the condition of mid-life remanufacturable products, achieving a level of remote interaction or EoL products processing previously unattainable, thereby extracting more value to meet the needs of the remanufacturing business. However, the remanufacturing process is more complex than manufacturing, thus, it is unwise to fully and directly transfer the Industry 4.0 paradigm to remanufacturing [146].

Another definition of smart remanufacturing, proposed by Okechukwu et al. is:

“Smart remanufacturing integrates the principles of Industry 4.0 (I4.0) and the circular economy to enhance the remanufacturing process. It modernises traditional remanufacturing methods by incorporating advanced technologies such as the Internet of Things (IoT), Virtual Reality (VR), and Augmented Reality (AR).” [17]

This definition emphasises the use of digital technology to shorten and strengthen the connections between product manufacturers, users, and remanufacturers. It aims to improve resource circulation and value creation through product service systems, adapting to changing social needs, user expectations, and workforce attributes.

As smart remanufacturing adopts these new technologies, it is expected to handle increased data and information flows, adding complexity but also increasing opportunities for innovation in the remanufacturing process. However, from a technological implementation perspective, the majority of remanufacturers are very small, resource-limited companies that cannot afford the cost of implementing smart manufacturing technologies.

Combining the above two definitions of smart remanufacturing, this chapter defines smart remanufacturing based on the constructed ‘three-stage, three-level’ CPRS as:

“Smart remanufacturing integrates the principles of closed-loop supply chains, Industry 4.0 technologies, and circular economy to achieve a highly efficient operational paradigm that is structured, transparent, and informational throughout the overall remanufacturing process.”

Distinct from the above definitions, this chapter's definition takes an integrated approach to the recycling and marketing stages of the remanufacturing process. This definition considers how to efficiently organise, manage, and optimise business processes, including production, service provision, and logistics. Given the multiple influencing factors of remanufactured products and markets, as well as related inherent uncertainties, smart remanufacturing can evolve and change in response to different technological developments, market demand dynamics, and updates in management concepts.

3.2.2 The Process of CPRS

The methodology employed in the proposed CPRS encompasses a series of stages: surface examination, disassembly, cleansing, sorting and inspection, reprocessing, reassembly, and testing. The essential technologies pertinent to these stages are depicted in Figure 3.1.

- **Surface inspection:** the heterogeneity and unpredictability of EoL products are pivotal factors that influence the efficacy of remanufacturing systems. A notable issue within this domain is the disconnect between remanufacturers and the original end-users of the EoL products. This separation often results in the loss of crucial information, thereby complicating the accurate assessment of the EoL products' condition [147]. To circumvent the costs associated with extensive data gathering and condition assessment, emphasis is placed on surface inspections upon receipt of EoL products. Such inspections serve as a



Figure 3.1: The process of CPRS.

preliminary step in determining the feasibility of remanufacturing an item. The evaluation primarily depends on various forms of data and information, such as usage duration, maintenance history, structural integrity, and visual examinations. This information, which can be collected from the end-users, is then analysed by the remanufacturer [148]. Effective surface inspections enhance the understanding of an EoL product's condition, providing a solid foundation for subsequent remanufacturing processes.

- **Disassembly:** represents a critical and mandatory phase in the remanufacturing cycle, distinguished from the linear methodology of assembly. This phase is characterised by its divergent nature, encompassing

varying levels, types, and routes of disassembly [149]. Disassembly levels are typically categorised into partial or complete. Partial disassembly targets the retrieval of valuable components, overlooking those deemed non-essential, and does not involve decomposing the EoL products into their individual parts. In terms of disassembly types, methods are classified as either destructive or non-destructive. Destructive disassembly, an irreversible process, is employed when certain components cannot be feasibly disassembled, often resulting in higher costs compared to its non-destructive counterpart. Furthermore, the selection of a disassembly route, also known as disassembly sequence planning, involves planning and optimising the order in which sub-assemblies or components are detached, taking into account the constraints of precedence and regulations pertaining to fasteners.

- **Cleaning:** constitutes an essential stage in the remanufacturing process, aimed at removing contaminants such as rust and paint from components to achieve a specified level of cleanliness, which is crucial for ensuring the quality and performance of the components [15]. Various cleaning technologies are employed, including jet, chemical, and ultrasonic cleaning. The choice of technology is influenced by the materials, physical structure, and chemical properties of the components. It is also common to utilise a combination of these technologies to effectively clean different types of components. Moreover, it is critical to prevent secondary contamination of the components during the

cleaning process to maintain the integrity and effectiveness of the re-manufacturing.

- The **sorting** process in remanufacturing is integrally linked to the inspection phase. The primary objective of the **inspection** process is to ascertain the geometric accuracy, surface and internal integrity, and the quality and physical properties of the components. To ensure that the inspection does not introduce defects or alter the existing condition of the components, non-destructive testing (NDT) methods are employed. These methods typically include ultrasonic testing (UT), radio-graphic testing (RT), and magnetic particle testing (MPT). Based on the results of the inspection and an analysis of cost efficiency, the sorting process categorises components into groups designated for maintenance, reprocessing, or replacement. Furthermore, the classification of maintenance and reprocessing components is refined according to the type of defect and physical condition of the components [150].
- **Reprocessing** in remanufacturing involves a series of physical interventions aimed at restoring both the structural and functional integrity of components [149]. Unlike continuous process manufacturing, which transforms raw materials into components, reprocessing is typically conducted in batch production settings, offering flexibility to address diverse maintenance needs and specific types of defects. In recent developments, additive manufacturing has emerged as an innovative re-

processing technique that offers both cost efficiency and enhanced precision. Furthermore, the scheduling of components within the remanufacturing process presents an optimisation challenge. This scheduling can be effectively integrated and optimised in conjunction with the planning of the disassembly process sequence [64].

- **Reassembly** constitutes the methodical integration of maintained, reprocessed, and replaced components into remanufactured products, effectively serving as the inverse of the disassembly process. Unlike standard assembly operations in manufacturing, reassembly is characterised by significant uncertainty, variability, and instability, traits inherited from the disassembly process. These factors critically impact the reliability and longevity of remanufactured products [151]. Furthermore, reassembly and disassembly processes often share the same machinery within a unified remanufacturing system, thereby linking the planning of disassembly/reassembly sequences and resource allocation to unique optimisation challenges in the field of remanufacturing.
- **Testing** represents the concluding phase in the remanufacturing process, wherein the precision of the physical structure, functionality, and durability predictions are assessed to validate the performance of remanufactured products. The outcomes of these tests must align with the standards set for new products [150]. The primary objective of the testing phase is to detect and eliminate any defects that may have

arisen during the remanufacturing process, thereby ensuring the operational integrity of the remanufactured products. It is imperative that the methodologies and criteria used for evaluating the performance of remanufactured products are consistent with those applied to new products.

3.3 The Conceptual Framework of CPRS

To enhance the automation and intelligence of smart remanufacturing systems, this chapter proposes a conceptual framework called CPRS by leveraging advanced technologies such as the Internet of Things (IoT), Information and Communication Technology (ICT), Cyber-Physical Systems (CPS), and Digital Twins (DT). Inspired from Chao et al. [152], The architecture of CPRS is structured into three distinct layers: the physical layer, the edge layer, and the cloud service layer as shown in Figure 3.2. The physical layer, located at the base, comprises tangible entities and facilitates communication among various components. Above this, the edge layer serves as a bridge, translating physical entities into virtual counterparts via digital twins and connecting to the physical layer through network interfaces. The topmost layer, the cloud service layer, provides comprehensive system-level applications and integrated services for remanufacturing. This layer supports iterative optimisation to enhance cloud services, which, in turn, guide the operational decisions at the edge layer. Communication between the edge and cloud service layers is primarily conducted through protocols that

govern the interaction among different mechanical systems. The framework exhibits increasing levels of digitisation and visualisation as one moves from the lower to the upper layers, and horizontally, it demonstrates enhanced cooperation and adaptability. Further details about each layer's components are expounded in subsequent sections.

3.3.1 Physical Layer

In the remanufacturing system, the objectives encompass EoL products and accompanying technological components, including machinery, interactive devices, and sensors, as illustrated in Figure 3.3. EoL products undergo remanufacturing via diverse types of machinery. Interactive and sensor devices facilitate communication among these machines and monitor the processes involving EoL products. Consequently, the proposed physical layer of the system is composed of five segments: EoL products, interactive equipment, actuator equipment, sensor equipment, and the environment. These components collectively support all stages of the remanufacturing process.

- **EoL products** represent the primary targets for remanufacturing. Due to their inherently uncertain characteristics, remanufacturing these products cannot adhere to a uniform standard process. Consequently, the availability of comprehensive supplementary information on EoL products enhances the creation of a robust knowledge base for the remanufacturing process. Data pertaining to EoL products are categorised into two types: static and dynamic. Static data include the

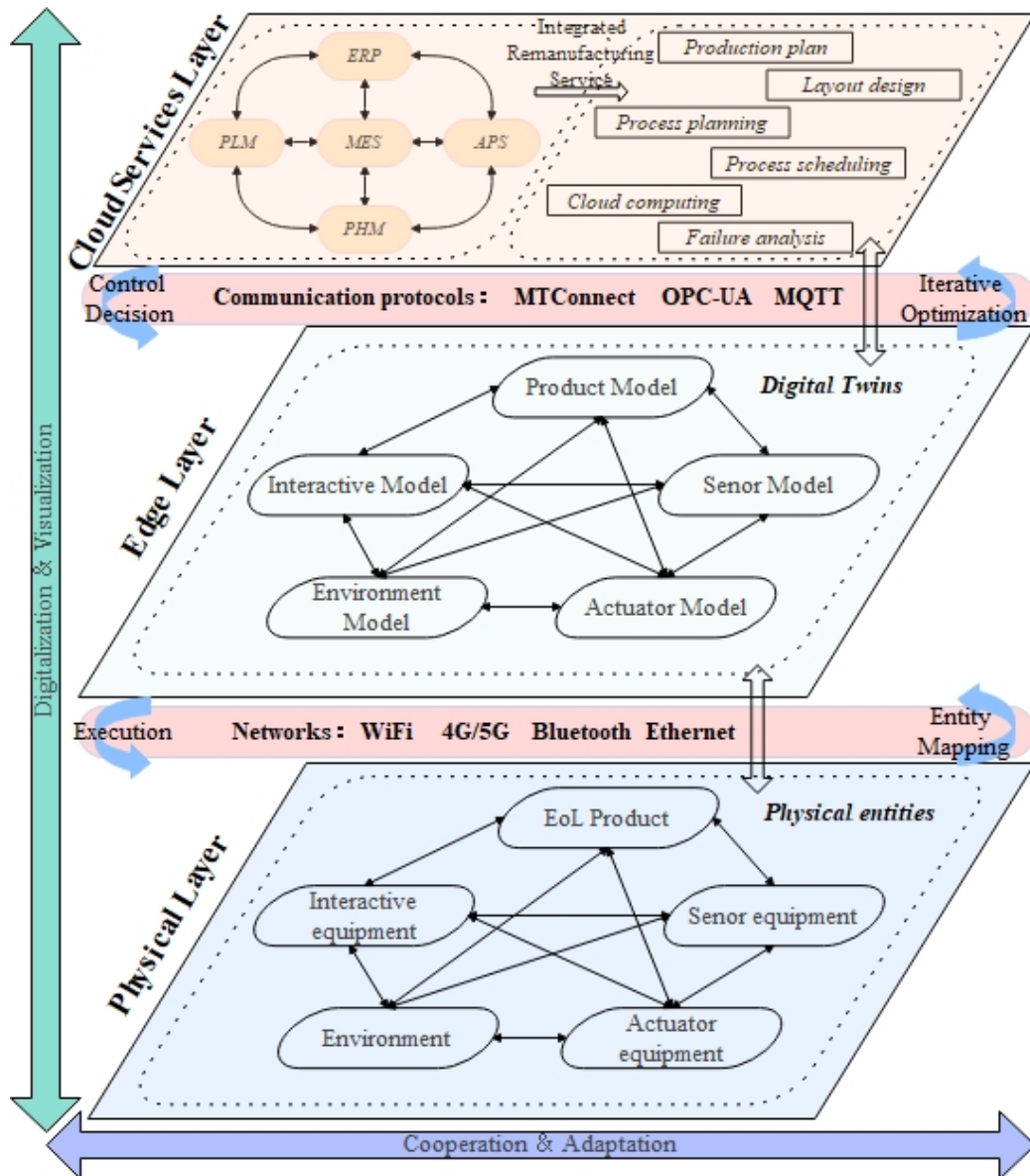


Figure 3.2: The structure of proposed CPRS.

bill of materials (BOM), which lists the categories and quantities of raw materials vital for disassembly. Additional static data encompass

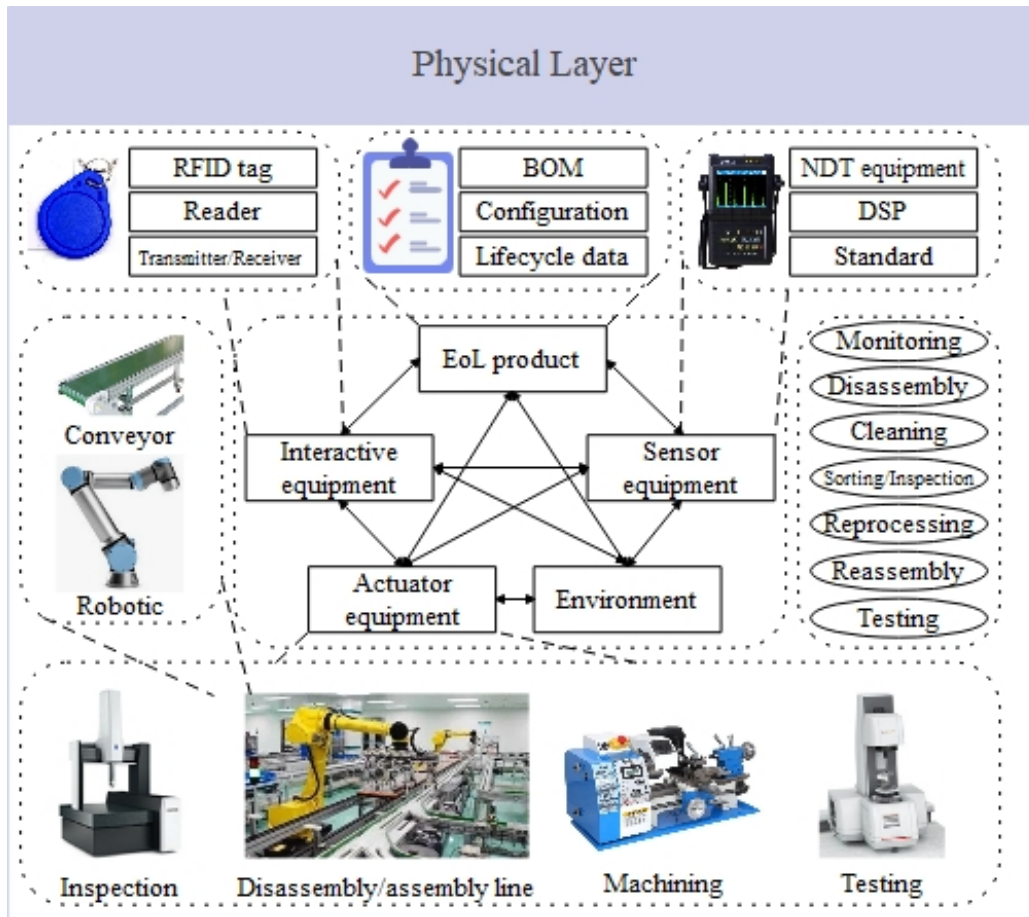


Figure 3.3: Physical layer of CPRS.

geometric parameters and constraints among the product components. Dynamic data, on the other hand, typically encapsulate life-cycle information detailing maintenance types and components, which are crucial for the inspection processes in remanufacturing. However, not all collected data are beneficial for remanufacturing purposes; redundant data can obscure pertinent information and diminish the operational efficiency of the remanufacturing system. Therefore, it is imperative

to scrutinise the scope of data collection related to EoL products to support and streamline the remanufacturing process effectively.

- **Interactive equipment** plays a crucial role in enabling communication between machinery and End-of-Life (EoL) products, which otherwise lack the capability to interact autonomously. Leveraging the Internet of Things (IoT), interactive devices facilitate the establishment of interconnected systems between various pieces of machinery and EoL products. Radio-frequency identification (RFID) serves as a key example of such wireless communication technologies. It operates by identifying, reading, and transmitting stored data via radio signals without the need for direct physical contact. This technology has found extensive applications in logistics management and smart manufacturing due to its efficiency and the ability to operate without physical connectivity. RFID systems primarily utilise RFID tags, which are capable of storing and processing information that can be wirelessly transmitted and received by reading devices operating at specific radio frequencies.
- **Actuator equipment** encompasses various machinery aligned with the sequential stages of the remanufacturing process. To accommodate the diverse and increasing volume of remanufactured products, a mixed disassembly/assembly line has been implemented, which includes the integration of robotic arms to advance towards an autonomous reman-

ufacturing process. Machine tools are predominantly used for reprocessing within these systems. Additionally, the equipment designated for inspection and testing varies to suit different types of EoL products. Cleaning, however, is primarily conducted manually and thus does not involve specialised machinery equipment [152]. All actuator devices are interconnected through interactive equipment, enabling the monitoring of the remanufacturing process for EoL products.

- **Sensor equipment**, though primarily utilised in the inspection and testing phases of the remanufacturing system, extends its applications to performance assessment and prediction of components. An example of such technology is Ultrasonic Testing (UT), where the equipment comprises a probe and a sensor that collect raw digital signals. These signals are subsequently processed by a digital signal processor (DSP) to produce analogue signal data, characterised by its continuity and high resolution. Beyond Non-Destructive Testing (NDT) equipment, it is imperative to incorporate temperature and humidity sensors within the remanufacturing system. These sensors play a crucial role in monitoring the environmental conditions of the process, thereby preventing failures that could arise from adverse conditions affecting the actuator equipment.
- The **environment** constitutes a critical component that cannot be overlooked in remanufacturing systems, which represent a specialised

mode within the broader manufacturing domain. The triadic system engineering framework of "man-machine-environment" remains pivotal in these systems. Within a remanufacturing context, the environment primarily oversees and regulates factors such as temperature, humidity, and other necessary conditions for remanufacturing. Adherence to these environmental standards is essential not only for minimising wear and tear on actuator equipment but also for enhancing the quality of the remanufactured products. This integrated approach ensures that operational conditions are optimised to support the longevity and functionality of the products processed.

3.3.2 Edge Layer

Digital Twin (DT) offers a high-fidelity and precise virtual representation of the entire life-cycle of physical entities [143]. Utilising the DT model, Product Life-cycle Management (PLM) can be efficiently and cost-effectively executed in a virtual environment. Additionally, the digital twin enables the simulation, analysis, and optimisation of the physical entity.

Within the conceptual framework of the CPRS, the edge layer serves as the virtual counterpart to the physical components found in the physical layer. This includes models of EoL products, interactive devices, actuators, sensors, and the environmental conditions, as depicted in Figure 3.4.

- **Product model:** the fidelity and precision of the DT model for EoL products, which mirrors the physical attributes of these products, are

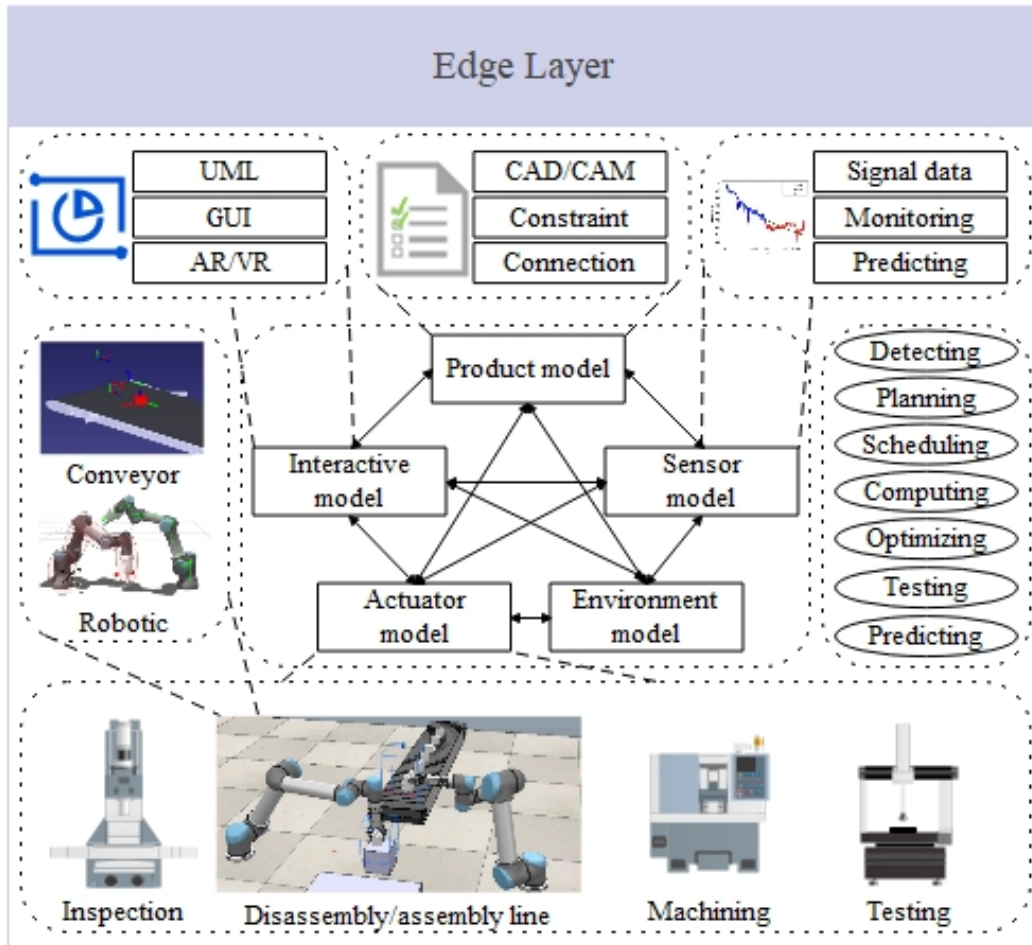


Figure 3.4: Edge layer of CPRS.

essential for the effective execution of the remanufacturing process in a virtual environment. Nonetheless, completeness in this context does not imply exhaustive information about EoL products, as extraneous data can introduce redundancy and complicate data collection efforts. The accuracy of this data is critical, as it influences the disassembly, inspection, and testing stages in remanufacturing. Consequently,

data collection should prioritise capturing the constraints, connections, and geometric parameters essential for DT modelling of EoL products within the CPRS. CAD/CAM play pivotal roles in accurately representing the constraints and connections between sub-assemblies and components of EoL products in the virtual space. These technologies are adept at conveying explicit information about EoL products. However, implicit information often remains overlooked and requires the integration of auxiliary technologies such as ontology and knowledge graphs to uncover deeper insights into the EoL products.

- The **interactive model** primarily facilitates the exchange and communication of information data between EoL products and machinery equipment. Utilising the Unified Modelling Language (UML) and Graphical User Interface (GUI), this model enables effective communication across different machinery components, allowing for the visualisation of information data flows associated with EoL product models. This approach not only streamlines interactions but also enhances the clarity and accessibility of data within the remanufacturing process.
- The **actuator model** comprises DT representations of various machinery components, including robotic arms and machine tools, derived from their corresponding physical entities. Within the edge layer of the Cyber-Physical Remanufacturing System (CPRS), this model is utilised to implement diverse processes. It is integrated with in-

teractive and sensor models to enable the detection and monitoring of status information. Furthermore, the performance of the actuator model is influenced by the environmental conditions represented within the environment model, highlighting the interconnected nature of these system components.

- The **sensor model** encapsulates signal datasets gathered from physical sensor equipment. Within the edge layer of the CPRS, these signal datasets serve distinct purposes across various stages of the remanufacturing process. Monitoring signals provide insights into the condition of EoL products, while inspection signals help identify defects and assess the state of disassembled components. Additionally, testing signals are critical for evaluating the performance of remanufactured products and predicting their life cycle. For processes such as disassembly, reprocessing, and assembly, the sensor model plays a vital role in collecting data to monitor and adjust the workflow within CPRS, ensuring efficient process management and quality control.
- The **environment model** represents the characteristic attributes of the Cyber-Physical Remanufacturing System (CPRS) across both its physical and edge layers. This model is instrumental in assessing long-term degradation and failure performance under specific conditions, which are unattainable solely through the physical layer. Moreover, the environment model benefits from iterative simulations conducted

within the virtual edge layer. These simulations enhance the model's accuracy and effectiveness, facilitating the management and optimisation of processes in the physical layer. This dual-layer approach allows for a more comprehensive analysis and optimisation of environmental impacts on remanufacturing processes.

3.3.3 Cloud Service Layer

The cloud service layer constitutes the uppermost tier of the proposed conceptual framework. This layer is characterised by its computational and optimisation capabilities, essential for the operation of the CPRS. Within this layer, there are primarily two distinct levels of cloud services: system-level strategies and workshop-level executive applications. System-level strategies facilitate Product Life-cycle Management (PLM) utilising the Digital Twin model of End-of-Life (EoL) products. In operational processes such as disassembly, reprocessing, and assembly, advanced planning and scheduling (APS), enterprise resource planning (ERP), and manufacturing execution systems (MES) are comprehensively integrated. Additionally, prognostics health management (PHM) plays a crucial role in monitoring, inspection, and testing processes. These integrated strategies interact synergistically within the system, enhancing the overall efficiency and effectiveness of the remanufacturing process.

The integrated system-level strategies are implemented within the workshop-level executive applications at the edge layer, providing tailored services for

various stages of the remanufacturing process. In the phases of disassembly, reprocessing, and assembly, these strategies facilitate the optimisation of process planning, scheduling, and resource allocation. This optimisation is necessitated by the presence of multiple disassembly routes and the constraints posed by limited machinery availability. Additionally, layout design and production planning are intricately linked to both disassembly and assembly processes.

Furthermore, cloud computing plays a pivotal role through the cloud platform in the cloud service layer, offering robust capabilities for the storage and exchange of substantial resources and computational power within the CPRS. The effectiveness of the production plan and the overall performance of the remanufacturing services in CPRS are directly influenced by these integrated remanufacturing services.

3.4 Current Challenges and Future Perspectives of CPRS

At present, the comprehensive depiction of the CPRS remains in its nascent conceptual phase, which introduces several research challenges concerning its implementation. Consequently, these challenges are articulated to delineate the future research directions for CPRS, guiding further investigation and development within this domain.

3.4.1 EoL Product Modelling for CPRS

Remanufacturing diverges significantly from traditional manufacturing processes, which are typically convergent and standardised. In remanufacturing, processes are inherently divergent and variable, influenced by the conditions of EoL products. Accurately modelling the structure and condition of EoL products is essential for the effective execution of the remanufacturing process within the CPRS. Furthermore, the scope of information modelling for EoL products, which may include details such as component materials and colours, must be carefully managed to prevent information redundancy and interference.

Consequently, the modelling of EoL products emerges as a primary research area and challenge in CPRS. The information databases for EoL products in remanufacturing must be comprehensive and enhanced through advanced technologies. These databases should also support interactivity and repeatability to facilitate the remanufacturing of similar EoL products, optimising both efficiency and efficacy in the process.

3.4.2 Process Planning and Scheduling in CPRS

Disassembly, reprocessing, and assembly are the principal operational stages within a remanufacturing system, all of which typically share resources and equipment. This sharing necessitates careful process planning and scheduling. Notably, the disassembly process functions as the inverse of assembly. Yet, for complex and multiple End-of-Life (EoL) products, the routes and

sequences of the disassembly process can vary, presenting challenges in process planning within remanufacturing contexts. Given that the availability of machinery and workforce resources in the remanufacturing process is limited, effective resource management and enhancement of production performance become crucial. Consequently, optimising process planning and scheduling through the deployment of algorithms and adapting to uncertainties emerge as significant research topics and challenges in remanufacturing.

3.4.3 Data Exchange and Communication

In the proposed framework of CPRS, various types of machinery are employed at different stages of the process. Although these machines can be interconnected through the Internet of Things (IoT), challenges arise due to potential conflicts and recognition issues stemming from the disparate protocols and data formats used by different machines. This inconsistency can lead to inefficient data transmission and exchange, subsequently impacting the overall efficacy of the CPRS. Therefore, the development of standardised and effective protocols and data formats for managing inter-machine data within CPRS represents a significant research challenge.

3.5 Chapter Summary

Chapter 3 delves into the conceptual framework of Cyber-Physical Remanufacturing Systems (CPRS), starting with an introductory overview that sets the stage for understanding the importance of remanufacturing in the current

global sustainability and circular economy context. It outlines the remanufacturing process, beginning with the collection and sorting of End-of-Life (EoL) products, followed by disassembly, cleaning, refurbishing, and reassembly into like-new condition products. This process not only extends the lifecycle of products but also significantly reduces waste and resource consumption. The chapter then progresses to articulate the conceptual framework of CPRS, which is structured into three main layers: the physical layer, where the actual remanufacturing operations occur; the edge layer, which serves as the intermediary processing stage for real-time data; and the cloud service layer, which offers a centralised platform for data analysis, storage, and the provision of computational resources. This layered architecture facilitates a seamless integration of cyber and physical realms, enabling optimised operational efficiency through advanced data analytics, artificial intelligence, and machine learning.

The latter part of the chapter addresses the current challenges and future perspectives of CPRS, highlighting three main areas: EoL product modelling for remanufacturing, process planning and scheduling in remanufacturing, and data exchange and communication between the layers. Accurate modelling of EoL products is essential for effective remanufacturing, requiring sophisticated methods to assess and categorise products based on their condition and manufacturing ability. Process planning and scheduling are critical for ensuring the efficiency and effectiveness of remanufacturing operations, demanding advanced algorithms capable of handling the complexities

and variabilities inherent in EoL products. Lastly, the chapter underscores the importance of robust data exchange and communication protocols across the physical, edge, and cloud layers to support the dynamic and interconnected nature of CPRS. Addressing these challenges is crucial for advancing the capabilities of CPRS, paving the way for more sustainable manufacturing practices and contributing to the broader goals of the circular economy.

4

A Simulated Annealing-Based Hyper-Heuristic

Algorithm for Stochastic Parallel Disassembly Line

Balancing in CPRS

4.1 Introduction

Disassembly, an essential and very first step in the remanufacturing process, serves as the reverse of the assembly process. This involves the systematic

separation and retrieve of usable and valuable sub-assemblies or components from EoL products. Traditionally, disassembly can be executed either destructively or partially to extract core components with high residual value. However, within the remanufacturing context, it is imperative that disassembly be conducted non-destructively and dismantle thoroughly of EoL products. This ensures that the remanufactured products conform to the original specifications set by the original manufacturers [153]. Consequently, the disassembly process in remanufacturing necessitates a effective and automated approach to maintain the integrity and functionality of the components.

Recent advancements in technological innovation and material invention have led to a significant increase in the volume of EoL products. Consequently, the disassembly line has been recognised as an ideal configuration for managing the disassembly of these products, adeptly addressing their complexity and the demands of large-scale operations. The disassembly line balancing problem (DLBP) involves strategically allocating sequential disassembly tasks across a series of systematically arranged workstations. This allocation is aimed at improving performance metrics such as the number of stations, workload, and idle time [154]. Optimising DLBP is crucial for enhancing the productivity and efficiency of disassembly lines, which in turn contributes to increased operational efficiency and cost reduction [155].

As the variety of EoL products expands, traditional single, straight disassembly lines are insufficient to handle the diverse and voluminous categories of these products. Different layout configurations, such as two-sided

and U-shaped arrangements, have been explored to enhance the efficiency of disassembly lines by optimising the operating times at each workstation. However, these configurations still have limitations in managing the disassembly of multiple types of EoL products simultaneously. To address this challenge, the implementation of multiple disassembly lines, including parallel disassembly line setups, has been proposed to effectively manage the disassembly processes for various types of EoL products. Currently, research on parallel disassembly lines is in its early stages, with studies not considering the uncertain factors.

Consequently, this chapter research on the concept of the workshop-level parallel disassembly line, as outlined within the comprehensive system framework of the CPRS. To enhance the overall efficiency of these parallel disassembly lines, two primary contributions are presented in this chapter.

Firstly, a mathematical model for stochastic parallel complete disassembly line balancing (DLBP-SP) is proposed. Within the remanufacturing sector, it is essential that remanufactured products meet the same performance specifications as their original products [23]. As a result, EoL products must be completely disassembled prior to entering subsequent remanufacturing processes. Given the variable condition of EoL products, the disassembly times in this model are characterised as stochastic values. The optimisation goals for the parallel complete disassembly line encompass the number of workstations, workload index, and profitability. The inherent conflict among these optimisation objectives increases the computational complexity of the

model.

Secondly, a simulated annealing-based hyper-heuristic algorithm (HH) is proposed for addressing the multi-objective optimisation challenges of the DLBP-SP. This approach integrates partially mapped crossover and single-point insertion mutation operations to adhere to precedence constraints. By employing this algorithm, both the search and solution spaces are expanded and enhanced. The efficacy and superiority of this algorithm are validated through comparative experiments using an open-source dataset and previously established optimisation algorithms. Additionally, a case study in industrial disassembly is conducted to practically apply the proposed method. This case study serves to confirm the stability and robustness of the algorithm. Notably, this case study marks the first instance of employing a gearbox as a case study within the domain of DLBP.

The subsequent parts of this chapter are structured as follows: Section 4.2 delineates the problem description, assumptions, notations, and the mathematical model of DLBP-SP, supplemented by an illustrative example. Section 4.3 details the introduction of a novel simulated annealing-based hyper-heuristic algorithm, including an overview of its framework and the operational processes involved. Section 4.4 executes comparative experiments and a case study to analyse and confirm the efficiency and performance of the proposed algorithm. Finally, Section 4.5 offers a summary of this chapter.

4.2 Stochastic Parallel Disassembly Line Balancing Problem

4.2.1 Description of DLBP-SP

Figure 4.1 introduces the standard layout of a parallel disassembly line, consisting of two adjacent lines, labelled 1 and 2, designed to disassemble EoL products A and B concurrently. These products are conceptualised as layered industrial assemblies, with product A comprising five components and product B consisting of six components. In this setup, components shaded darker are prioritised for disassembly. Following disassembly, components are individually routed to subsequent remanufacturing processes. The sequence of disassembly adheres to a logical and feasible order, conforming to the precedence constraints imposed by the physical structure of the products. Complete disassembly, as shown for both EoL products A and B in Figure 4.1, entails the total separation of a product into its constituent components [156].

Workstations 1, 2, and 3 are sequentially placed between the parallel disassembly lines, designed to handle disassembly tasks from either or both lines. Initially, Workstation 1 undertakes the first two disassembly tasks for product A and the first disassembly task for product B. Subsequently, Workstation 2 is responsible for the next three disassembly tasks of product A and the following two disassembly tasks of product B, with both workstations

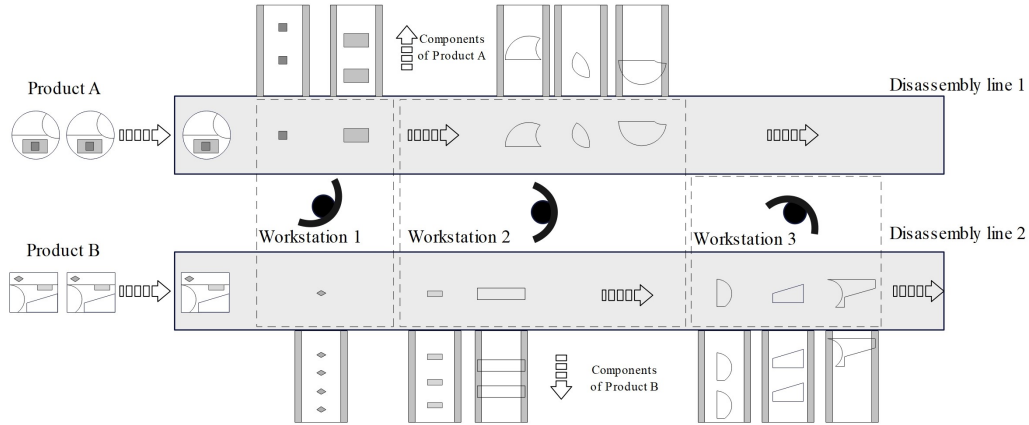


Figure 4.1: Parallel disassembly lines.

operating tasks across both lines. In contrast, Workstation 3, solely operating on disassembly line 2, handles the final three disassembly tasks of product B. Tasks are distributed among different workstations based on an optimisation algorithm to manage the disassembly of various EoL products.

This configuration allows for the simultaneous disassembly of multi-type products on parallel disassembly lines, where cycle times can be individually tailored for each line to enhance operational efficiency and flexibility. Furthermore, optimising the cycle times can reduce the idle periods of workstations, thereby improving overall efficiency.

4.2.2 Notations and Assumptions of DLBP-SP

In this subsection, the optimisation of the complete disassembly process for two distinct EoL products on parallel disassembly lines is examined. To develop a more applicable mathematical model for the stochastic parallel complete disassembly line balancing (DLBP-SP), various fundamental notations

are introduced. These notations are defined and described in Table 4.1.

Table 4.1: Definition and description of notations.

Notations	Definition and Description
m	Number of disassembly line, $m = 1, 2$
i_m	Number of disassembly tasks on disassembly line m , $i = 1, 2, \dots, I$, where I is the number of components of EoL product
K	Number of workstations, $k = 1, 2, \dots, K$, where K is the maximum number of workstations
j	The position of the disassembly process, $j = 1, \dots, J$, where J is the maximum number $J = I$.
r_i	Revenue from disassembly task i
C_w	Fix operation cost per unit time for workstations
C_p	Operating cost of workstations for parallel disassembly lines
C_c	Operating cost of workstations for single disassembly line
CT_m	Cycle time of disassembly line m
CT	Cycle time of parallel disassembly lines
T_k	Operation time of workstation k
ε_m	Coefficient value of CT and CT_m
\tilde{t}_{im}	Stochastic disassembly time of task i on disassembly line m
μ_{im}	Average disassembly time of task i on disassembly line m
σ_{im}^2	Variance of task i on disassembly line m
$1 - \alpha$	Confidence level
φ	Standard normal distribution function
LB	Theoretical minimum number of workstations
I	Workload smoothness index
P	Overall profit from complete disassembly process
$PAND(i_m)$	The set of <i>AND</i> predecessors of task i on disassembly line m
$POR(i_m)$	The set of <i>OR</i> predecessors of task i on disassembly line m
x_{ijm}	$= \begin{cases} =1, & \text{if task } i \text{ at position } j \text{ on line } m \\ =0, & \text{otherwise} \end{cases}$
y_{ijmk}	$= \begin{cases} =1, & \text{if task } i \text{ at position } j \text{ on line } m \text{ is assigned to workstation } k \\ =0, & \text{otherwise} \end{cases}$
S_k	$= \begin{cases} =1, & \text{if workstation } k \text{ is working on single disassembly line} \\ =0, & \text{otherwise} \end{cases}$
P_k	$= \begin{cases} =1, & \text{if workstation } k \text{ is working on parallel disassembly line} \\ =0, & \text{otherwise} \end{cases}$
Z_k	$= \begin{cases} =1, & \text{if workstation } k \text{ is available} \\ =0, & \text{otherwise} \end{cases}$

Drawing on the fundamental notations, a set of preliminary assumptions

has been established to facilitate the formulation of the mathematical model for the DLBP-SP.

1. Two disassembly lines are designed to be adjacent and parallel, and the workstations are located sequentially between them.
2. The cycle time of each disassembly line is pre-defined and can be different.
3. Workstations are operated by skilled workers who can work on single or both parallel disassembly lines and spend no travel time.
4. The workstations can only be allocated and process a single disassembly task at a time.
5. The precedence constraints and mean disassembly time of each disassembly task are known. Moreover, the precedence constraints of disassembly tasks should be satisfied during the disassembly process.
6. The EoL products are completely disassembled into their simplest single components. The revenue from each disassembled component is known.
7. Each disassembly task's actual process time is stochastic, following the standard normal distribution.
8. The sum of the actual process time of assigned disassembly tasks to a workstation should not exceed the cycle time. If exceeded, the number

of workstations should be added for taking the remaining disassembly tasks into new cycle time.

9. Materials and instruments are sufficient and infinite.

4.2.3 Mathematical Model of DLBP-SP

Using the established notations and assumptions, the parallel disassembly line balancing model with stochastic process times is formulated. This model is based on the defined common cycle time of the parallel disassembly lines, the multiple optimisation objectives, and the lower boundary conditions of the DLBP-SP. To demonstrate the application and functionality of the proposed mathematical model, an illustrative example is provided.

Cycle Time of Parallel Disassembly Lines

Cycle time is defined as the total elapsed time from the process beginning to the stop end of a workstation, which is pre-defined on the disassembly line [157]. Reflecting the unique attributes of parallel disassembly lines, each line's cycle time (CT_m) can be identical or distinct. To facilitate management and enhance the overall efficiency of parallel disassembly lines, a common cycle time (CT) is utilised. Drawing on the methodologies outlined in [158], this subsection employs the modified least common multiple (LCM) approach. The procedural steps of the LCM method tailored for the DLBP-SP are detailed as follows:

- Step 1: Determine the *LCM* as the common cycle time (CT) of two

different disassembly lines:

$$CT = [CT_1, CT_2], m = 2; \quad (4.1)$$

Step 2: Calculate the coefficient values ε_m by dividing each cycle time of the disassembly line (CT_m) by the common cycle time (CT):

$$\varepsilon_m = CT/CT_m; \quad (4.2)$$

Step 3: Modifying the stochastic process time of each disassembly line (\tilde{t}_{im}) into parallel disassembly lines based on the coefficient values ε_m :

$$\tilde{t}_{im} = N(\mu_{im}, \sigma_{im}) \quad (4.3)$$

$$\tilde{t}'_{im} = \varepsilon_m \cdot \tilde{t}_{im} \Rightarrow \tilde{t}'_{im} = N(\varepsilon_m \cdot \mu_{im}, \varepsilon_m^2 \cdot \sigma_{im}^2) \Rightarrow \tilde{t}_{im} = N(\mu'_{im}, \sigma'^2_{im}). \quad (4.4)$$

In the proposed DLBP-SP model, the calculated common cycle time (CT) and the updated stochastic process time (\tilde{t}'_{im}) are incorporated. This process will be further elucidated through an illustrative example.

Optimisation Goals of DLBP-SP

Generally, the objective of disassembly line balancing is to plan the allocation and optimise the sequence of disassembly tasks to enhance overall performance, with key performance indicators including productivity, efficiency, and profitability. In this context, to assess and validate the optimisation per-

formance, three optimisation objectives for DLBP-SP are considered in this subsection: the number of workstations (K), the workload smoothness index (I), and profit (P). The equations used to represent the multi-objective optimisation of DLBP-SP are presented below:

$$f_1 = \min(K) = \sum_{k=1}^K \max_{i=1}^I \left(\sum_{m=1}^M \sum_{j=1}^J x_{ijm} y_{ijmk} \right) \quad (4.5)$$

$$f_2 = \min(I) = \sqrt{\sum_{k=1}^K (CT - T_k)^2} \quad (4.6)$$

$$f_3 = \max(P) = \sum_{m=1}^M \sum_{i=1}^I r_i x_{ijm} - C_s \sum_{j=1}^J S_k - C_p \sum_{j=1}^J P_k - (CT \cdot C_w) \sum_{k=1}^K Z_k \quad (4.7)$$

$$F = \min [f_1, f_2, -f_3] \quad (4.8)$$

Equation 4.5 calculates the minimum number of workstations required, while Equation 4.6 assesses the smoothness index of workload distribution, aiming for minimisation. Equation 4.7 quantifies the maximum profit achievable through the comprehensive disassembly of various EoL products. Equation 4.8 encapsulates the multi-objective optimisation goals of the DLBP-SP, targeting the optimal solution that simultaneously minimises the number of workstations and workload while maximising profit.

The optimisation process for these multiple objectives may encounter inherent constraints and conflicts, where enhancing one objective could potentially compromise another. It is often impractical to achieve an optimal so-

lution that simultaneously optimises all objectives to their fullest extent. To address this, a Pareto optimal solution—also referred to as a non-dominated solution—is employed to evaluate the optimisation outcomes with the intent of achieving the best possible multi-objective performance [159]. The set of Pareto optimal solutions represents the boundary of optimal solutions, beyond which no objective can be improved without degrading another. The multi-objective optimisation equations must also adhere to the following constraint equations:

$$\sum_{k=1}^K y_{ijmk} \leq 1, \forall i \in I, j \in J \quad (4.9)$$

$$\sum_{m=1}^M \sum_{i=1}^{I_m} x_{ijm} y_{ijmk} \geq 1, \forall k = 1, 2, \dots, K \quad (4.10)$$

$$y_{ijmk} \leq \sum_{o=1}^k y_{ijmo}, \forall i \in I, k \in K, o \in PAND(i) \quad (4.11)$$

$$y_{ijmk} \leq \sum_{o=1}^k \sum_{o \in OR(i)} y_{ijmo}, \forall i \in I, k \in K, o \in OR(i) \quad (4.12)$$

$$\sum_{m=1}^M \sum_{k=1}^K \sum_{i=1}^I T_k x_{im} \leq CT, \forall i \in I, j \in J, k \in K \quad (4.13)$$

$$x_{ijm}, y_{ijmk}, Z_k \in \{0, 1\}, \forall m, i, k \quad (4.14)$$

Equation 4.9 specifies that each disassembly task may only be assigned to one workstation at any given time. Equation 4.10 confirms that there are no workstations remaining idle. Equation 4.11 stipulates that a disassem-

bly task can only be assigned once all preceding tasks, linked by an *AND* relationship, have been completed. Conversely, Equation 4.12 allows a disassembly task to be allocated if at least one of its predecessors, connected through an *OR* relationship, has been assigned. Equation 4.13 ensures that the total estimated uncertainty and processing time for all tasks assigned to a workstation do not exceed the defined cycle time. In Equation 4.14, the decision variables are defined as binary (0 or 1).

Definition of Lower Bound

The concept of the lower bound was initially introduced by Gökçen et al. [160] as a theoretical construct representing the minimum number of stations required to balance a parallel assembly line under specific conditions. The original lower bound (LB_o) is calculated using the following formula:

$$LB_o = \left\lceil \sum_{m=1}^M \frac{\sum_{i=1}^{I_m} \mu_{im}}{CT_m} \right\rceil, LB_o \in N^+ \quad (4.15)$$

In Equation 4.15, the term μ_{im} denotes the deterministic component that represents the average disassembly time. However, if the disassembly time is treated as a stochastic variable, as Özcan discussed [158], the lower bound (LB) for the proposed DLBP-SP model is modified accordingly, as shown in Equation 4.16.

$$LB = \left\lceil \sum_{m=1}^M \frac{\sum_{i=1}^{I_m} \mu_{im} + \varphi^{-1}(1 - \alpha) \sqrt{\sum_{i=1}^{I_m} \sigma_{im}^2}}{CT_m} \right\rceil, LB \in N^+ \quad (4.16)$$

In this equation, the disassembly time is treated as a stochastic variable, following a standard normal distribution. In practical applications, disassembly times may increase due to unpredictable factors such as tool malfunctions or components sticking, leading to a potential surpass the workstation's cycle time by the total disassembly time of the tasks assigned to it. To account for this, a confidence level $(1 - \alpha)$ is employed to quantify the probability that the total stochastic disassembly time of the assigned tasks remains within the workstation's cycle time. Following the approach from Özcan [158], this subsection adopts confidence levels of 0.9 and 0.975. Additionally, the random variances in disassembly tasks are generated and categorised into low variance $([0, (\mu_{im}/4)^2])$ and high variance $([0, (\mu_{im}/2)^2])$, serving as the initial parameters for the comparative experiments discussed in Section 4.4.

The Explanatory Example

In this subsection, a detailed example is presented to demonstrate the proposed mathematical model for the DLBP-SP. The parallel disassembly line presented in Figure 4.1 serves as the basis for this example, with the pre-determined cycle time for each disassembly line (CT_m) and relevant data on various EoL products provided in Tables 4.2 and 4.3. The analysis assumes

low task variances for the disassembly tasks, allowing for the calculation of cycle time (CT) and coefficient values (ε_m) using the Least Common Multiple (LCM) method as derived from Equations 4.1 to 4.4. The adjusted information for products A and B on the parallel disassembly lines is summarised in Table 4.4.

Table 4.2: The information of product A on disassembly line 1.

Cycle Time of Disassembly Line 1 (CT_1)		15				
Task ID (i_1)		1	2	3	4	5
Average disassembly time (μ_{i1})		4	6	3	4	2
Variance (σ_{i1}^2)		0.50	1.20	0.70	0.60	0.20
Precedence constraints		-	1	1, 2	1, 2	1, 2

Table 4.3: The information of product B on disassembly line 2.

Cycle Time of Disassembly Line 2 (CT_2)		20					
Task ID (i_2)		1	2	3	4	5	6
Average disassembly time (μ_{i2})		3	4	2	6	7	4
Variance (σ_{i2}^2)		0.40	0.30	0.10	1.20	1.50	0.30
Precedence constraints		-	1	1, 2	1, 2, 3	1, 2	1, 2, 3, 4

Table 4.4: The modified information of product A and B on parallel disassembly lines.

$CT = 60$											
$\varepsilon_1 = 4, \varepsilon_2 = 3$											
TaskID	A1	A2	A3	A4	A5	B1	B2	B3	B4	B5	B6
μ'_i	16	24	12	16	8	9	12	6	18	21	12
$\sigma_i^{2'}$	8.00	19.20	11.20	9.60	3.20	3.60	2.70	0.90	10.80	13.50	2.70

The minimum number of workstations is determined to be 3, based on the calculation from Equation 4.15. Table 4.5 presents a feasible optimal disas-

sembly sequence, along with the corresponding task allocation and operating rate.

Table 4.5: A feasible disassembly sequence of the DLBP-SP.

Number of Workstation	1			2			3				
Sequential task ID	A1	B1	A2	B2	B3	A3	A4	A5	B4	B5	B6
μ	16	9	24	12	6	12	16	8	18	21	12
i	8.00	3.60	19.20	2.70	0.90	11.2	9.60	3.20	10.80	13.50	2.70
Sum of	49			54			51				
Operating rate (%)	76.67			90.00			85.00				

This disassembly sequence obtains the theoretical minimum number of workstations, qualifying it as one of the potential optimal solutions. However, this solution is not unique. When considering the operating rate as an additional optimisation objective, it may no longer remain optimal. Conversely, if both the number of workstations and the operating rate are optimised simultaneously, this solution could be considered a Pareto optimal solution. To address this multi-objective optimisation, the following subsections will introduce the proposed HH algorithm.

4.3 The Proposed Hyper-Heuristic Algorithm for DLBP-SP

This section introduces the novel simulated annealing-based hyper-heuristic algorithm (HH). The process begins with the representation and encoding of the precedence constraints of EoL products using a precedence graph. Following this, the operational procedure and framework of the proposed HH

are described in detail. Lastly, the decoding process is outlined to illustrate the multi-objective optimisation results achieved by the HH algorithm.

4.3.1 Encoding Strategy

All feasible disassembly sequences are required to comply with the precedence constraints of EoL products. Following the approach from Bentaha et al. [161], a precedence graph is utilised to construct the precedence matrix, ensuring adherence to these constraints and facilitating the generation of a feasible initial solution. The precedence matrix for EoL products is defined using binary variables to represent the precedence relationships among the components of EoL products. As illustrated in Equation 4.17, the precedence matrix for an EoL product on disassembly line m is denoted as P_m :

$$P_m = [P_{ijm}]_{(N_m * N_m)}, \forall i, j = 1, 2, \dots, N_m; m = 1, 2, \dots, M \quad (4.17)$$

As shown in Equation 4.18, P_{ijm} represents the precedence relationship between disassembly task i and task j . The equation must satisfy the decision variable:

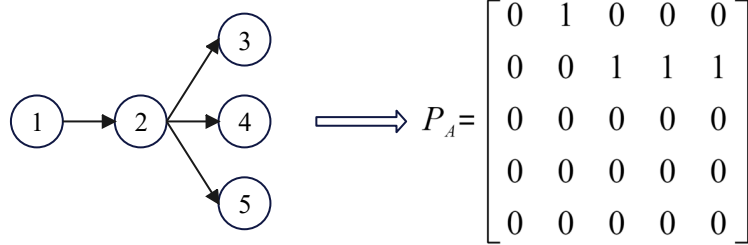
$$P_{ijm} = \begin{cases} = 1, & \text{if task } i \text{ immediate predecessor of task } j \\ = 0, & \text{otherwise} \end{cases} \quad (4.18)$$

Different EoL products are associated with varying precedence constraints. To effectively manage these constraints within the context of the DLBP-SP, a composite precedence matrix is developed. This matrix represents the relationships among the different EoL products, as depicted in Equation (4.19) [45]:

$$P^* = \begin{bmatrix} P_1 & 0 & 0 & 0 & 0 \\ 0 & \dots & 0 & 0 & 0 \\ 0 & 0 & P_m & 0 & 0 \\ 0 & 0 & 0 & \dots & 0 \\ 0 & 0 & 0 & 0 & P_M \end{bmatrix} \quad (4.19)$$

The composite precedence matrix P^* is structured as a diagonal matrix, where the precedence matrices for the various EoL products are placed sequentially along the diagonal, while all other elements in P^* are zero matrices.

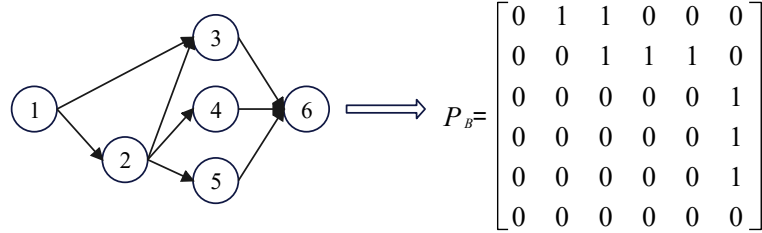
For instance, in the illustrative example, the precedence graphs and corresponding precedence matrices for EoL products A and B are depicted in Figure 4.2. The resulting composite precedence matrix P^* is presented in Equation 4.20.



(a) Precedence graph

(b) Precedence matrix

(A) The precedence graph and matrix of product A.



(a) Precedence graph

(b) Precedence matrix

(B) The precedence graph and matrix of product B.

Figure 4.2: The precedence graph and matrix of product.

$$P^* = \begin{bmatrix} \begin{bmatrix} 0 & 1 & 0 & 0 & 0 \\ 0 & 0 & 1 & 1 & 1 \\ 0 & 0 & 0 & 0 & 0 \\ 0 & 0 & 0 & 0 & 0 \\ 0 & 0 & 0 & 0 & 0 \end{bmatrix} & 0 \\ 0 & \begin{bmatrix} 0 & 1 & 1 & 0 & 0 & 0 \\ 0 & 0 & 1 & 1 & 1 & 0 \\ 0 & 0 & 0 & 0 & 0 & 1 \\ 0 & 0 & 0 & 0 & 0 & 1 \\ 0 & 0 & 0 & 0 & 0 & 1 \\ 0 & 0 & 0 & 0 & 0 & 0 \end{bmatrix} \end{bmatrix} \quad (4.20)$$

The composite precedence matrix serves as the foundational input for generating the initial solution in DLBP-SP. The steps involved in identifying a feasible disassembly sequence are outlined below, based on the illustrative example:

Step 1: Identify the disassembly tasks that do not have any predecessor tasks, designating them as priority tasks. In this case, the priority disassembly tasks would be A_1 or B_1 .

Step 2: Once all priority disassembly tasks have been assigned, update the composite precedence matrix accordingly. For example, prior to assigning task A_1 , the original matrix element $P^*(A_1, A_2)$ equals 1. After assigning task A_1 , the updated matrix element $P^{*'}(A_1, A_2)$ becomes 0. Additionally, the upper-left sub-matrix becomes zero, allowing it to be removed during the disassembly task sequencing process.

Step 3: Randomly select the next disassembly tasks from those that do not have *AND* predecessor tasks or have *OR* predecessor tasks, such as A_2 or B_2 .

Step 4: Repeat steps 2 and 3 until the composite precedence matrix P^* is reduced to $P^* = [0]$. At this point, all disassembly tasks in the DLBP-SP will have been assigned and sequenced.

In the example provided, Table 4.5 illustrates one possible disassembly sequence for the DLBP-SP. Although the constraints and components for products A and B are relatively simple, the sequencing process becomes increasingly complex as the scale of EoL products grows.

4.3.2 Procedure of Proposed Hyper-Heuristic Algorithm

Distinct from conventional heuristic approaches, hyper-heuristics represent a systematic method designed to select or create heuristics that effectively address multi-objective optimisation challenges [162]. Typically, the structure of a hyper-heuristic framework facilitates the deployment of a high-level heuristic algorithm (HLH), which orchestrates an array of low-level heuristic algorithms (LLHs) to derive the best possible solution [163].

Low-Level Heuristic Algorithms

LLHs are crucial elements within the HH framework, significantly influencing its complexity and effectiveness. In the design of LLHs, it is imperative to adopt principles that are straightforward yet robust, to enhance the overall efficacy of HH. This section utilises three distinct types of heuristic algorithms as LLHs: the non-dominated sorting genetic algorithm 2 (NSGA2), strength Pareto evolutionary algorithm 2 (SPEA2), and multi-objective evolutionary algorithm based on decomposition (MOEAD). Each of these algorithms possesses unique strengths and limitations.

1. NSGA2 [164]: employs rapid sorting and an elitist strategy to enhance the algorithm's convergence and precision, while introducing a crowding distance measure to ensure diversity and even distribution of solutions. NSGA2 demonstrates robust convergence capabilities in addressing multi-objective optimisation problems. Nevertheless, it is observed that the distribution of optimal solutions produced by NSGA2 lacks

uniformity.

2. SPEA2 [165]: utilises a fitness assignment strategy coupled with density information, making it well-suited for tackling multi-objective optimisation problems. This algorithm is characterised by its rapid convergence and reduced computational complexity relative to the other algorithms discussed.
3. MOEAD [166]: reformulates multi-objective optimisation problems into several sub-scalar problems, each defined by a uniformly distributed weight vector. It addresses each sub-scalar problem using an aggregation function to optimise the overarching multi-objective challenges. However, among the low-level heuristic algorithms discussed, MOEAD exhibits the highest computational complexity.

The chosen three types of LLHs are comparatively straightforward and apt for use within the HH framework. Each LLH necessitates the implementation of crossover and mutation processes to manipulate initial solutions and produce a set of optimal solutions. The following subsection incorporates the use of partially mapped crossover and single-point insertion mutation specifically for the DLBP-SP scenario.

Partially Mapped Crossover

Generally, the random crossover method is preferred for its simplicity in producing offspring solutions from optimal parental configurations. However,

within the DLBP-SP context, this method may lead to infeasible solutions that breach precedence constraints, thereby diminishing the effectiveness of LLHs. Consequently, this subsection adopts the partially mapped crossover method to enhance the performance of LLHs.

Consider the previous illustrative example where the operation of partially mapped crossover is depicted in Figure 4.3. In this method, any two feasible solutions may serve as parents, with the mapping section established between two randomly selected crossover points. Within the exchange mapping section, a list for swapping is chosen, such as $B_2 \leftrightarrow A_3, A_5 \leftrightarrow A_4$. Subsequent steps involve updating individuals that present conflicts according to the mapping list, while non-conflict individuals are directly copied from their respective parents. Ultimately, this process results in the generation of offspring solutions.

Single-Point Insertion Mutation

Like the crossover operation, traditional random mutation methods often result in the creation of infeasible solutions. According to Wang et al. [45], the single-point insertion mutation method enhances the performance of LLHs.

Illustrating this process, Figure 4.4 demonstrates the operation of single-point insertion mutation. A mutation point, such as B_3 , is chosen randomly. Subsequently, the predecessor and successor tasks, B_2 and B_6 respectively, are identified. The chosen point, B_3 , must then be positioned either after B_2 or before B_6 . In the original parental solution where B_3 follows B_2 , the only

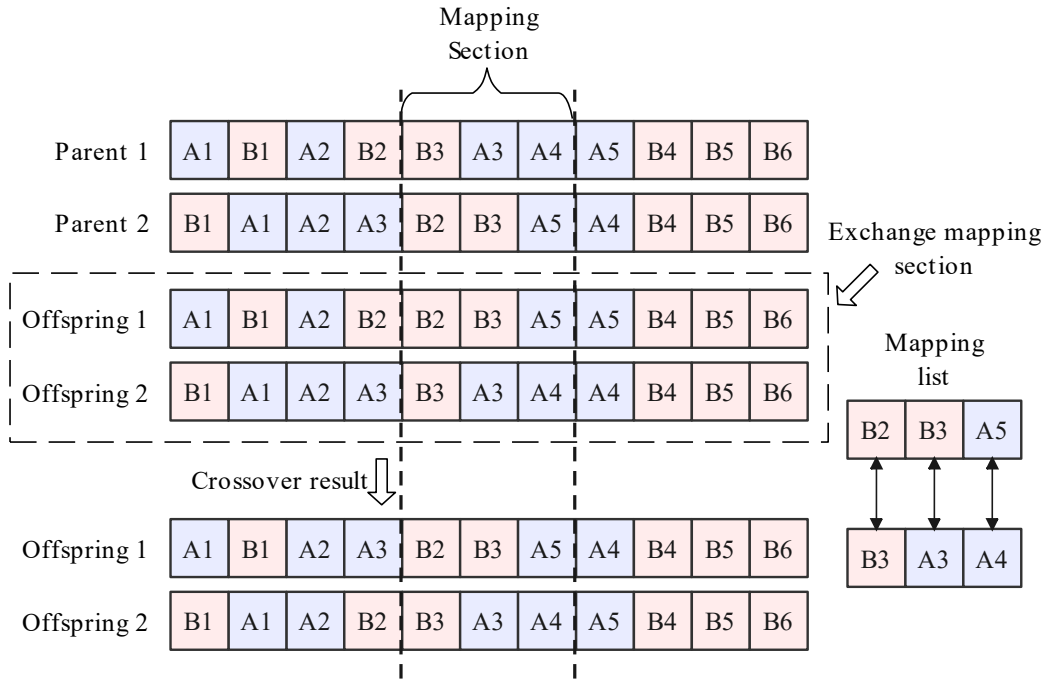


Figure 4.3: Operation process of the partial mapped crossover.

feasible offspring solution positions B_3 immediately before B_6 .

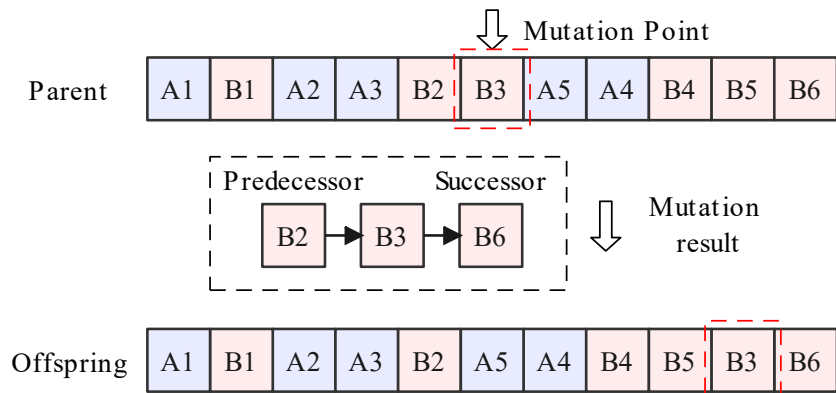


Figure 4.4: Operation process of single-point insertion mutation.

4.3.3 Simulated Annealing Based High-Level Heuristic Algorithm

The HLH is a critical element that significantly impacts the overall effectiveness of a HH system. The choice of an appropriate high-level strategy is crucial for addressing optimisation problems effectively. Presently, HLHs are classified into four main categories based on their operational mechanisms: random selection, greedy strategy, meta-heuristic algorithms, and learning methods [167]. In this subsection, the simulated annealing algorithm (SA) is utilised as the HLH for the DLBP-SP scenario.

The SA algorithm is proficient in handling complex, parallel multi-objective optimisation problems. It is noted for its straightforward computational complexity and exhibits considerable robustness and versatility. However, the efficacy of the SA algorithm is contingent upon the initial values and pre-defined parameters; it also has a comparatively slow convergence rate. Employing SA as the HLH in a HH framework can effectively circumvent local optima and achieve superior global solutions by coordinating multiple solution spaces derived from LLHs. The methodology for the SA-driven HH is outlined in Algorithm 1.

4.3.4 Decoding Process

The decoding process involves assigning optimally sequenced disassembly tasks to workstations while adhering to the cycle time constraints of DLBP-

Algorithm 1 Proposed SA based HH.

Input: Objective Function, F ; Crossover, p_c ; Mutation, p_m ; Initial temperature, T_0 ; Stopping temperature, T_f ; Cooling rate, α ; Initial population, P_0 ; Iteration time, K ; Precedence matrix, P^* ; Population size, N

Output: Optimal solution set, S_*

```

1:  $t \leftarrow 0$ 
2: Random generate  $N$  individuals as the initial population
3: while  $t \leq K$  or  $S_t \neq S_{t-1}$  do
4:   for  $i = 1$  to  $N$  do
5:     Generate initial solution sets  $S_0$  through mapping, crossover ( $p_c$ )
     and mutation ( $p_m$ ) based on LLHs ( $H_i$ )
6:     while  $T_0 \geq T_f$  do
7:       Randomly select a heuristic  $h_i \in H_i$ , combine  $S_0$  to generate
       new solution sets through neighborhood mutation  $S_i$ , Calculate  $\Delta E_k =$ 
        $F(S_1) - F(S_0)$ 
8:       if  $\Delta E_k \geq 0$  then
9:          $S_* = S_1$ 
10:      else
11:        generate a random number  $x \sim U(0, 1)$ 
12:        if  $x < \exp(-\Delta E_k/t)$  then
13:           $S_* = S_1$ 
14:        else
15:           $S_* = S_0$ 
16:        end if
17:      end if
18:    end while
19:  end for
20:   $t = t + 1$ 
21: end while

```

SP. As the illustrative example and optimal sequences in Table 4.5, under specific conditions, the optimal minimum number of workstations is 3. The sequences of disassembly tasks allocated to each workstation are as follows: $K_1 = A_1 \rightarrow B_1 \rightarrow A_2$, $K_2 = B_2 \rightarrow B_3 \rightarrow A_3 \rightarrow A_4 \rightarrow A_5$, and

$K_3 = B_4 \rightarrow B_5 \rightarrow B_6$. According to the non-deterministic polynomial (NP) characteristic of DLBP-SP, the optimal solution is not identical.

4.4 Computational Experiments

This section presents a comparative experiment and a case study. Initially, the comparative experiment involves assessing the performance of the proposed HH against existing algorithms using benchmark test datasets. Subsequently, a case study focusing on two types of industrial splitter gearboxes is introduced. The outcomes of both the comparative experiment and the case study are analysed and discussed in this section. The implementation of the proposed HH was carried out using Python on a computer equipped with an Intel(R) Core(TM) i7-9700K CPU at 3.6 GHz and 32 GB of RAM.

4.4.1 Comparison Experiment

The proposed HH algorithm is evaluated in comparison with existing methods. Specifically, it is benchmarked against the Tabu search algorithm (TS) designed for addressing the stochastic parallel assembly line balancing problem as introduced from Özcan [158], and the genetic simulated annealing algorithm (GSA) developed for solving the partially parallel stochastic disassembly line balancing problem (DLBP), as introduced from Wang et al. [45].

Description of The Experiment Dataset

The benchmark datasets utilised in this experiment are sourced from Özcan [158], encompassing 16 distinct named datasets, including those labelled as Jaeschke, Jackson, etc. Each dataset comprises a varying number of disassembly tasks, precedence constraints, and average process times for each task. To suit applications in parallel disassembly lines, problems were generated by pairing datasets with themselves and with other datasets (e.g., Jaeschke-Jaeschke, Jackson-Jaeschke). This experiment considers 31 different experimental problems, with a total of 372 experiments conducted using various indicators such as cycle times (CT_1 , CT_2), the number of tasks (N_1 , N_2), task variances, and confidence levels (0.9 and 0.975). The primary optimisation objective in these computational experiments is the number of workstations (N). Comparative results for the TS and GSA algorithms are derived from references [45, 158].

Results and Analysis

The findings of the computational experiments are detail presented in Tables 4.6 and 4.8. The proposed HH algorithm consistently achieves solutions that are nearly identical to those of the existing algorithms under conditions of low task variance, but with limited enhancements. Specifically, the HH's rates of obtaining identical solutions compared to the TS and GSA under low task variance are 87.10% and 84.94% versus 73.12% and 80.64%, respectively. Conversely, under high task variance conditions, the HH algorithm

demonstrates significant improvement, achieving better solutions at rates of 89.24% and 97.84% compared to 86.02% and 97.84% for TS and GSA, respectively. These results suggest that the HH algorithm performs comparably to TS and GSA under low variance conditions, where the limited variety and search space for mean disassembly times facilitate the attainment of optimal solutions. Under high variance conditions, the expanded search space enables the HH to outperform, confirming its superior efficacy in more complex scenarios.

To assess the effectiveness of the proposed HH algorithm, the gap percentage (%Gap) from the LB , defined as $LB = \frac{Min(K)-LB}{LB}$, has been introduced. A lower %Gap indicates that the computed outcomes are closer to the theoretical minimum number of workstations, reflecting the performance of the optimisation algorithm. According to the data presented in Table 4.8, the %Gap from LB for confidence levels $(1 - \alpha) = 0.9$ and $(1 - \alpha) = 0.975$ under low task variance are 9.37% and 14.29%, respectively. Under conditions of high task variance, these gaps are 7.63% and 13.17%.

Comparative analysis with the TS and GSA algorithms shows that under low task variance, the %Gap from the HH algorithm exhibits marginal improvements. However, under high task variance, the %Gap reductions are more significant: 9.2% for $(1 - \alpha) = 0.9$ and 8.86% for $(1 - \alpha) = 0.975$ relative to TS, and 10.88% for $(1 - \alpha) = 0.9$ and 17.84% for $(1 - \alpha) = 0.975$ compared to GSA. These results not only highlight the HH algorithm's superior performance in challenging scenarios but also its consistency across different

task variances, demonstrating its stability.

The outcomes of the computational experiments substantiate that the proposed HH algorithm is validated and demonstrates suitability for complex and uncertain environments.

Table 4.6: Computational results (Part 1).

Problem	N1	N2	CT ₁	CT ₂	Low task variances								High task variance									
					(1 - α) = 0.9				(1 - α) = 0.975				(1 - α) = 0.9				(1 - α) = 0.975					
					LB	TS	GSA	HH	LB	TS	GSA	HH	LB	TS	GSA	HH	LB	TS	GSA	HH		
Jaeschke-Jaeschke	9	9	10	14	7	8	8	8	8	10	9	7	11	10	8	8	13	13	10			
					10	10	8	10	10	9	12	12	12	8	14	14	10	10	15	15	12	
					18	10	7	7	7	7	7	7	8	8	7	9	9	8	8	11	11	9
Jackson-Jaeschke	11	9	10	10	14	8	9	9	9	8	11	10	10	8	11	11	10	8	13	13	11	
					10	10	9	12	12	12	9	14	14	14	9	14	14	12	10	15	15	14
					21	18	5	5	5	5	5	6	6	6	6	6	6	6	6	6	7	7
Jackson-Jackson	11	11	10	13	9	11	11	11	9	12	12	12	9	11	11	11	9	14	13	12		
					14	14	8	9	9	8	8	9	9	8	8	9	9	8	8	10	10	9
					21	14	7	7	7	7	7	7	7	7	7	7	7	7	7	7	8	8
Roszieg-Jackson	25	11	18	21	11	11	11	11	11	12	12	12	11	13	12	11	11	14	13	12		
					21	21	10	10	10	10	10	11	10	10	10	11	10	10	10	12	12	11
					25	14	10	10	10	10	10	11	11	11	11	11	11	11	11	10	12	12
Roszieg-Roszieg	25	25	18	25	14	14	14	15	14	15	15	15	14	16	16	15	14	17	17	16		
					21	21	13	15	14	15	14	16	15	15	14	16	16	15	14	18	17	16
					32	25	11	11	11	11	11	11	11	11	11	11	11	11	11	11	13	12
Sawyer-Roszieg	30	25	41	32	13	15	14	14	13	15	15	15	14	16	15	15	14	17	17	15		
					47	25	14	14	14	14	14	15	15	15	14	16	15	14	14	18	17	15
					54	21	13	14	14	14	14	15	15	15	14	16	15	14	14	18	17	15
Sawyer-Sawyer	30	30	36	41	18	21	20	21	18	22	22	22	19	24	22	21	19	27	26	23		
					36	36	19	22	22	23	19	24	24	25	20	25	24	23	20	28	28	25
					75	54	11	12	12	12	11	13	13	13	12	13	13	12	12	14	14	13
Gunther-Sawyer	35	30	61	75	14	15	15	15	14	16	16	16	14	17	16	15	14	19	18	16		
					69	54	14	16	15	16	14	17	17	15	18	17	16	15	20	19	17	
					81	36	16	19	18	19	16	20	19	20	17	21	20	19	17	24	23	20
Gunther-Gunther	35	35	61	69	17	19	19	19	17	20	20	20	17	22	21	19	17	25	24	21		
					69	69	16	18	17	18	16	19	19	19	16	20	20	18	16	24	22	19
					81	61	15	17	17	17	16	18	18	18	16	20	19	18	16	23	22	19
Kilbridge-Gunther	45	35	79	81	14	15	15	15	15	16	16	16	15	17	17	15	15	19	19	16		
					69	69	17	18	18	18	17	19	19	19	17	20	19	18	17	22	22	20
					184	61	12	13	13	13	12	14	14	14	13	15	15	13	13	17	16	14
Kilbridge-Kilbridge	45	45	79	184	11	12	12	12	12	12	12	12	12	12	12	12	12	13	13	12		
					92	92	13	14	14	14	14	15	15	15	14	15	15	14	14	16	16	15
					138	110	10	10	10	10	11	11	11	11	11	11	11	11	11	11	12	12
Hahn-Kilbridge	53	45	2338	92	13	14	14	14	14	14	15	15	15	14	15	15	14	14	16	16	15	
					2004	69	16	18	18	18	17	19	19	19	17	19	19	18	17	21	21	19
					2338	184	10	10	10	11	11	11	11	11	11	11	11	11	11	11	12	12
Hahn-Hahn	53	53	2004	4676	11	12	12	12	11	13	13	13	12	13	13	12	12	14	14	13		
					2806	2806	11	12	12	12	11	13	12	12	12	13	12	12	12	14	15	13
					4676	3507	8	8	8	8	8	9	8	8	9	9	9	9	9	9	9	9

4.4.2 Case Study

This subsection implements the proposed HH algorithm for the multi-objective optimisation of the DLBP-SP involving two similar types of gearboxes from

Table 4.7: Computational results (Part 2).

Problem	N1	N2	CT ₁	CT ₂	Low task variances								High task variance							
					(1- α) = 0.9				(1- α) = 0.975				(1- α) = 0.9				(1- α) = 0.975			
					LB	TS	GSA	HH	LB	TS	GSA	HH	LB	TS	GSA	HH	LB	TS	GSA	HH
			293	2004	20	22	22	23	16	24	24	24	21	25	25	23	21	28	27	24
Tonge-Hahn	70	53	410	2806	14	13	13	16	14	14	14	17	15	14	14	16	15	16	16	17
			468	3507	12	13	13	13	12	14	14	14	13	14	14	13	13	16	16	14
			364	410	19	21	21	21	19	22	22	22	19	23	23	21	19	26	26	22
Tonge- Tonge	70	70	468	468	16	17	17	17	16	18	18	18	16	19	19	17	16	21	21	18
			527	293	19	22	22	22	19	23	23	23	20	24	24	22	20	27	27	23
			50	320	42	55	50	55	42	63	62	64	43	63	62	56	43	71	67	65
Wee-Mag-Tonge	75	70	52	364	40	48	45	48	40	57	55	57	40	60	56	54	40	66	62	61
			54	527	35	42	40	41	36	49	44	48	35	54	48	41	36	58	56	53
			50	56	57	77	67	77	57	95	90	95	58	103	98	79	59	113	109	98
Wee-Mag-Wee-Mag	75	75	52	52	58	82	74	81	58	104	103	105	60	107	104	82	60	113	112	107
			56	54	54	67	65	67	55	83	76	82	55	97	91	69	57	108	106	85
			5048	50	45	59	54	58	46	67	63	65	47	70	63	60	47	74	72	68
Arcus83-Wee-Mag	83	75	5408	54	42	50	49	50	42	56	55	56	43	62	60	51	44	70	69	58
			5853	56	39	47	46	47	39	51	49	51	40	58	54	48	41	66	61	51
			5048	5408	29	34	34	34	29	36	35	36	31	38	37	34	31	43	42	36
Arcus83- Arcus83	83	83	6883	6883	22	25	25	25	22	26	26	26	24	28	28	25	24	31	31	27
			8898	6309	20	23	23	23	20	24	24	24	22	26	26	24	22	29	29	25
			110	6309	29	31	31	31	29	33	33	33	29	35	35	31	29	39	38	33
Lutz3-Arcus83	89	83	127	7571	25	27	26	27	25	28	28	28	25	29	29	27	25	32	32	28
			150	8898	21	22	22	22	21	23	23	23	21	24	24	22	21	27	27	23
			110	150	28	30	30	30	28	32	32	32	28	33	33	31	28	37	37	32
Lutz3- Lutz3	89	89	118	118	30	33	33	33	30	35	34	35	30	37	36	33	30	41	40	35
			137	127	27	29	29	29	27	31	31	31	27	32	32	29	27	36	36	31
			301	137	28	30	30	30	28	32	32	32	28	33	33	31	28	37	37	32
Mukherje-Lutz3	94	89	324	118	29	31	31	31	29	33	33	33	29	35	35	32	29	39	38	34
			351	150	25	26	27	26	25	28	28	28	25	29	29	27	25	32	32	28
			301	301	29	33	33	33	29	35	35	35	30	36	36	33	30	40	40	35
Mukherje- Mukherje	94	94	301	351	27	30	30	30	27	32	32	32	28	33	33	30	28	37	37	32
			351	324	26	29	29	29	26	31	31	31	27	32	32	29	27	36	35	31
			8847	301	32	36	36	36	32	39	38	39	33	40	40	37	33	45	45	39
Arcus111- Mukherje	111	94	9400	324	30	34	34	34	30	36	36	36	31	38	37	34	31	42	42	36
			10027	351	28	31	31	31	28	33	33	33	29	35	34	32	29	39	38	33
			8847	9400	34	39	39	34	42	41	42	35	44	43	40	40	35	49	48	42
Arcus111- Arcus111	111	111	11378	11378	28	31	31	31	28	33	32	33	28	33	33	31	28	37	37	33
			17067	10743	23	26	26	26	23	28	28	28	24	29	29	26	24	32	32	28
			564	11378	25	26	26	26	25	28	28	28	25	29	29	26	25	31	31	28
Bartholdi-Arcus111	148	111	705	11570	22	24	24	24	22	25	25	25	23	26	26	24	23	28	28	25
			805	7571	28	31	31	31	28	33	33	33	28	35	34	31	28	37	38	33
			513	564	22	23	24	23	22	24	25	24	23	25	25	23	23	27	28	24
Bartholdi- Bartholdi	148	148	626	626	19	20	20	20	19	21	21	21	20	21	22	20	20	23	23	21
			805	705	16	17	17	17	16	17	17	17	17	18	18	17	17	19	19	18
			1510	564	26	28	29	28	26	30	30	30	27	31	31	28	27	34	34	30
Lee-Bartholdi	205	148	2077	626	21	22	23	22	21	23	23	23	22	24	24	22	22	26	26	23
			2832	705	17	18	18	18	17	19	19	19	18	19	19	18	18	20	21	19
			1699	2643	23	25	25	25	23	26	26	26	23	27	27	25	23	29	29	26
Lee-Lee	205	205	2266	2266	22	23	23	23	22	23	24	24	22	24	24	23	22	26	26	24
			2832	2454	19	19	20	20	19	20	20	20	19	21	21	20	19	22	22	21
			1935	2831	46	50	50	50	46	52	52	52	46	54	54	50	46	60	60	52
Scholl-Lee	297	205	2247	1699	46	50	50	50	46	53	53	53	46	54	54	50	46	60	60	52
			2787	1510	42	45	45	45	42	47	47	47	42	49	49	45	42	53	53	47
			2049	2680	62	68	67	67	67	71	71	71	62	73	73	68	62	81	81	71
Scholl- Scholl	297	297	2111	2111	68	75	75	75	68	78	78	78	68	82	81	75	68	90	90	79
			2787	2247	58	63	63	63	58	66	66	66	58	68	68	63	58	75	74	66

Hansa Tmp Co., Ltd. The efficacy of the HH algorithm is evidenced by the number of non-dominated solutions it yields in comparison to both LLHs (NSGA2, SPEA2, and MOEAD) and the conventional SA algorithm. The

Table 4.8: Analysis of the computational results.

Computational Results analysis	VS TS				VS GAS			
	Low task variance		High task variance		Low task variance		High task variance	
	$(1-\alpha) = 0.9$	$(1-\alpha) = 0.975$						
Number of better solutions	6	9	83	91	5	1	80	91
Number of identical solutions	81	79	9	1	68	75	12	1
Number of worse solutions	6	5	1	1	20	17	1	1
Rate of better solutions (%)	6.45%	9.68%	89.24%	97.84%	5.38%	1.08%	86.02%	97.84%
Rate of identical solutions (%)	87.10%	84.94%	9.68%	1.08%	73.12%	80.64%	12.90%	1.08%
Rate of worse solutions (%)	6.45%	5.38%	1.08%	1.08%	21.50%	18.28%	1.08%	1.08%
%Gap of TS and GAS	9.67	14.37	16.83	22.03	9.51	16.98	18.51	31.01
%Gap	9.37	14.29	7.63	13.17				

advantage of the HH algorithm is particularly highlighted by its ability to generate a higher number of non-dominated solutions. Additionally, the stability and robustness of the HH algorithm are further corroborated by the hyper-volume index, reinforcing its effectiveness in handling complex optimisation scenarios.

Descriptions of The Gearboxes

Gearboxes represent a prevalent and fundamental type of industrial machinery. On one hand, most malfunctions in splitter gearboxes typically involve minor issues with a single component while the majority of primary components remain fully operational, as noted by Wang et al. [168]. On the other hand, the configuration of components within a gearbox is relatively straightforward, theoretically permitting complete disassembly without the need for destructive methods. Consequently, gearboxes hold significant potential for remanufacturing. This case study considers two similar models of gearboxes, specifically the splitter gearbox series 85000 and 90000, as detailed in Appendix 8.1.

This case study concentrates exclusively on gathering information pertinent to the disassembly process, thus it does not take into account detailed

operational parameters and data. Information on the installation of the splitter gearboxes is compiled, which includes the type and quantity of components (expressed as average disassembly process time), variance in operation times, and revenue derived from each disassembled component.

Comprehensive details on the bill of materials and associated relationship constraints of the components for these gearboxes are obtained from an open-source platform, the link to which is provided in Appendix 8.1. Moreover, the related data (mean process time and deviation) are referenced from Marruganti and Frizziero [169], where 1 time measurement unit (TMU) is proposed to represent 0.0036 seconds. Based on the open-source platform and a similar disassembly process used in this case study, the related data have been simulated and calculated, as presented in Appendix 8.1.

The splitter gearbox series 85000 comprises 30 parts, while the series 90000 contains 35 parts. The exploded views of both gearbox series are illustrated in Figure 4.5, sourced from an open-source catalogue and detailed in the materials section. The precedence constraints and disassembly sequences for the splitter gearboxes series 85000 and 90000 are developed based on the spare parts list and the manufacturing processes. The disassembly procedure is conceptualised as the reverse of the manufacturing process, with arrows in the diagrams indicating the immediate precedence of each disassembly task. This case study assumes that both series of splitter gearboxes can be completely disassembled without destructive processes. The precedence relationships for both series are depicted in Figure 4.6.

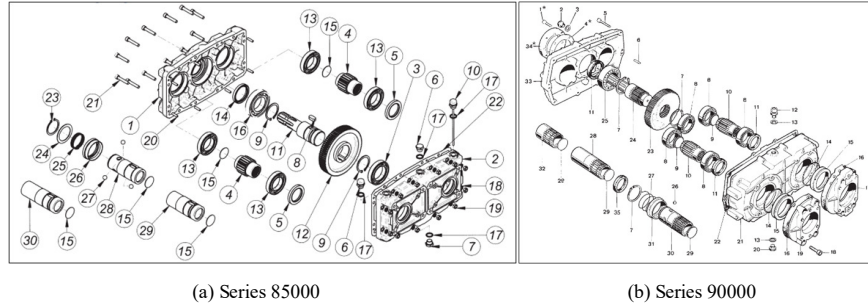


Figure 4.5: Explosion diagram of splitter gearboxes.

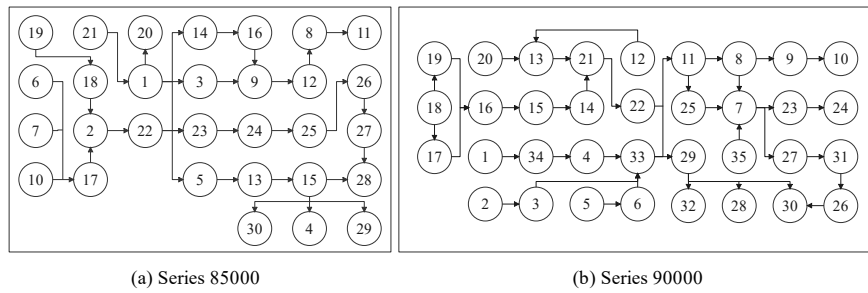


Figure 4.6: Precedence relationship of splitter gearboxes.

Experiments and Analysis

In this subsection, various combinations of cycle times for each disassembly line are established. The cycle times of each parallel disassembly line are set as $CT_1 = \{8, 27, 50, 60, 90\}$ and $CT_2 = \{10, 24, 60, 65, 108\}$, respectively. The combination of different experimental parameters is shown in Table 4.9.

For each algorithm involved in this experiment, the initial population is set to 50 individuals. The probabilities for crossover and mutation in the relevant algorithms are determined to be 0.8 and 0.2, respectively. Additionally, the initial temperature for processes requiring thermal parameters is established at 200, with a cooling rate of 0.975. The process is designed

to continue until reaching a final minimum temperature of 10.

Table 4.9: The combination of experiment parameters.

No.	CT_1	CT_2									
1	8	11	8	27	65	15	39	89	22	84	24
2	8	24	9	27	72	16	67	11	23	84	65
3	8	65	10	27	89	17	67	24	24	84	72
4	8	72	11	39	11	18	67	65	25	84	89
5	8	89	12	39	24	19	67	72			
6	27	11	13	39	65	20	67	89			
7	27	24	14	39	72	21	84	11			

Table 4.10 outlines three optimisation objectives alongside the number of non-dominated solutions derived from various experiments. It is observed that when the cycle time for one disassembly line is fixed, the required number of workstations (K) decreases as the cycle time for the other line increases. In a specific instance where both disassembly lines have the same cycle time ($CT_1 = CT_2 = 60$), the minimum workload smoothness index (I) and the maximum profit (P) are realised, highlighting a unique scenario for parallel disassembly lines. Nevertheless, there is no direct correlation between I and P ; for example, experiments 7 and 8, 13 and 14 yield similar I values but markedly different P outcomes. Additionally, three experiments resulted in costs that deem them impractical to consider further.

Moreover, a higher count of non-dominated solutions is indicative of superior performance by the optimisation algorithm. The results from Table 4.10 demonstrate that the proposed hyper-heuristic (HH) algorithm is capable of achieving a significantly greater number of non-dominated solutions, registering the highest count in 24 out of 25 experiments.

Table 4.10: Multi-objective optimisation results and the number of non-dominated solutions.

No.	CT_1	CT_2	K	I	P	MOEAD	SPEA2	NSGAI	SA	HH
1	8	10	51	781.8	359.8	6	6	7	6	7
2	8	24	39	421.3	495.8	5	5	6	5	6
3	8	60	31	1866.6	479.8	6	6	7	7	7
4	8	65	31	8127.6	79.8	6	6	7	7	7
5	8	108	29	3259.8	403.8	7	7	8	7	7
6	27	10	38	3991.9	259.8	8	8	8	8	8
7	27	24	25	620.2	443.8	5	5	5	5	5
8	27	60	16	619.8	209.8	9	9	9	9	10
9	27	65	15	1767.9	-995.2	10	10	11	11	11
10	27	108	13	102.9	671.8	6	6	7	6	7
11	50	10	33	681.2	529.8	6	6	6	6	6
12	50	24	20	1505.8	109.8	5	5	5	5	5
13	50	60	11	124.1	499.8	7	7	8	7	8
14	50	65	10	127.9	159.8	6	6	8	7	8
15	50	108	8	486.8	-1870.2	9	9	10	10	10
16	60	10	32	803.4	529.8	6	6	6	6	6
17	60	24	19	290.9	599.8	3	3	3	3	3
18	60	60	10	19.9	749.8	11	10	10	11	11
19	60	65	9	142.6	39.8	6	6	7	6	7
20	60	108	7	46.6	299.8	3	3	3	3	3
21	90	10	30	1154.6	519.8	6	6	7	6	7
22	90	24	17	797.4	379.8	6	6	6	6	6
23	90	60	8	25.3	649.8	6	6	7	6	7
24	90	65	8	256.3	-340.2	6	6	7	6	7
25	90	108	6	116.0	309.8	10	10	10	10	10
	Best number in 25 times					8	7	22	12	24
	Rate (%)					32	28	88	48	96

Tables 4.11-4.13 highlight three selected optimal solutions derived from different cycle time combinations for detailed analysis.

Table 4.11 presents an optimal solution for the cycle times $CT_1 = 50$, $CT_2 = 60$. The corresponding Gantt chart, shown in Figure 4.7, provides a visual representation of the disassembly tasks allocation. This solution achieves a minimum of 11 workstations, with workstation 6 dedicated solely to dis-

assembly line 1, while the remaining workstations serve both lines. The workload balancing index is recorded at 124.12, and the total profit from the disassembly operations amounts to 499.8. The utilisation rates of the workstations vary from 96.1% to 61.4%, with the first two workstations showing relatively lower rates due to the time-intensive nature of certain tasks (such as B5 and A21), which pose challenges in practical application. Excluding these two, the utilisation rates of the other nine workstations exceed 85%.

Table 4.11: One optimal sequence of the disassembly process ($CT_1 = 50, CT_2 = 60$).

Workstation No.	Working load balance	Profit	Time	$\Delta(\%)$	Task sequence on each workstation
1	124.12	499.8	184.2	61.4%	'A6'→'B5'→'B35'→'B2'→ 'B20'
2			239.0	79.7%	'A21'→'B6'→'A10'
3			287.5	95.8%	'B18'→'B1'→'B3'→'B34'→ 'B19'→'B12'→'B4'
4			281.0	93.7%	'A1'→'B13'→'A19'→'B33'→'A7'
5			265.5	88.5%	'B17'→'A20'→'A18'→'A17'
6			260.0	86.7%	'B16'→'B15'→'B14'→'B21'→ 'B22'→'B29'
7			288.8	96.3%	'A2'→'A22'→'A23'→'B32'→ 'A3'→'B11'→'B28'
8			271.5	90.5%	'A24'→'A14'→'A5'→'B8'
9			279.8	93.2%	'B25'→'A25'→'A16'→'B7'→ 'B23'→'B9'
10			279.2	93.0%	'A26'→'A27'→'A9'→'B24'→ 'A13'→'B27'→'A15'→'B31'→ 'A4'→'B26'→'A29'
11			289.0	96.3%	'A30'→'B30'→'A28'→'A12'→ 'B10'→'A8'→'A11'

Table 4.12 details an optimal solution derived under the condition where the cycle times for both disassembly lines are identical ($CT_1 = CT_2 = 60$), representing a unique case within parallel disassembly line configurations.

This scenario facilitates a minimum of 10 workstations. The working load balancing index is notably low at 19.87, while the total profit from the disassembly process amounts to 749.8. The utilisation rates for all workstations exceed 85.0%. The exceptionally low workload balancing index and the maximization of revenue are attributed to the uniform cycle times across disassembly lines, which allows for optimal workstation performance without inter-line conflicts.

Table 4.12: One optimal sequence of the disassembly process ($CT_1 = CT_2 = 60$).

Workstation No.	Working load balance	Profit	Time	$\Delta(\%)$	Task sequence on each workstation
1	19.87	749.8	53.0	88.3%	'A19'→'B35'→'B2'→'A6'→ 'A18'→'B1'
2			56.6	94.3%	'B5'→'A21'
3			44.6	89.2%	'A1'→'B20'→'A20'→'A7'→ 'A10'→'B18'
4			57.8	96.3%	'B17'→'B19'→'B16'→'B3'→ 'B6'→'B34'
5			57.6	96.0%	'A17'→'A2'→'B4'→'B12'→ 'B15'→'A22'→'A14'→'B13'
6			51.0	85.0%	'A23'→'B3'→'B14'→'B21'→ 'A5'→'A24'→'A13'→'A3'→ 'A15'
7			55.4	92.3%	'A16'→'A4'→'A9'→'A25'→ 'A29'→'A30'→'A12'→'A8'
8			58.4	97.3%	'B22'→'B11'→'B29'→'A26'→ 'B28'→'A27'→'B25'
9			49.2	82.0%	'A28'→'B32'→'B8'→'B9'→ 'A11'
10			53.8	89.7%	'B7'→'B27'→'B31'→'B10'→ 'B23'→'B24'→'B26'→'B30'

Table 4.13 outlines an optimal solution for the cycle times $CT_1 = 90$, $CT_2 = 108$, which represent the longest duration considered in this case study. This

configuration results in a minimum of six workstations, a working load balancing index of 115.97, a total profit from the disassembly process of 309.8, and workstation utilisation rates ranging from 96.1% to 76.6%. When compared to the scenario with cycle times $CT_1 = 50, CT_2 = 60$, there is a slight reduction in the working load balance and a decrease in overall profit. This comparison suggests that longer cycle times do not necessarily enhance performance, as they can lead to prolonged operational duration without necessarily improving workstation utilisation rates. Therefore, it is crucial to carefully determine the cycle times for each parallel disassembly line during the initial design phase, particularly in the context of disassembling EoL products.

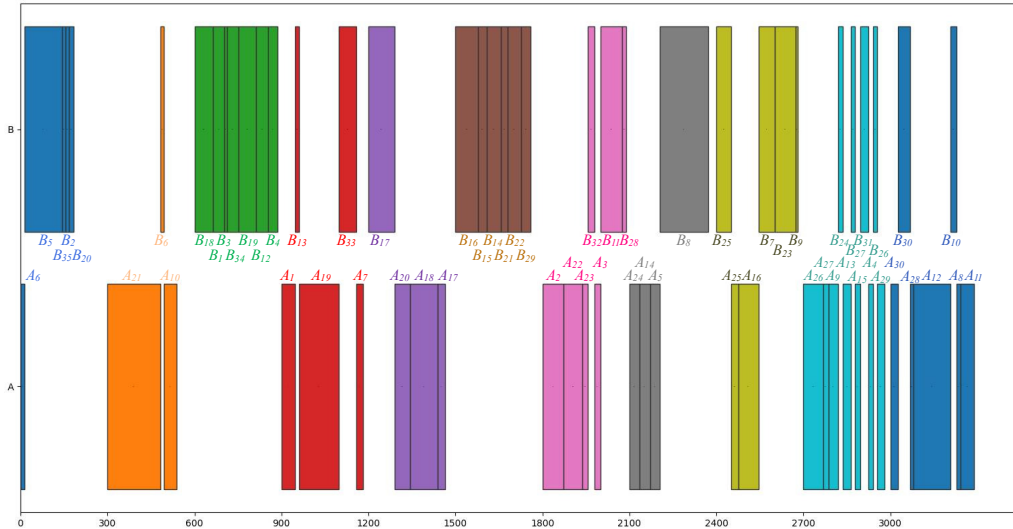


Figure 4.7: The Gantt chart of optimal solution ($CT_1 = 50, CT_2 = 60$).

Additionally, this case study utilises the hypervolume index as a metric

Table 4.13: One optimal sequence of the disassembly process ($CT_1 = 90, CT_2 = 108$).

Workstation No.	Working load balance	Profit	Time	$\Delta(\%)$	Task sequence on each workstation
1			490.9	90.9%	'B5'→'A19'→'B12'→'B6'→ 'B1'→'A7'→'A10'→'B18'
2	115.97	309.8	508.1	94.1%	'B17'→'A21'→'A18'→'A1'→ 'B34'→'B20'→'B2'→'B13'→ 'B35'
3			512.2	94.9%	'B4'→'B19'→'B16'→'B3'→ 'A6'→'A20'→'A17'→'B15'→ 'B14'→'B33'→'A2'→'B21'
4			519.1	96.1%	'B22'→'B29'→'B11'→'B28'→ 'B25'→'A22'→'B8'→'A14'→ 'B9'→'B32'
5			481.4	89.1%	'A16'→'B10'→'A3'→'B7'→ 'B23'→'A9'→'B24'→'A23'→ 'B27'→'A24'→'A25'→'A26'→ 'A5'
6			413.8	76.6%	'A12'→'A13'→'B31'→'A15'→ 'B26'→'B30'→'A30'→'A8'→ 'A11'→'A29'→'A27'→'A4'→ 'A28'

to assess the efficacy of the proposed HH algorithm. The hypervolume index quantifies the volume encompassed by the hypercube formed between individual points in the solution set and a reference point within the target space [170]. This metric is particularly apt for evaluating both the convergence and the distribution of solution sets derived from multi-objective optimisation algorithms. Superior performance of the algorithm is indicated by a higher average hypervolume value and a reduced number of outliers, reflecting better convergence and uniform distribution of solutions.

From the analysis of three disassembly schemes described earlier, the re-

sults for three hypervolume indices are depicted in Figure 4.8. The data illustrate that the HH algorithm consistently achieves superior outcomes, devoid of outliers within its solution sets. The performance of low-level heuristic algorithms appears comparable, indicating a minimal performance disparity among them, with the basic SA algorithm outperforming these lower-level heuristics. The extent of convergence and distribution is represented by the span of the box plot. Among all evaluated algorithms, the HH algorithm demonstrates the most effective convergence and the most uniform distribution.

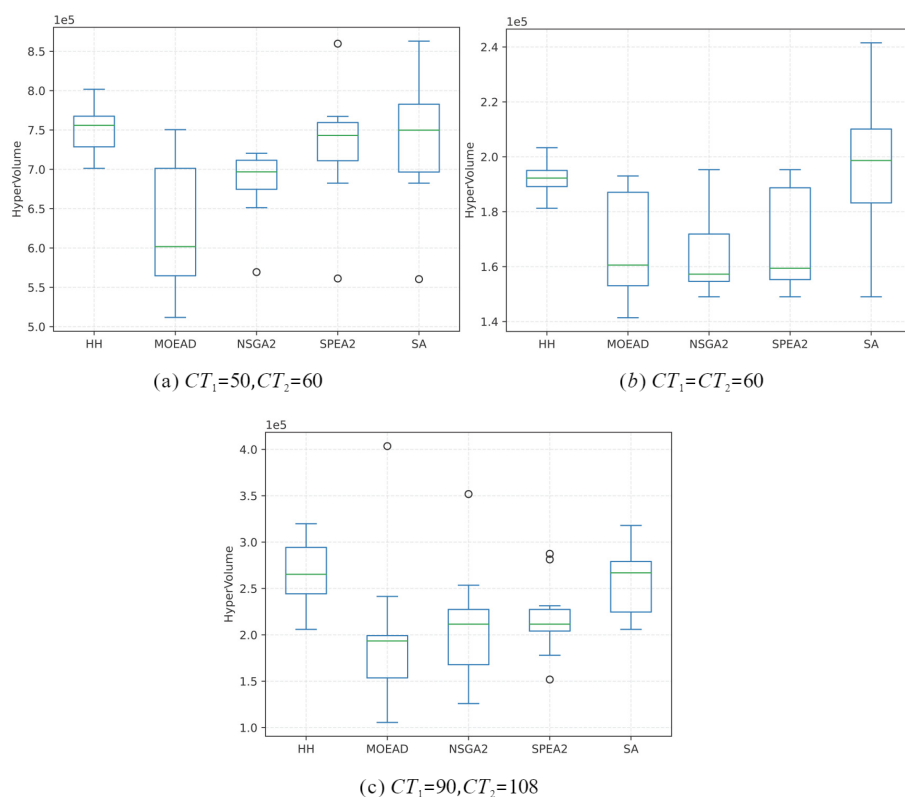


Figure 4.8: Box plots of hypervolume.

Experiments Discussion and Conclusion

In conclusion, the effectiveness and superior performance of the proposed HH algorithm are confirmed through comparative analysis with both the TS and GSA. Employing two types of splitter gearboxes as a case study, the HH algorithm was utilised for multi-objective optimisation in the disassembly of industrial equipment. The algorithm's enhanced performance is substantiated by the quantity of non-dominated solutions it produces. Furthermore, evaluations using the hypervolume index demonstrate the HH algorithm's stability and robustness relative to low-level heuristic algorithms and the simulated annealing (SA) algorithm.

The primary aim of this section is to propose the mathematical model and develop a methodology to optimise the DLBP-SP, setting a foundation for implementing parallel disassembly lines in practical settings. Nevertheless, the current approach has limitations, notably the absence of dynamic planning and real-time monitoring capabilities. Recent advancements in sensing technologies present opportunities to enhance the intelligence and efficiency of these parallel disassembly lines. For instance, mobile visual sensor systems could be incorporated for real-time monitoring, allowing for the detection of anomalies and failures that facilitate dynamic planning and further optimisation of the disassembly processes [171]. Additionally, the integration of autonomous robotics, automated guided vehicles (AGVs), and smart sensor devices holds considerable promise. As described by Indri et al. [172], a vir-

tual sensor network could be embedded into parallel disassembly lines to aid in manual robot guidance and collision detection. This network, equipped with a variety of physical sensors like light beamers, vision sensors, and HD cameras, could offer real-time decision-making capabilities to enhance operational efficiency. Future research will explore the integration of these varied sensing technologies into the proposed methodology.

4.5 Chapter Summary

This chapter presents a workshop-level demonstration of the proposed conceptual framework of CPRS. The introduced HH algorithm effectively manages the disassembly sequencing and optimises associated objectives for a diverse and substantial quantity of EoL products. There are two main research contributions:

Firstly, this chapter develops the mathematical model of DLBP-SP in remanufacturing context. This model more accurately reflects the uncertainties inherent in EoL products by incorporating stochastic disassembly times. An illustrative example underscores the complexity involved in managing stochastic parallel disassembly lines and highlights the necessity for advanced algorithms that optimise key performance metrics like cycle time and throughput.

Secondly, the other contribution of the chapter details the specialised HH algorithm proposed for DLBP-SP, describing its distinctive elements such as the encoding strategy, the algorithm's procedural framework, and the

integration of low-level heuristic algorithms with innovative operations like partially mapped crossover and single-point insertion mutation. The simulated annealing-based high-level heuristic algorithm plays a crucial role in efficiently navigating the solution space, employing a temperature-controlled exploration process that adeptly balances between exploration and exploitation. The decoding process is intricately detailed, illuminating how solutions are translated into practical adjustments on the parallel disassembly lines.

Subsequent computational experiments validate the proposed HH algorithm's effectiveness, featuring comparative analyses with existing methods and a case study on gearbox disassembly that collectively highlight the algorithm's enhanced performance in optimising disassembly line configurations under uncertain conditions. The comparison experiment results show that under low task variance, the rates of obtaining identical solutions are 87.10%, 84.94%, and for high task variance, the rates of achieving better solutions are 89.24%, 97.84%, respectively, compared to the TS and GSA algorithms, confirming the algorithm's validity and superiority.

Furthermore, the case study in this chapter is pioneering in applying the DLBP-SP to gearboxes, demonstrating their suitability for complete non-destructive disassembly. The research outlines the potential to extend and adapt this approach to design parallel disassembly lines for a vast array of gearbox types within remanufacturing systems. The multi-objective optimisation performed in the case study involving two gearbox types shows that the proposed HH algorithm produces the highest number of non-dominated

solutions relative to four other basic algorithms. Additionally, the hyper-volume index box plots of the proposed algorithm show the highest mean number and absence of noise points, evidencing improved stability and convergence. The versatility of the proposed HH solution is further validated across both single and multiple optimisation problems.

5

An ontology and rule-based method for human-robot collaborative disassembly planning in CPRS

5.1 Introduction

Unlike the advanced automation and intelligence characterising assembly processes, disassembly operations remain nascent, largely due to unpredictable variations in quality and failure mechanisms inherent in EoL products [173]. Consequently, there is significant value in developing models and manage-

ment strategies for these EoL products. Most disassembly operations are currently performed manually, resulting in inefficiencies and elevated costs. The incorporation of industrial robots into these processes is seen as a potential solution to enhance both automation and intelligence. Industrial robots, known for their precision, sensitivity, and consistency, excel at executing basic and repetitive tasks in disassembly, ensuring uniform performance [174]. Nevertheless, these robots have not yet achieved the capability to completely eliminate the need for human intervention in the disassembly process [175]. In cases involving complex or ambiguous tasks, the inflexible nature of robot operations, combined with a lack of situational awareness, can lead to the inadvertent damage of valuable components, diminishing their remaining value [176].

Within the scope of modern semi-automatic manufacturing, HRCD has emerged as an optimal approach. In this paradigm, industrial robots are deployed for basic and repetitive tasks, simultaneously aiding humans with more complex disassembly activities [177]. Human operators, equipped with comprehensive information about EoL products, are able to make informed, adaptive decisions that facilitate the seamless execution of tasks, thus enhancing overall disassembly efficiency [178]. The HRCD method leverages the strengths of both human and robotic capabilities, advancing automation and intelligence while retaining essential flexibility and adaptability [179]. This collaborative model effectively mitigates the uncertainties inherent in disassembly processes, thereby improving operational efficiency.

Nevertheless, HRC D sequence planning encounters several obstacles:

1. The variability and unpredictability of EoL products mean that existing product information models are inadequate and not effectively tailored for HRC D applications. There is an absence of a standardised, universal model that can efficiently encapsulate the diversity of EoL products.
2. Presently, common strategies for devising and identifying the optimal disassembly sequence typically employ heuristic optimisation algorithms. These algorithms, however, yield results and procedural steps that are challenging to interpret and confirm as optimal. It would be more beneficial to develop a new, structured, and easily interpretable method that ensures optimal planning and execution of disassembly sequences and schemes.
3. Disassembly itself is a divergent process, involving the breakdown of EoL products into subassemblies or components, which can often be conducted simultaneously. Within the HRC D framework, various disassembly approaches may be applied to each individual task. Consequently, there exists a plethora of potential disassembly methods and sequences, complicating the identification of the most suitable scheme, particularly for complex EoL products.

To overcome these challenges, this chapter concentrates on the individual-level of CPRS, introducing a general ontology model and a rule-based approach for the HRC D sequence planning of EoL products.

The proposed disassembly-related ontology model captures and stores knowledge pertinent to each component of EoL products, offering a standardised and structured framework for knowledge representation in human-robot collaborative disassembly. This facilitates the systematic organisation and management of disassembly knowledge, allowing for rapid extraction from extensive data associated with EoL products. Building on this foundation, a Semantic Web Rule Language (SWRL) rule-based reasoning method for HRCd has been developed. This method determines the precedence constraints and potential disassembly methods for each task, leading to the formulation of an optimal disassembly plan. To demonstrate the practicality of these methods, the chapter includes a case study on the HRCd planning of a gearbox. The comprehensive workflow of this chapter is depicted in Figure 5.1.

The subsequent sections of this chapter are structured as follows: Section 5.2 details the development of the ontology for human-robot collaborative disassembly and outlines the semantic model for EoL products. Section 5.3 explicates the established rules for reasoning and formulating the optimal disassembly scheme. Section 5.4 showcases a case study that evaluates the viability and effectiveness of the proposed methodology. A summary of this chapter is provided in Section 5.5.

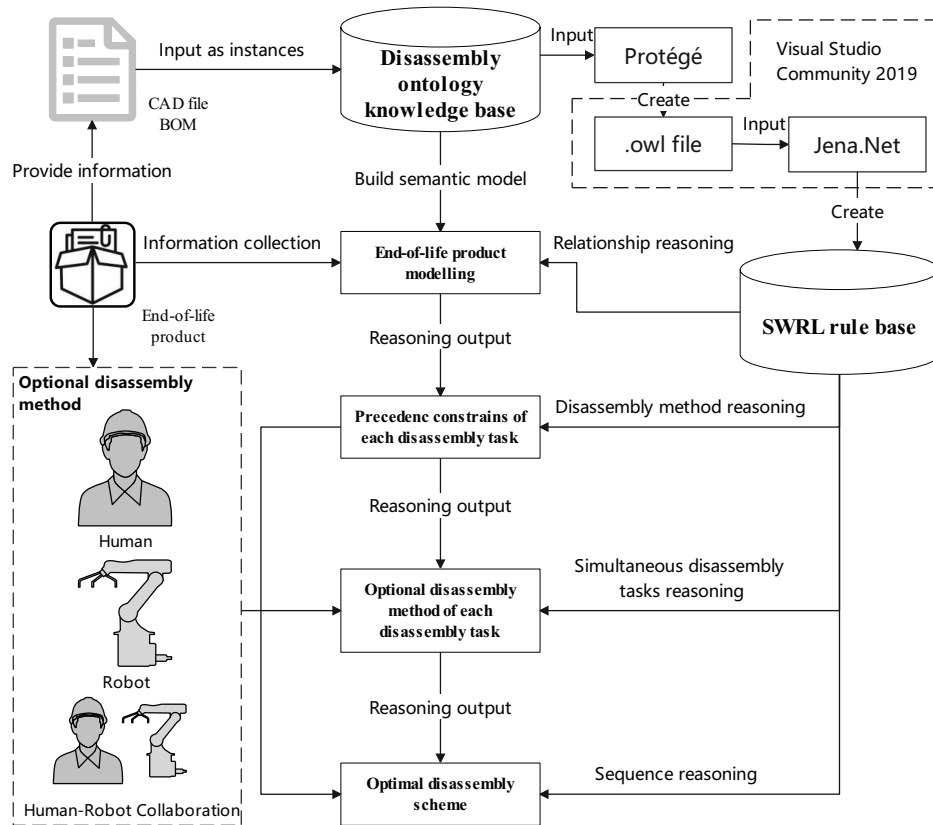


Figure 5.1: Overall workflow of this chapter.

5.2 HRC Product Disassembly Ontology and Product Semantic Model

This subsection introduces the ontology for HRC product disassembly. It formalises and semantically represents information related to the disassembly processes of EoL products.

5.2.1 The Proposed HRCO Ontology

A domain ontology is crafted to encapsulate the knowledge within a specific area, providing a semantic framework that details the concepts and their interrelations within that domain [180]. The primary objective of constructing such an ontology is to consolidate related knowledge, which aids in resolving ambiguities and reducing redundancies across concepts and terminologies. This type of ontology fosters a standardised, shared, and comprehensive understanding of the domain-specific knowledge [181]. The development process of an ontology involves delineating a set of classes, object properties, and data properties [182]. Classes are defined as collections of instances that exhibit common properties or characteristics. These classes are linked and interact via object properties. Instances, which are the core elements of the ontology model, act as the objects [183].

The class hierarchy within the proposed ontology for HRCO is illustrated in Figure 5.2. At the apex of this hierarchy sits the class designated as *owl:Thing*, which encompasses all conceivable entities. This ontology introduces twelve subclasses under *owl:Thing*, each specifically devised to encapsulate the knowledge pertinent to HRCO. These subclasses provide a structured vocabulary and framework for the upper ontology, rooted in essential concepts.

Two subclasses are proposed to describe the EoL product-level structure:

1. *Product* (p) denotes an abstract concept encompassing a set of EoL

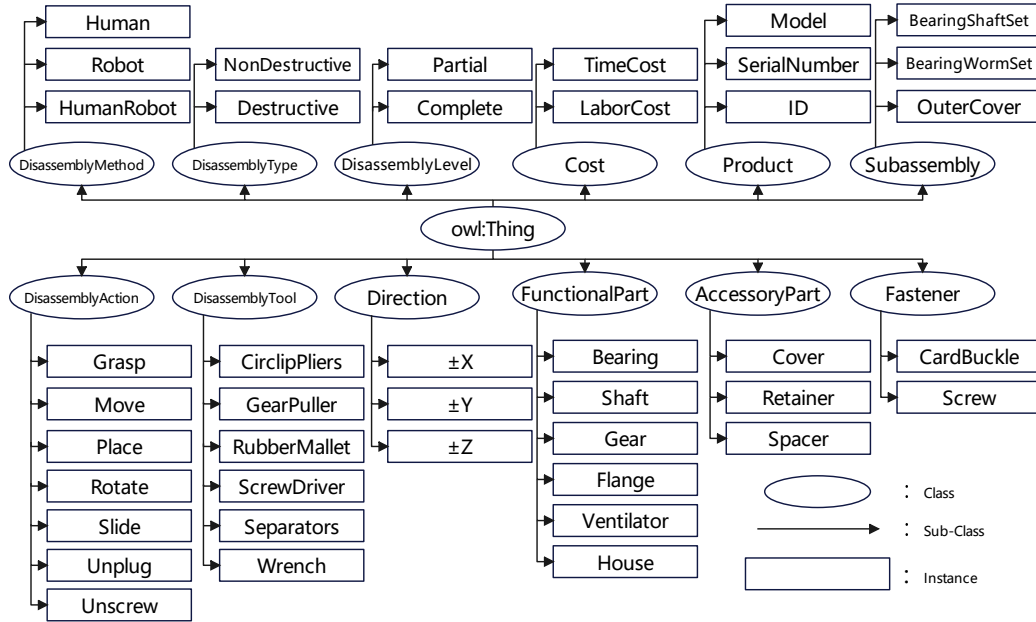


Figure 5.2: The class hierarchy of the proposed HRCO ontology.

products, which serve as the focal point of research in remanufacturing. This concept may apply to any mechanical product approaching the end of its life-cycle.

2. *Subassembly (sa)* refers to a group of components that, when combined, function collectively as a unit within a larger assembly or product. Typically assembled in a specific sequence during manufacturing, a subassembly (*sa*) is considered a singular component within an EoL product during disassembly. This classification simplifies the disassembly process by reducing the total number of individual components and potential disassembly sequences required for EoL products.

The aforementioned two subclasses are commonly utilised in product-

level modelling. In contrast to conventional classifications and modelling techniques at the component level, this study proposes three unique categories for modelling the components of EoL products. These categories are designed to align with the performance demands of the disassembly process in remanufacturing.

1. *FunctionalPart* (fp) refers to a category of crucial components that are central to the primary functions of a product and critical to its operation and performance. These components often retain substantial residual and remanufacturing value. Typically, in the remanufacturing process, the fp is targeted for reclamation, reprocessing, and reuse in the production of remanufactured goods.
2. *AccessoryPart* (ap) designates a category of supplementary components that augment a product's features, convenience, appearance, or safety through their specific functions. These components, while enhancing the product, are not crucial to its core functionality or performance. Accessory Parts are characterised by their reparability and interchangeability. Commonly, in the remanufacturing process, aps undergo reprocessing via additive manufacturing techniques to enhance the grades and qualities of the remanufactured products.
3. *Fastener* (f) refers to a category of hardware devices that mechanically secure or attach two or more components. These devices, designated as fs , are widely utilised to connect or fasten fps or aps in a manner

that is secure yet non-permanent. This functionality facilitates the disassembly of *fps* or *aps* without necessitating a destructive process.

The aforementioned subclasses are utilised to hierarchically delineate the structural connections and relationships among components in EoL products. These subclasses are specifically proposed to facilitate the management of disassembly-related knowledge within a human-robot collaborative manner. Additionally, this ontology model includes seven other proposed subclasses:

1. *DisassemblyAction* (*DA*) encompasses a range of activities necessary for the removal of components, including grasping, moving, placing, etc. These actions can be performed by either humans or robots, and all disassembly tasks may be carried out through either a single action or a combination of multiple actions.
2. *DisassemblyTool* (*DTI*) refers to the instruments employed for detaching component connections in EoL products, including tools such as screwdrivers, separators, and pullers. Both humans and robots are capable of utilising these disassembly tools, with each disassembly task generally necessitating specific types of tools.
3. *DisassemblyMethod* (*DM*) encompasses three distinct approaches for executing disassembly tasks: human, robot, and human-robot collaborative methods. The appropriate *DMs* for each task are determined based on the specific *DAs* and *DTIs* required.

4. *DisassemblyType* (*DTy*) categories disassembly into non-destructive and destructive forms. Destructive disassembly may lead to irreversible damage, thereby reducing the residual value of components. Conversely, non-destructive disassembly is favoured in remanufacturing due to its ability to preserve component integrity and value.
5. *DisassemblyLevel* (*DL*) describes the extent of the disassembly process, encompassing both complete and partial disassembly. The specific components targeted within EoL products dictate the level of disassembly required, which in turn impacts the strategic planning of the disassembly sequence.
6. *Direction* (*Dir*) denotes the constraints on component movement along six coordinate axes ($\pm X, \pm Y, \pm Z$).
7. *Cost* (*C*) encompasses the time and labor expenses involved in performing the disassembly task, which vary depending on the *DMs* employed. Each method utilises different *DAs* and *DTls*, influencing the overall cost.

5.2.2 Object and Data Properties of HRCD Ontology

The Web Ontology Language (OWL) is the preferred language for ontology representation within the framework of semantic web standards [184]. It builds upon the Resource Description Framework (RDF) Schema to enhance the depiction of complex classes, attribute characteristics, and property con-

straints. OWL facilitates comprehensive semantic descriptions and logical reasoning, which helps in minimising redundancies in knowledge representation and enhances knowledge sharing and semantic operations. These features are especially beneficial for encapsulating complex knowledge in areas such as human-robot collaborative disassembly within remanufacturing [185]. Ontologies crafted in OWL are both machine-readable and computation-friendly, thereby supporting efficient storage and development processes. Within the OWL-based framework, object properties clarify the attributes and relational constraints between classes. The relationships among classes in the proposed human-robot collaborative disassembly ontology are illustrated in Figure 5.3.

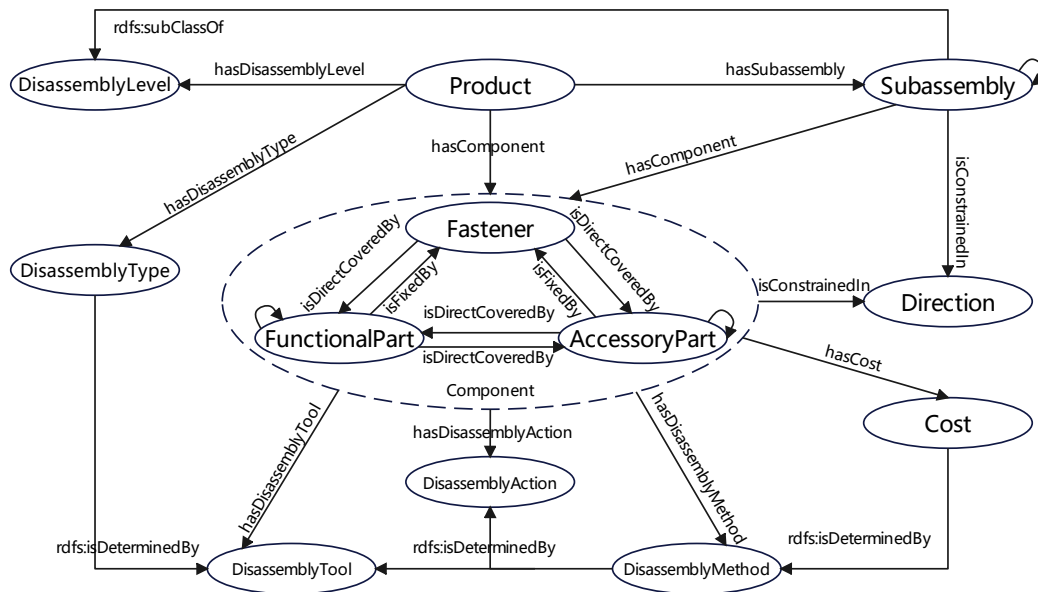


Figure 5.3: The class relationships of the proposed HRCD ontology.

The inner circle of the diagram displays the semantic representation of

the structural relationships at the component level within EoL products. Specifically, the structural interconnections among the three categories of components in the EoL product are depicted by the relationships *isDirectCoveredBy* (*iDCB*) and *isFixedBy* (*iFB*). The *iDCB* relationship denotes that a *f*, an *ap*, or a *fp* is directly covered by another *ap* or *fp*. Conversely, the *iFB* relationship indicates that *aps* or *fps* are fastened by a *f*.

To illustrate the product level more effectively and clearly, all categories of components are collectively referred to as *component* (*cp*) in this figure. Relationships within a *p* that include *sa* are denoted by *hasSubassembly* (*hsa*), while *cp* contained within a *p* or *sa* are indicated by *hasComponent* (*hc*). It is important to acknowledge that a *sa* can also serve as a component for another *sa*, demonstrating the modular nature of subassemblies within the product structure.

The additional disassembly-related classes are also interconnected and applied through semantic expressions. Movement constraints for *sa* and *cp* are captured by *isConstrainedIn* (*iCI*), which delineates the six directional (*Dir*) limitations. The *DL* and *DTy* of a *p* can be described through *hasDisassemblyLevel* (*hDL*) and *hasDisassemblyType* (*hDTy*), respectively. Within this framework, *sa* is a subclass of *DL*. When *sa* is empty ($sa=\emptyset$), the *DL* is classified as complete disassembly. The *cp* is defined by its required *DTl*, *DA*, *DM*, and *cp* through the object properties *hasDisassemblyTool* (*hDTl*), *hasDisassemblyAction* (*hDA*), *hasDisassemblyMethod* (*hDM*), and *hasCost* (*hC*), respectively.

Furthermore, this chapter delineates that the *DM* encompasses three distinct approaches: human, robot, and human-robot collaborative. The choice of an appropriate *DM* for a given disassembly task is influenced by the required *DTIs* and *DAs* specific to each *cp*. The determination of *DMs* and *C* for a *cp* is guided by these requirements, utilising a rule-based reasoning approach that integrates *DTIs* and *DAs*.

Expanding upon the ontology object properties discussed by Chen et al. and Yu et al. [104, 105], this chapter introduces a set of object properties specifically designed for the human-robot collaborative disassembly ontology. These properties are detailed in Table 5.1.

This table outlines that the *domain* of an object property identifies the class to which the property may be applied, while the *range* specifies the class that can assume the value of the property. The *domain* and *range* define the permissible associations within an ontology, thus ensuring conformity to the ontology's logical framework. The object properties introduced are as follows:

- Object properties 1-12 delineate the assembly relationships among product components along the six coordinate axis directions (+X/-X/+Y/-Y/+Z/-Z), collectively defining the complete assembly structure of the EoL product. Specifically, properties 1-6 detail the coverage relationships between different components, whereas properties 7-12 address the fastening relationships involving fasteners and both functional and accessory parts.

Table 5.1: Object properties in the HRCO ontology.

No.	Object property	Domain	Range	Inverse property
1	dC_plusX	<i>fp, ap, sa</i>	<i>f, fp, ap, sa</i>	iDCB_minusX
2	dC_plusY	<i>fp, ap, sa</i>	<i>f, fp, ap, sa</i>	iDCB_minusY
3	dC_plusZ	<i>fp, ap, sa</i>	<i>f, fp, ap, sa</i>	iDCB_minusZ
4	iDCB_plusX	<i>f, fp, ap, sa</i>	<i>fp, ap, sa</i>	dC_minusX
5	iDCB_plusY	<i>f, fp, ap, sa</i>	<i>fp, ap, sa</i>	dC_minusY
6	iDCB_plusZ	<i>f, fp, ap, sa</i>	<i>fp, ap, sa</i>	dC_minusZ
7	fix_plusX	<i>f</i>	<i>fp, ap, sa</i>	iFB_minusX
8	fix_plusY	<i>f</i>	<i>fp, ap, sa</i>	iFB_minusY
9	fix_plusZ	<i>f</i>	<i>fp, ap, sa</i>	iFB_minusZ
10	iFB_plusX	<i>fp, ap, sa</i>	<i>f</i>	fix_minusX
11	iFB_plusY	<i>fp, ap, sa</i>	<i>f</i>	fix_minusY
12	iFB_plusZ	<i>fp, ap, sa</i>	<i>f</i>	fix_minusZ
13	iPO	<i>f, fp, ap, sa</i>	<i>sa, p</i>	hPO
14	cBDI	<i>f, fp, ap, sa</i>	<i>Dir</i>	N/A
15	hDA	<i>f, fp, ap, sa</i>	<i>DA</i>	N/A
16	cBDB	<i>f, fp, ap, sa</i>	<i>DTL</i>	N/A
17	hDM	<i>f, fp, ap, sa</i>	<i>DM</i>	N/A
18	hTBDA	<i>f, fp, ap, sa</i>	<i>f, fp, ap, sa</i>	N/A
19	hTBDDA	<i>f, fp, ap, sa</i>	<i>f, fp, ap, sa</i>	N/A
20	hPT	<i>f, fp, ap, sa</i>	<i>C</i>	N/A
21	hC	<i>f, fp, ap, sa</i>	<i>C</i>	N/A
22	cBDS	<i>f, fp, ap, sa</i>	<i>f, fp, ap, sa</i>	N/A
23	dF	<i>f, fp, ap, sa</i>	<i>Dir, DTL</i>	N/A

- Object property 13 represents the hierarchical relationship among products, subassemblies, and individual components.
- Object property 14 indicates the potential disassembly directions of a subassembly or component in an EoL product.
- Object properties 15-17 respectively identify the necessary disassembly actions, tools, and viable disassembly methods for each task.
- Object properties 18-19 elucidate the precedence relationships in disassembly between subassemblies and components, establishing the se-

quence of disassembly for the product. This property is transitive, allowing components with direct disassembly precedence to be treated as subassemblies.

- Object properties 20-21 convey the time and operational costs required for the disassembly of subassemblies and components.
- Object property 22 identifies which subassemblies or components may be disassembled concurrently.
- Object property 23 is utilised primarily to evaluate whether different subassemblies or components can be disassembled simultaneously. In this evaluation, *Dir* and *DTI* are employed as two indices, corresponding to Auxiliary rules 67-69 as presented in Table 5.5.

Data properties are utilised to define the characteristics, attributes, or other data-centric information pertaining to entities across different classes [185]. Similar to object properties, each data property is associated with a specific domain and range. The definitions and detailed descriptions of these relevant data properties are documented in Table 5.2.

5.2.3 An Illustrative Example

In the dynamic field of smart remanufacturing, the disassembly of EoL products is recognised as a pivotal element, necessitating organised and methodical strategies. A key innovation in this area is the development of a product semantic model tailored for disassembly, which serves as a critical conduit

Table 5.2: Data properties in the HRCD ontology.

No.	Data Property	Domain	Range	Description
1	cBDI_plusX	<i>f, fp, ap, sa</i>	boolean	Record the optional disassembly direction of a <i>f, fp, ap</i> or <i>sa</i>
	cBDI_plusY			
	cBDI_plusZ			
	cBDI_minusX			
	cBDI_minusY			
cBDI_minusZ				
2	iD	<i>f, fp, ap, sa, p</i>	string	Record the identity of a <i>f, fp, ap, sa</i> or <i>p</i>
3	nameOfComponent	<i>f, fp, ap, sa</i>	string	Record the name of a <i>f, fp, ap</i> or <i>sa</i>
4	quantity	<i>f, fp, ap</i>	int	Record the quantity of a <i>f, fp, ap</i> or <i>sa</i> in the <i>p</i>
5	humanProcessTime	<i>f, fp, ap, sa</i>	float	Record the process time of disassemble a <i>f, fp, ap</i> or <i>sa</i> using human, robot or human-robot <i>DM</i>
	robotProcessTime			
	humanRobotProcessTim			

linking EoL products with other remanufacturing processes. This ontology model provides an exhaustive representation of products, capturing not only their physical structure and attributes but also incorporating relevant data such as maintenance histories and failure modes. Utilising semantic technologies, the model comprehensively delineates complex relationships, dependencies, and hierarchies among EoL product components. By mapping out both hierarchical and connection-based relationships within product architectures, the semantic model enhances the efficiency, clarity, and effectiveness of the disassembly process.

The product semantic model is integrated within the broader framework of the proposed HRCD ontology model, which delineates the components and their interrelationships within EoL products. This section aims to elucidate the product semantic model by using the belt roller support assembly as a case study. Figure 5.4 illustrates the interactions among the three categorised components of the belt roller support assembly: bolts (depicted in grey) function as fasteners, bushes (shown in light blue) serve as accessory parts,

and the base (in navy blue), shaft (in yellow), bracket (in green), and roller (in red) are identified as functional parts. Utilising the product semantic model alongside the object properties outlined in Table 5.1, Table 5.2, and Figure 5.3, we have constructed the topological structures of the belt roller support assembly, highlighting its connections and hierarchical relationships. Descriptions and semantic expressions of the belt roller support assembly are detailed below:

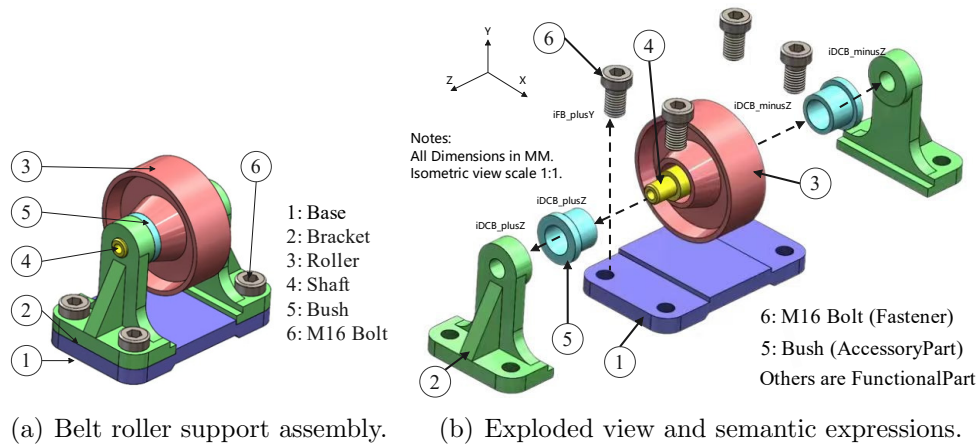


Figure 5.4: An illustrative example.

- Bracket iFB_plusY bolt: brackets are fixed by bolts from +Y direction.
- Base iDCB_plusZ bracket: the base is directly covered by brackets from +Y direction.
- Bush iDCB_plusZ bracket: the left bush is directly covered by the left bracket from +Z direction.

- Bush iDCB_minusZ bracket: the right bush is directly covered by the right bracket from +Z direction.
- Shaft iDCB_plusZ bracket: the shaft is directly covered by the left bracket from +Z direction.
- Shaft iDCB_minusZ bracket: the shaft is directly covered by the right bracket from +Z direction.
- Roller iDCB_plusZ shaft: the roller is directly covered by the shaft from +Z direction.

Normally, the -Y direction, which is associated with gravity, is not considered in the disassembly process.

5.3 Rule-Based Reasoning for HRC D Sequence Planning

In this section, the Semantic Web Rule Language (SWRL) and Semantic Query-enhanced Web Rule Language (SQWRL) are utilised to develop a rule-based reasoning approach. The first subsection introduces rules concerning the product structure. These rules are designed to reason about and establish precedence constraints necessary for disassembling subassemblies or components within an EoL product. The second subsection outlines rules that ascertain the disassembly method for each component, aiming to formulate an optimal human-robot collaborative disassembly strategy.

5.3.1 Rules for Reasoning Disassembly Precedence Constraints

Building upon the disassembly relationships between fp and f as discussed in previous papers [104, 105], this thesis extends the analysis to include relationships among fp , ap , and f . Disassembly tasks are conducted from five coordinate axes directions, excluding the -Y direction. The rules and guidelines for establishing disassembly precedence constraints are detailed in Table 5.3. In mechanical products, situations where f s are attached to each other typically do not occur and are therefore not included in the considerations. Three specific relationships are defined as direct disassembly: f/fp , f/ap , and ap/ap . These relationships promote consistent disassembly practices and actions and help minimise changes in the disassembly direction. Based on these established rules, it is feasible to determine the precedence constraints among fp , ap , and f within an EoL product.

The belt roller serves as a case study to verify the accuracy and completeness of the disassembly precedence constraint set. By utilising the CAD file, which is accessible through the open-source link provided in Appendix 8.3, and the relational semantic descriptions found in Section 5.2.3, the actual disassembly procedures and the precedence constraint graph are depicted in Figure 5.5. The disassembly sequence begins with the removal of the bolts, followed by the brackets, bushes, and shaft. During this sequence, the roller and base are automatically separated. The graph illustrates nine precedence

Table 5.3: Rules for generating the precedence constrains of components.

No.	SWRL/SQWRL	Description
1-6	$f (?f) \wedge fp (?fp) \wedge iDCB_Dir (?f, ?fp) \rightarrow hTBDDA (?f, ?fp)$	If a f is directly covered by a fp in any disassembly-direction of the f , then the f shall be direct disassembled after the fp
7-12	$f (?f) \wedge ap (?ap) \wedge iDCB_Dir (?f, ?ap) \rightarrow hTBDDA (?f, ?ap)$	If a f is directly covered by an ap in any disassembly-direction of the f , then the f shall be direct disassembled after the ap
13-18	$ap (?ap) \wedge fp (?fp) \wedge iDCB_Dir (?ap, ?fp) \rightarrow hTBDA (?ap, ?fp)$	If an ap is directly covered by a fp in any disassembly-direction of the ap , then the ap shall be disassembled after the fp
19-24	$fp (?fp) \wedge ap (?ap) \wedge iDCB_Dir (?fp, ?ap) \rightarrow hTBDA (?fp, ?ap)$	If a fp is directly covered by an ap in any disassembly-direction of the fp , then the fp shall be disassembled after the ap
25-30	$fp (?fp) \wedge f (?f) \wedge iFB_Dir (?fp, ?f) \rightarrow hTBDDA (?fp, ?f)$	If a fp is fixed by a f in any direction, then the fp shall be direct disassembled after the f
31-36	$ap (?ap) \wedge f (?f) \wedge iFB_Dir (?ap, ?f) \rightarrow hTBDDA (?ap, ?f)$	If an ap is fixed by a f in any direction, then the ap shall be direct disassembled after the f
37-42	$fp (?fp) \wedge fp (?fp1) \wedge iDCB_Dir (?fp, ?fp1) \rightarrow hTBDA (?fp, ?fp1)$	If a fp A is directly covered by a fp B in any direction, then the fp A shall be disassembled after the fp B
43-48	$ap (?ap) \wedge ap (?ap1) \wedge iDCB_Dir (?ap, ?ap1) \rightarrow hTBDDA (?ap, ?ap1)$	If an ap A is directly covered by an ap B in any direction, then the ap A shall be disassembled after the ap B

**Dir* represents *plusX*, *minusX*, *plusY*, *plusZ*, *minusZ*, respectively.

constraints among the components of the belt roller. Although various disassembly sequences are possible, the set of precedence constraints is singular and fixed, necessitating strict adherence throughout the disassembly process.

The ontology for the product, along with specific instances of the belt roller, has been constructed utilising Protégé version 5.5.0, employing Hermit as the integrated reasoning engine. This process resulted in the generation of nine assertions based on the established rules:

1. ‘Bracket_left hTBDDA Bolts’: The left bracket, directly fixed by bolts from the +Y direction, has to be direct disassembled after removing the bolts (from rules 25-30)
2. ‘Bracket_right hTBDDA Bolts’: The right bracket, directly fixed by bolts from the +Y direction, has to be direct disassembled after removing the bolts (from rules 25-30).

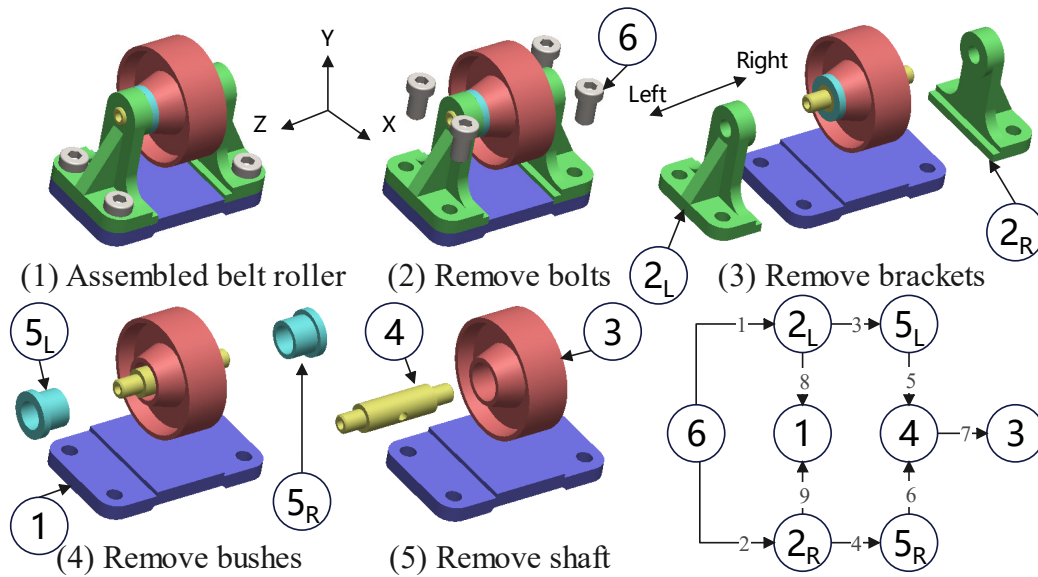


Figure 5.5: Disassembly procedures and precedence constraints of the belt roller.

3. ‘Bush_left hTBDA Bracket_left’: The left bush, directly covered by the left bracket from the +Z direction, has to be disassembled after the left bracket (from rules 13-18).
4. ‘Bush_right hTBDA Bracket_right’: The right bush, directly covered by the right bracket from the -Z direction, has to be disassembled after the right bracket. (from rules 13-18).
5. ‘Shaft hTBDA Bush_left’: The shaft, directly covered by the left bush from the +Z direction, has to be disassembled after the left bush. (from rules 19-24).
6. ‘Shaft hTBDA Bush_right’: The shaft, directly covered by the right

bush from the -Z direction, has to be disassembled after the right bush. (from rules 19-24).

7. ‘Roller hTBDA Shaft’: The roller, directly covered by shaft from the +Z direction, has to be disassembled after the shaft. (from rules 37-42).
8. ‘Base hTBDA Bracket_left’: The base, directly covered by the left bracket from the +Y direction, has to be disassembled after the left bracket. (from rules 37-42).
9. ‘Base hTBDA Bracket_right’: The base, directly covered by the right bracket from the +Y direction, has to be disassembled after the right bracket. (from rules 37-42).

In this case analysis, a single assertion is derived from the selected rule according to the specified direction. The accuracy and completeness of the precedence constraint set can be evaluated based on the following criteria:

1. Correctness of the precedence constraint set: The SWRL rules proposed in this study ensure the absence of contradictions, and all reasoning outcomes produced by these rules are consistent with the intended precedence constraints. The resulting precedence constraints for the belt roller effectively reflect the true sequence requirements for the components.
2. Completeness of the precedence constraint set: The set, which comprises the outcomes derived from the proposed SWRL-based rules, en-

compasses nine precedence constraints. This total corresponds exactly with the actual precedence constraint set for the belt roller.

The disassembly precedence constraint set generated by the proposed SWRL rules 1-48 corresponds with the actual precedence constraint set of the belt roller. However, rules 1-12, 31-36, and 43-48 do not establish any precedence constraints among the components, which is attributable to the lack of specific component relationships and semantic descriptions within the belt roller. Despite this, these rules are not considered redundant, as they are designed to encompass and describe all possible scenarios or inferences, including potential relationships within an EoL product.

5.3.2 Rules for Determining Disassembly Method

Collaborative robots are well-suited for efficiently handling repetitive and straightforward tasks within human-robot collaboration environments, addressing the limitations of manual disassembly, such as lower efficiency and higher costs. However, their effectiveness is influenced by several factors, including worker safety, the complexity of the disassembly tasks, and the constraints of available tools and resources. For more complex disassembly tasks, humans have demonstrated greater flexibility and efficiency compared to robots. This advantage is due to human capabilities such as detection, observation, critical thinking, and manual dexterity, which robots currently lack. Therefore, complex disassembly processes are best approached through human-robot collaboration, combining the flexibility of human work-

ers with the precision of robots. This synergy between human adaptability and robotic accuracy is more effective in managing complex disassembly tasks than either humans or robots working independently.

In the context of HRCd, existing knowledge does not provide a standard methodology for determining the disassembly methods for various components, primarily due to the absence of a standardised approach for evaluating task complexity. To address this, we draw on evaluation criteria from the literature [186] and consider the number and type of disassembly actions, as well as the disassembly tools, as key factors in identifying the most suitable disassembly methods for each disassembly task. The disassembly actions are based on nine fundamental actions identified in previous study [187], and the tools include common items such as wrenches and screwdrivers, along with specialised tools like bearing pullers. Building on these criteria, this section introduces a set of rules that leverage disassembly-related knowledge—specifically the required disassembly actions and tools—to determine the optimal disassembly method for each component in an EoL product. The proposed rules and their corresponding descriptions are detailed in Table 5.4. The potential disassembly methods for a component fall into four primary categories: those that can be executed by either humans or robots, those that are feasible solely for humans, those that are suitable exclusively for robots, and those that require human-robot collaboration.

- Rules 49-54 specify that if a c can be disassembled using a single DA and requires one or fewer DTI , then the disassembly of the c can be

Table 5.4: Rules for determining disassembly method.

No.	SWRL/SQWRL	Description
49	$fp(?fp) \wedge hDA(?fp, ?a) \wedge hDTI(?fp, ?t) \wedge sqwrl:count(?a) = 1 \wedge sqwrl:count(?t) \leq 1$ $\rightarrow hDM(?fp, ?r) \wedge Robot(?r) \wedge hasProcessTime(?fp, ?pt)$	For any fp , ap or f that has a single DA that uses less than or equal to one DTI ,
50	$fp(?fp) \wedge hDA(?fp, ?a) \wedge hDTI(?fp, ?t) \wedge sqwrl:count(?a) = 1 \wedge sqwrl:count(?t) \leq 1$ $\rightarrow hDM(?fp, ?h) \wedge Human(?h) \wedge hasProcessTime(?fp, ?pt)$	then the fp , ap or f can be disassembled by robot or human through certain process time
51	$ap(?ap) \wedge hDA(?ap, ?a) \wedge hDTI(?ap, ?t) \wedge sqwrl:count(?a) = 1 \wedge sqwrl:count(?t) \leq 1$ $\rightarrow hDM(?ap, ?r) \wedge Robot(?r) \wedge hasProcessTime(?ap, ?pt)$	
52	$ap(?ap) \wedge hDA(?ap, ?a) \wedge hDTI(?ap, ?t) \wedge sqwrl:count(?a) = 1 \wedge sqwrl:count(?t) \leq 1$ $\rightarrow hDM(?ap, ?h) \wedge Human(?h) \wedge hasProcessTime(?ap, ?pt)$	
53	$f(?f) \wedge hDA(?f, ?a) \wedge hDTI(?f, ?t) \wedge sqwrl:count(?a) = 1 \wedge sqwrl:count(?t) \leq 1$ $\rightarrow hDM(?f, ?r) \wedge Robot(?r) \wedge hasProcessTime(?f, ?pt)$	
54	$f(?f) \wedge hDA(?f, ?a) \wedge hDTI(?f, ?t) \wedge sqwrl:count(?a) = 1 \wedge sqwrl:count(?t) \leq 1$ $\rightarrow hDM(?f, ?h) \wedge Human(?h) \wedge hasProcessTime(?f, ?pt)$	
55	$fp(?fp) \wedge hDA(?fp, ?a) \wedge hDTI(?fp, ?t) \wedge sqwrl:count(?a) = 2 \wedge sqwrl:count(?t) \leq 1$ $\rightarrow hDM(?fp, ?r) \wedge Robot(?r) \wedge hasProcessTime(?fp, ?pt)$	For any fp , ap or f that has two DAs that uses less than or equal to one DTI ,
56	$ap(?ap) \wedge hDA(?ap, ?a) \wedge hDTI(?ap, ?t) \wedge sqwrl:count(?a) = 2 \wedge sqwrl:count(?t) \leq 1$ $\rightarrow hDM(?ap, ?r) \wedge Robot(?r) \wedge hasProcessTime(?ap, ?pt)$	then the fp , ap or f can be disassembled by robot through certain process time
57	$f(?f) \wedge hDA(?f, ?a) \wedge hDTI(?f, ?t) \wedge sqwrl:count(?a) = 2 \wedge sqwrl:count(?t) \leq 1$ $\rightarrow hDM(?f, ?r) \wedge Robot(?r) \wedge hasProcessTime(?f, ?pt)$	
58	$fp(?fp) \wedge hDA(?fp, ?a) \wedge hDTI(?fp, ?t) \wedge sqwrl:count(?a) = 2 \wedge sqwrl:count(?t) = 2$ $\rightarrow hDM(?fp, ?h) \wedge Human(?h) \wedge hasProcessTime(?fp, ?pt)$	For any fp , ap or f that has two DAs that uses two $DTIs$, then the fp , ap or f can only be disassembled by human through certain process time
59	$ap(?ap) \wedge hDA(?ap, ?a) \wedge hDTI(?ap, ?t) \wedge sqwrl:count(?a) = 2 \wedge sqwrl:count(?t) = 2$ $\rightarrow hDM(?ap, ?h) \wedge Human(?h) \wedge hasProcessTime(?ap, ?pt)$	
60	$f(?f) \wedge hDA(?f, ?a) \wedge hDTI(?f, ?t) \wedge sqwrl:count(?a) = 2 \wedge sqwrl:count(?t) = 2$ $\rightarrow hDM(?f, ?h) \wedge Human(?h) \wedge hasProcessTime(?f, ?pt)$	
61	$fp(?fp) \wedge hDA(?fp, ?a) \wedge hDTI(?fp, ?t) \wedge sqwrl:count(?a) > 2 \wedge sqwrl:count(?t) >= 2$ $\rightarrow hDM(?fp, ?hr) \wedge HumanRobot(?hr) \wedge hasProcessTime(?fp, ?pt)$	For any fp , ap or f that has more than two DAs that uses two and more than two $DTIs$, then the fp , ap or f can be disassembled by human-robot collaboration through certain process time
62	$ap(?ap) \wedge hDA(?ap, ?a) \wedge hDTI(?ap, ?t) \wedge sqwrl:count(?a) > 2 \wedge sqwrl:count(?t) >= 2$ $\rightarrow hDM(?ap, ?hr) \wedge HumanRobot(?hr) \wedge hasProcessTime(?ap, ?pt)$	
63	$f(?f) \wedge hDA(?f, ?a) \wedge hDTI(?f, ?t) \wedge sqwrl:count(?a) > 2 \wedge sqwrl:count(?t) >= 2$ $\rightarrow hDM(?f, ?hr) \wedge HumanRobot(?hr) \wedge hasProcessTime(?f, ?pt)$	

performed by either a human or a robot.

- Rules 55-57 suggest that if a c requires two DAs and no more than one DTI , then the disassembly process for the c should be carried out by a robot.
- Rules 58-60 indicate that if a c requires two DAs and two $DTIs$, then the disassembly of the c should be performed by a human.
- Rules 61-63 state that if a c requires more than two DAs and two or more $DTIs$, the disassembly process for the c should apply human-robot collaboration.

After determining the disassembly methods for each component through

reasoning, the corresponding disassembly time costs are incorporated as supplementary knowledge.

5.3.3 Auxiliary Rules

In addition to the rules previously established, there are several supportive auxiliary rules proposed to specify and infer the optimal disassembly sequence as shown in Table 5.5.

Table 5.5: Auxiliary rules

No.	SWRL/SQWRL	Description
64	$fp(?fp) \rightarrow dD_plusX(?fp, 1) \wedge dD_minusX(?fp, 1) \wedge dD_plusY(?fp, 1) \wedge dD_minusY(?fp, 1) \wedge dD_plusZ(?fp, 1) \wedge dD_minusZ(?fp, 1)$	Update and get the disassemble direction of a <i>fp</i> , <i>ap</i> or <i>f</i> .
65	$ap(?ap) \rightarrow dD_plusX(?ap, 1) \wedge dD_minusX(?ap, 1) \wedge dD_plusY(?ap, 1) \wedge dD_minusY(?ap, 1) \wedge dD_plusZ(?ap, 1) \wedge dD_minusZ(?ap, 1)$	
66	$f(?f) \rightarrow dD_plusX(?f, 1) \wedge dD_minusX(?f, 1) \wedge dD_plusY(?f, 1) \wedge dD_minusY(?f, 1) \wedge dD_plusZ(?f, 1) \wedge dD_minusZ(?f, 1)$	
67	$fp(?fp) \wedge ap(?ap) \wedge hDD(?fp, ?d1) \wedge hDD(?ap, ?d2) \wedge swrlb:dF(?d1, ?d2) \wedge hDM(?fp, ?m1) \wedge hDM(?ap, ?m2) \wedge swrlb:dF(?m1, ?m2) \wedge sqwrl:not(hTBDA(?fp, ?ap)) \wedge sqwrl:not(hTBDA(?ap, ?fp)) \rightarrow cBDS(?fp, ?ap)$	Determine if the <i>fp/ap</i> , <i>fp/f</i> or <i>ap/f</i> have different disassembly directions, can be disassembled by different method, and have no specified requirement for one part to be disassembled after the other. If these conditions are met, the rule infers that the referred parts can be disassembled simultaneously
68	$fp(?fp) \wedge f(?f) \wedge hDD(?fp, ?d1) \wedge hDD(?f, ?d2) \wedge swrlb:dF(?d1, ?d2) \wedge hDM(?fp, ?m1) \wedge hDM(?f, ?m2) \wedge swrlb:dF(?m1, ?m2) \wedge sqwrl:not(hTBDA(?fp, ?f)) \wedge sqwrl:not(hTBDA(?f, ?fp)) \rightarrow cBDS(?fp, ?f)$	
69	$ap(?ap) \wedge f(?f) \wedge hDD(?ap, ?d1) \wedge hDD(?f, ?d2) \wedge swrlb:dF(?d1, ?d2) \wedge hDM(?ap, ?m1) \wedge hDM(?f, ?m2) \wedge swrlb:dF(?m1, ?m2) \wedge sqwrl:not(hTBDA(?ap, ?f)) \wedge sqwrl:not(hTBDA(?f, ?ap)) \rightarrow cBDS(?ap, ?f)$	
70	$hTBDDA(?f, ?fp) \rightarrow sa(?f) \wedge sa(?fp)$	If a <i>f</i> has to be direct disassembled after a <i>fp</i> or <i>ap</i> , the <i>fp</i> or <i>ap</i> has to be direct disassembled after the <i>f</i> . <i>Ap</i> A has to be direct disassembled after <i>ap</i> B. Then the <i>f</i> and <i>f/ap</i> can be regarded as a <i>sa</i>
71	$hTBDDA(?fp, ?f) \rightarrow sa(?fp) \wedge sa(?f)$	
72	$hTBDDA(?f, ?ap) \rightarrow sa(?f) \wedge sa(?ap)$	
73	$hTBDDA(?ap, ?f) \rightarrow sa(?ap) \wedge sa(?f)$	
74	$hTBDDA(?ap1, ?ap2) \rightarrow sa(?ap1) \wedge sa(?ap2)$	

- Rules 64-66 are employed to update the disassembly direction available for each component.

- Rules 67-69 are designed to determine whether two components can

be disassembled concurrently, taking into account their disassembly direction and method, while ensuring that there are no precedence constraints. For simultaneous disassembly to be possible, the components must be oriented in different disassembly directions and must utilise distinct disassembly methods, excluding those involving human-robot collaboration. Typically, components of the same type share identical disassembly methods, which precludes concurrent disassembly. Additionally, these rules aim to minimise changes in the disassembly direction and maintain continuity in the disassembly actions.

- Rules 70-74 suggest that if a f has an hTBDDA relationship with another fp or ap , then f and fp/ap can be treated as a single sa . Similarly, if an ap has an hTBDDA relationship with another ap , these two aps can also be grouped as a sa . These rules facilitate the grouping of components, thereby simplifying the disassembly sequence planning by reducing the need for changes in disassembly direction. This approach enhances the efficiency and capability of the rule-based reasoning method, particularly when dealing with larger and more complex EoL products.

In this chapter, subassemblies are categorised based on the types of components they contain. If a sa is composed exclusively of a single type of fp , ap , or f , it is classified as that specific component type. However, if a sa contains two or more different types of components, it is classified as an fp .

5.3.4 Process for Generating The Optional Disassembly Scheme

The research workflow of this chapter, built upon the developed product semantic model, consists of two main phases: first, establishing disassembly precedence constraints among product components and determining their respective disassembly methods; second, generating the optimal disassembly scheme.

Workflow for Generating Disassembly Precedence Constraints

The workflow for generating disassembly precedence constraints among components is illustrated in Figure 5.6. Before applying the relevant reasoning rules, three empty sets are initialised: Set f , Set fp , and Set ap . The primary input in this chapter consists of the lowest-level components of the EoL product. Components are categorised and assigned to the appropriate sets based on their classification. Disassembly-related information for these components is stored and transmitted across the different sets. After reading and inputting the complete list of product components, rules 1-48 are applied to establish disassembly precedence constraints among the various components. These constraints are constructed on the foundation of traditional And/Or graphs but retain additional information about the components, enhancing the subsequent decision-making processes. Next, according to rules 70-74, related components are grouped and treated as subassemblies, thereby reducing the total number of product components and shrinking the solution

space for feasible disassembly sequences. The types of sub-components are determined by the categories of the components they contain, with the sets being updated accordingly. Finally, rules 49-63 are used to infer the potential disassembly methods for each component, and the time cost associated with each method is recorded as part of the known knowledge base.

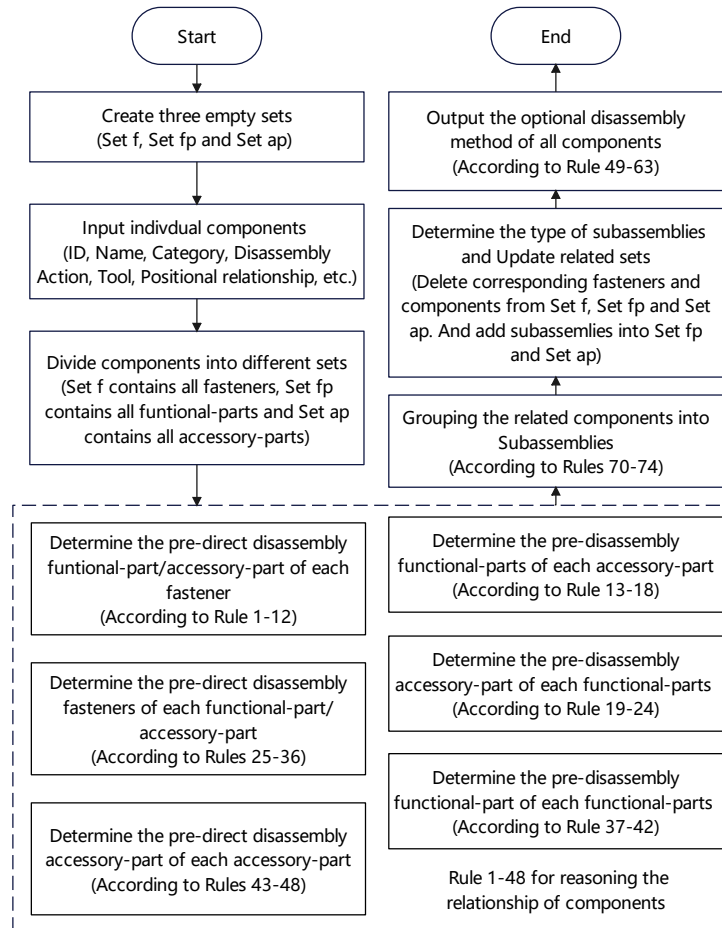


Figure 5.6: Workflow for generating precedence constraints of EoL product.

Workflow for Generating Optimal Disassembly Scheme

Based on the precedence constraints established in section 5.3.4, all possible disassembly sequences and the optimal disassembly scheme can be generated and determined using subsequent rules. The overall workflow for determining the optimal disassembly scheme is illustrated in Figure 5.7. According to the grouping and categorisation process detailed in section 5.3.4, *sas* have already been sequentially grouped and categorised as *fps*, *aps*, or *fs*. Following this, all components are divided into three distinct sets—*fp*, *ap*, and *f*—based on their attributes within the EoL product. It is important to note that any relationship in which an *f* is directly covered by another *fp* or *ap* is eliminated through the grouping and generation of *sas*. This procedure not only reduces the number of components involved in the disassembly sequence planning but also aligns with the standard practices of disassembly consistency.

After applying rules 64-66, the available disassembly directions and all executable components are identified and initialised. Following conventional disassembly practices, where components are typically loosened first, the *f* components are prioritised for disassembly. If the *f* set is non-empty, one executable *f* is selected as the current disassembly task. Simultaneously, the potential for simultaneous disassembly with another executable *fp* or *ap* is assessed using rules 68-69. If a compatible *fp* or *ap* is identified, the *f* and the *fp/ap* are disassembled together. Otherwise, the *f* is disassembled individually. Once this task is completed, the disassembly directions for the

remaining components are reinitialised using rules 64-66, and the relevant sets are updated. This process continues iteratively.

When the f set is empty, the ap set is then evaluated. Typically, aps are incorporated to improve the overall performance of the product, serving as connectors between fs and fps . If the ap set is non-empty, an executable ap is selected as the next disassembly task. Rule 67 assists in determining whether this ap can be disassembled concurrently with any remaining fp . If a suitable fp is identified, they are disassembled together; if not, the ap is disassembled on its own. After the ap is disassembled, the disassembly directions for the remaining fps or aps are updated in accordance with rules 64-65, leading to the subsequent updating of sets fp and ap .

When the ap set is empty, the fp set is examined last. If the fp set is non-empty, an executable fp is selected as the current task. Typically, these remaining fps have a higher residual value and are disassembled using similar methods. As a result, no further evaluation is needed to identify other fps that could be disassembled concurrently. This process continues iteratively until the fp set is empty, at which point it can be concluded that all components of the EoL product have been fully disassembled. Following this, all possible HRCD sequences are generated and output by sequentially following the disassembly tasks. The optimal HRCD scheme can then be determined based on specific criteria.

Additionally, to address conflicts and uncertainties in multi-optional simultaneous disassembly tasks, the selection of executable components is pri-

oritised in the order of +Y, +X, +Z, -X, and -Z, with -Y generally representing the gravitational direction and therefore not considered for disassembly tasks.

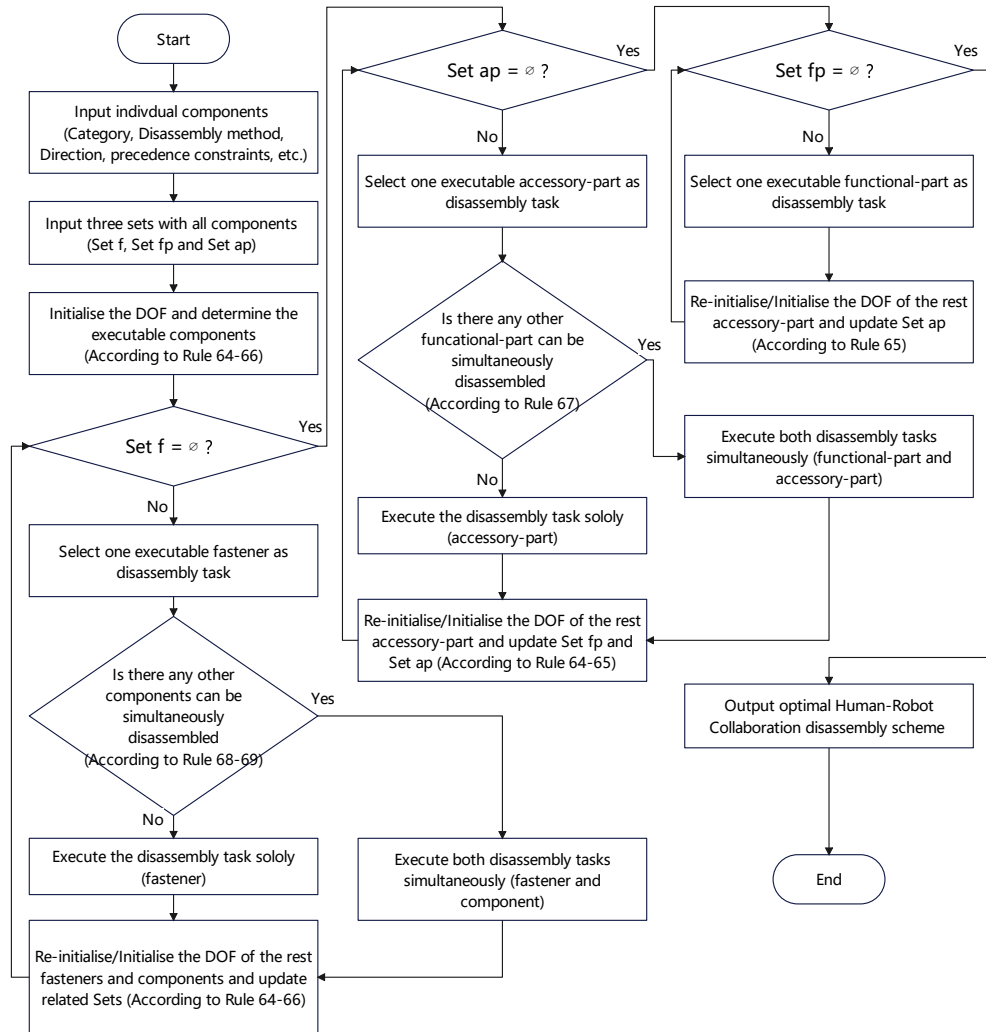


Figure 5.7: Workflow for generating optimal disassembly schemes.

5.4 Case Study

In this section, a case study is proposed involving the disassembly sequence planning of a worm gear reducer gearbox to validate the feasibility and efficiency of the proposed HRC methods. The exploded view and bill of materials (*BOM*) for the gearbox are shown in Figure 5.8 and Table 8.3, respectively. The CAD file and *BOM* are accessible via the link provided in Appendix 8.3. This case study is designed to validate the effectiveness of the proposed human-robot collaborative disassembly ontology and inference rules. In this scenario, the gearbox is assumed to undergo a complete non-destructive disassembly. The *ProcessingTime* for this case study is measured in dimensionless units.

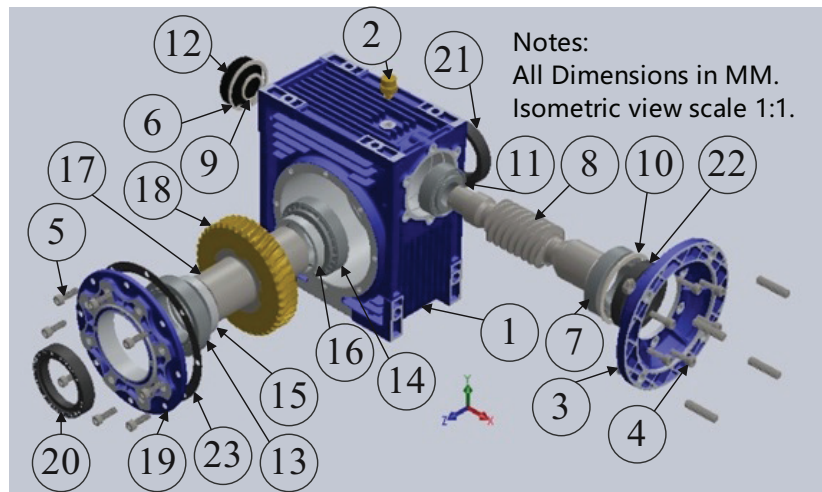


Figure 5.8: Exploded view of the gearbox.

5.4.1 HRCO Ontology Model of Gearbox

In this subsection, the disassembly ontology of the gearbox is constructed using the modelling tool Protégé 5.5.0. Building upon the general disassembly ontology model developed earlier, the gearbox components are input as instances. The established classes, object properties, data properties, and individuals associated with the gearbox are depicted in Figure 5.9. The created gearbox ontology is saved in the Web Ontology Language (OWL) format as an .owl file. The rules relevant to HRCO are developed using Microsoft Visual Studio Community 2019, with the C# programming language. This process integrates the open-source .Net library (dotNetRDF), which provides a comprehensive API for using SPARQL, and Jena.Net, a .NET port of the Jena semantic web toolkit. The ontology file generated and saved in Protégé (.owl file) is imported into Visual Studio. Subsequently, SPARQL and the Jena Ontology API are used to construct and execute the corresponding rule inferences, enabling the generation of the optimal human-robot collaborative disassembly scheme.

5.4.2 Precedence Constraints of The Gearbox

The relationships concerning the semantic disassembly of fasteners, accessory components, and functional components within the gearbox are delineated in Tables 5.6, 5.7, and 5.8. The precedence constraints for the gearbox, which were derived from the process outlined in Section 5.3.4, are depicted in Figure 5.10. Furthermore, the relationships of component disassembly

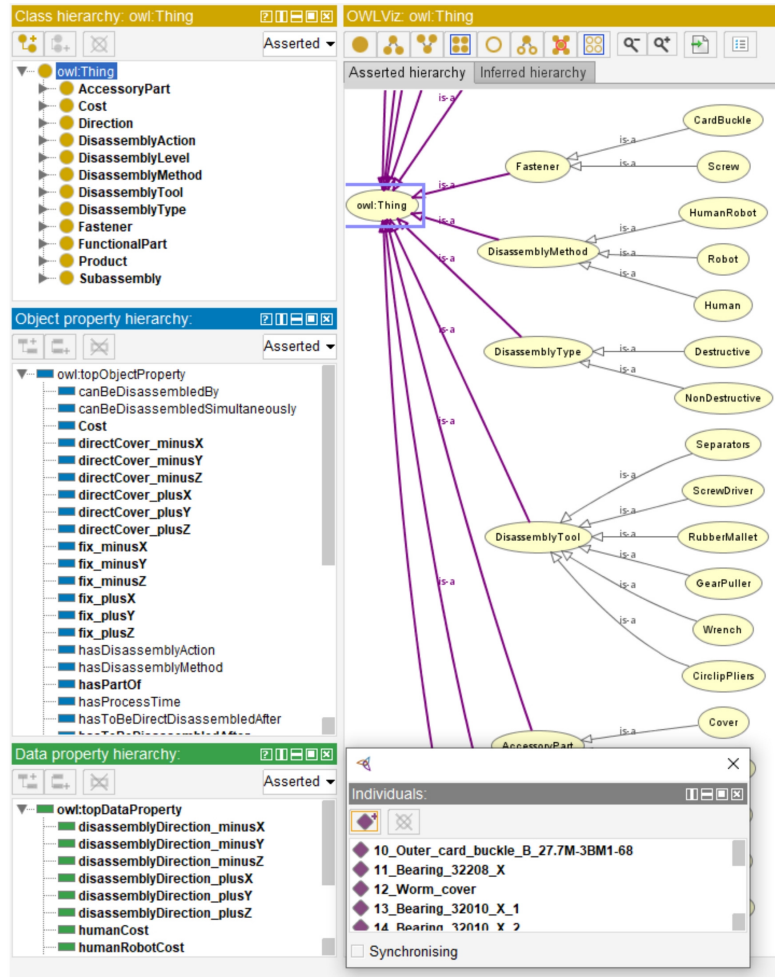


Figure 5.9: Screenshot of the human-robot disassembly ontology of gearbox in Protégé.

precedence, as deduced from Rules 1-48, are displayed in Figure 5.10(a). By applying additional Rules 49-63 and 70-74, the streamlined disassembly precedence relationships are illustrated in Figure 5.10(b). The analysis of

precedence constraint graphs indicates a reduction in constraints from 22 to 7. This condensation of optional disassembly sequences enhances the efficiency of the planning process, particularly through the application of Rules 70-74. Detailed information regarding the resultant subassemblies and the residual components is provided in Table 5.9. Notably, the assembly process yielded five subassemblies, with the S2 subassembly categorised as an accessory part and the others classified as functional parts.

Table 5.6: Semantic assembly-relations of fasteners in the gearbox.

<i>f</i> No.	iDCB_plusX	iDCB_minusX	iDCB_plusY	iDCB_minusY	iDCB_plusZ	iDCB_minusZ
4	-	-	-	-	-	-
5	-	-	-	-	-	-
<i>f</i> No.	cBDI_plusX	cBDI_minusX	cBDI_plusY	cBDI_minusY	cBDI_plusZ	cBDI_minusZ
4	1	0	0	0	0	0
5	0	0	0	0	1	0

Table 5.7: Semantic assembly-relations of accessory parts in the gearbox.

<i>ap</i> No.	iDCB_plusX	iDCB_minusX	iDCB_plusY	iDCB_minusY	iDCB_plusZ	iDCB_minusZ
6	-	12	-	-	-	-
9	-	6	-	-	-	-
10	22	-	-	-	-	-
15	-	-	-	-	13	-
16	-	-	-	-	-	14
19	-	-	-	-	20	-
20	-	-	-	-	-	-
21	-	-	-	-	-	-
22	3	-	-	-	-	-
23	-	-	-	-	19	-
<i>ap</i> No.	iFB_plusX	iFB_minusX	iFB_plusY	iFB_minusY	iFB_plusZ	iFB_minusZ
6	-	-	-	-	-	-
9	-	-	-	-	-	-
10	-	-	-	-	-	-
15	-	-	-	-	-	-
16	-	-	-	-	-	-
19	-	-	-	-	5	-
20	-	-	-	-	-	-
21	-	-	-	-	-	-
22	-	-	-	-	-	-
23	-	-	-	-	-	-

Table 5.8: Semantic assembly-relations of functional parts in the gearbox.

<i>fp</i> No.	iDCB_plusX	iDCB_minusX	iDCB_plusY	iDCB_minusY	iDCB_plusZ	iDCB_minusZ
1	8	-	2	-	18	21
2	-	-	-	-	-	-
3	-	-	-	-	-	-
7	10	-	-	-	-	-
8	7	11	-	-	-	-
11	-	9	-	-	-	-
12	-	-	-	-	-	-
13	-	-	-	-	23	-
14	-	-	-	-	-	21
17	-	-	-	-	15	16
18	-	-	-	-	17	-
<i>fp</i> No.	iFB_plusX	iFB_minusX	iFB_plusY	iFB_minusY	iFB_plusZ	iFB_minusZ
1	-	-	-	-	-	-
2	-	-	-	-	-	-
3	4	-	-	-	-	-
7	-	-	-	-	-	-
8	-	-	-	-	-	-
11	-	-	-	-	-	-
12	-	-	-	-	-	-
13	-	-	-	-	-	-
14	-	-	-	-	-	-
17	-	-	-	-	-	-
18	-	-	-	-	-	-

Table 5.9: Output of optional disassembly methods of components in the gearbox.

No.	Components	Quantity	Category	<i>DA</i>	<i>DTI</i>	<i>DM</i>	ProcessTime
S1	3,4,10,22	9	<i>fp</i>	Grasp, Unscrew, Unplug	Screwdriver, Puller, Circlip pliers	H	34
S2	6,9,12	3	<i>ap</i>	Unplug	Circlip pliers	H/R	39/26
S3	7,8,11	3	<i>fp</i>	Place, Grasp, Move, Unplug, Slide, Rotate	Puller, Separators, Circlip pliers	HR	86
S4	5,19,20,23	9	<i>fp</i>	Unscrew, Move, Grasp, Unplug	Screwdriver, Puller, Rubber Mallet, Circlip pliers	HR	42
S5	13-18	6	<i>fp</i>	Place, Grasp, Move, Slide, Unplug, Rotate	Puller, Separators, Circlip pliers	HR	120
2	-	1	<i>fp</i>	Rotate	Wrench	H/R	10/8
21	-	1	<i>ap</i>	Grasp, Unplug	Puller, Circlip plier	H	15

5.4.3 Optimal HRCDD Scheme of The Gearbox

This subsection delineates the generation of all viable disassembly sequences and identifies the optimal scheme for human-robot collaborative disassembly of the gearbox, employing the methodologies introduced in this study.

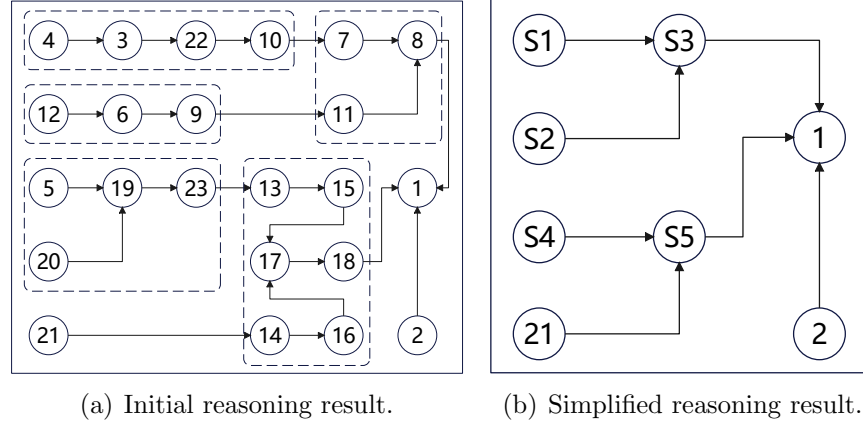


Figure 5.10: Precedence constraints of the gearbox.

Moreover, a selection of basic heuristic optimisation algorithms is utilised as benchmarks to illustrate the enhanced efficacy of our proposed approach.

Our Approach

Utilising the simplified component precedence constraints, accessory part S2 was initially designated as the primary disassembly task. Application of Rule 67 revealed that S2 could be disassembled simultaneously with functional part 2. Following the workflow described in Section 5.3.4, this analysis led to the generation of two viable disassembly solutions, labelled Solution 1 and Solution 2, which are detailed in Table 5.10.

Table 5.10: Optional HRCd sequence schemes.

No.	Disassembly sequence	DM	ProcessTime
1	$\langle S2(-X), 2(+Y) \rangle \rightarrow 21(-Z) \rightarrow S1(+X) \rightarrow S3(+X) \rightarrow S4(+Y) \rightarrow S5(+Y)$	$\langle H, R \rangle \rightarrow H \rightarrow HR \rightarrow HR \rightarrow HR \rightarrow HR$	336
2	$\langle S2(-X), [2(+Y), 21(-Z)] \rangle \rightarrow S1(+X) \rightarrow S3(+X) \rightarrow S4(+Y) \rightarrow S5(+Y)$	$\langle R, [H] \rangle \rightarrow H \rightarrow HR \rightarrow HR \rightarrow HR \rightarrow HR$	308

In Solution 1, the disassembly task involving accessory part S2 is undertaken by a human operator, whereas a robot performs the disassembly of

functional component 2. This configuration yields a total disassembly time of 336 time units. In contrast, Solution 2 proposes the robotic disassembly of accessory part S2 in parallel with the human-led disassembly of functional component 2. This arrangement allows the human to commence the disassembly of the subsequent accessory part 21 immediately upon completing their initial task, optimising workflow continuity. The efficient synchronisation achieved in Solution 2 reduces the total disassembly time to 308 units, thereby establishing it as the more efficient option.

Comparison Experiments

This case study pioneers the resolution of the HRCD sequence planning problem by integrating an ontology model with a rule-based reasoning approach. Using a gearbox as a case study, the case study develops an optimal disassembly scheme through this novel method. In the absence of directly comparable methodologies to validate the superiority of the proposed approach, this case study assesses its feasibility and effectiveness through comparative analysis with established optimisation algorithms.

The review paper [133] identifies several prominent and frequently utilised techniques for HRCD sequence planning and task allocation, including genetic algorithm (GA), artificial bee colony (ABC), ant colony optimisation (ACO), particle swarm optimisation (PSO), linear programming (LP), and Tabu search (TS). Given that linear programming demands a formal mathematical model which falls outside the scope of this case study, the compar-

ative experiment in this study will focus on the remaining five algorithms.

The disassembly-related data and alternative disassembly techniques presented in Table 8.3 serve as inputs for this chapter. Additionally, the precedence constraints depicted in Figure 5.10 are incorporated as constraints within the analysis. Tasks lacking precedence constraints are capable of being disassembled concurrently with other tasks using various directions and methods. Furthermore, the consideration of subassemblies is omitted in these optimisation algorithms.

The primary objective of the comparative experiment discussed herein is to evaluate the feasibility and effectiveness of the method proposed. The detailed design, parameter configuration, and performance optimisation of the optimisation algorithms are not within the focus of this investigation. Consequently, this study utilises five representative optimisation algorithms sourced from an open-source library (details available in Appendix 8.3), with parameters configured to their default settings as stipulated by the library. These parameter settings are detailed in Table 5.11.

For the comparison experiment described, the number of iterations is established at 1000, which constitutes one criterion for termination. Another termination condition is met if a solution is identified during these iterations and remains unchanged in the subsequent four iterations; at this juncture, the iterations cease, and the prevailing solution is deemed optimal. To verify the fairness and efficacy of these optimisation algorithms, 20 experiments were conducted under identical conditions. The results of the optimal experiments

Table 5.11: Parameter settings for comparison experiments.

Method	Parameters	Values	Method	Parameters	Values
TS	Number of iterations	1000	ABC	Population size	50
	Number of neighbours	10		Number of iterations	1000
	Tabu size	10		N_limits	25
GA	Population size	50	AC	Population size	50
	Number of iterations	1000		Number of iterations	1000
	Crossover Probability	0.9		Sample count	25
	Mutation Probability	0.1		Intent factor	0.5
PSO	Number of iterations	1000		Deviation distance ratio	1.0
	Local coefficient	2.05			
	Global coefficient	2.05			
	Inertia factor	0.4			

are displayed in Table 5.12.

Table 5.12: Comparison experiment results.

No.	Disassembly sequence	Direction Change Times	ProcessTime
TS	12(-X)→21(-Z)→5(+Z)→14(-Z)→20(+Z)→16(-Z)→	19	311
	4(+X)→6(-X)→19(+Z)→3(+X)→22(+X)→9(-X)→		
	23(+Z)→10(+X)→11(-X)→13(+Z)→15(+Z)→2(+Y)→		
	17(+Z)→7(+X)→18(+Z)→8(+X)		
ABC	12(-X)→20(+Z)→6(-X)→4(+X)→5(+Z)→3(+X)→	12	314
	22(+X)→19(+Z)→23(+Z)→9(-X)→11(-X)→13(+Z)→		
	15(+Z)→21(-Z)→14(-Z)→16(-Z)→17(+Z)→18(+Z)→		
	2(+Y)→10(+X)→7(+X)→8(+X)		
AC	20(+Z)→12(-X)→6(-X)→4(+X)→21(-Z)→3(+X)→	13	315
	9(-X)→2(+Y)→14(-Z)→5(+Z)→19(+Z)→22(+X)→		
	10(+X)→7(+X)→11(-X)→8(+X)→16(-Z)→23(+Z)→		
	13(+Z)→15(+Z)→17(+Z)→18(+Z)		
PSO	2(+Y)→4(+X)→3(+X)→21(-Z)→12(-X)→22(+X)→	12	319
	10(+X)→6(-X)→20(+Z)→9(-X)→11(-X)→7(+X)→		
	8(+X)→14(-Z)→5(+Z)→19(+Z)→16(-Z)→23(+Z)→		
	13(+Z)→15(+Z)→17(+Z)→18(+Z)		
GA	12(-X)→4(+X)→2(+Y)→5(+Z)→3(+X)→20(+Z)→	15	313
	19(+Z)→6(-X)→9(-X)→21(-Z)→11(-X)→14(-Z)→		
	8(+X)→13(+Z)→15(+Z)→22(+X)→10(+X)→7(+X)→		
	23(+Z)→16(-Z)→17(+Z)→18(+Z)		
Ours	{S2(-X), [2(+Y), 21(-Z)]}→S1(+X)→S3(+X)→S4(+Y)→S5(+Y)	3	308

The table outlines the results of disassembly sequences obtained using five representative optimisation algorithms. The outcomes for *ProcessTime* are relatively consistent, ranging between 310 and 320 units. Among these, TS

demonstrates the greatest efficiency with a process time of 311 units, closely approaching the optimal result. GA, ABC, ACO exhibit process times of 313, 314, and 315 units respectively. Conversely, PSO records the highest process time at 319 units, indicating a minor delay in comparison to the other algorithms. It is important to note that none of the algorithms assessed were able to match the optimal process time of 308 units achieved by our proposed method.

In the conducted comparison experiment, no specific preferences or restrictions were placed on the disassembly direction, yet the selected algorithms proposed various initial disassembly directions. For example, TS, ABC, and GA commence disassembly in the -X direction for the same task, whereas PSO and ACO initiate in the +Y and +Z directions, respectively. Each algorithm results in over 10 directional changes throughout the disassembly process. Such frequent changes in direction can escalate time and labor costs and pose increased safety risks, which are sub-optimal for practical disassembly operations. In contrast, our method, which is informed by expert knowledge and specific disassembly preferences, tends to execute successive operations in consistent directions, significantly reducing directional changes to only three throughout the disassembly process.

The representative optimisation algorithms exhibit inherent limitations stemming from their default parameter configurations. These algorithms necessitate additional adjustments to their parameters to enhance the quality of solutions and approach the global optimum more closely. The absence

of expert insights and real-world context complicates the parameter tuning process, making it both challenging and uncertain. The notable benefits of our proposed method, as demonstrated in the comparative analysis, are summarised in Table 5.13.

Table 5.13: Comparison between our method and optimisation algorithms.

	Our method (OM)	Optimisation algorithms (OAs)
Principle	OM is proposed based on SWRL rules, which are a formal semantic expression derived from expert knowledge and real-world scenarios.	OAs are proposed based on a defined objective function and are subject to various constraints, but they lack expert knowledge and descriptions of real-world scenarios.
Procedure	Transparent and explicit.	Opaque
Predictability	OM reasoning outcomes are predictable. Outcomes are consistent as long as the input conditions are the same.	The results of OAs are unpredictable due to the randomness of OAs.
Traceability	OM is easy to trace back to specific rules.	OAs act as a black box, and the intermediate processes are hard to trace.
Complexity	The semantic expressions and SWRL rules in OM are easier to implement and understand.	OAs are more complex to implement, which require algorithm design and constant adjustment of parameters.
Replicability	The SWRL rules in OM can directly encode, store, and integrate the expert knowledge into different scenarios.	OAs are designed, and parameters are adjusted to a specific scenario.
Optimisation Result	OM can generate an exact optimal solution.	OAs generate a near-optimal solution and are unable to confirm that the solution is optimal.

5.5 Chapter Summary

This chapter introduces a human-robot disassembly ontology model along with a rule-based reasoning method aimed at identifying the optimal disassembly scheme for EoL products. This model develops a standardised and semantically structured framework that represents disassembly precedence constraints and various optional disassembly methods for each component of EoL products. Relative to methodologies developed in other studies [104, 105], the approach adopted in this chapter exhibits several innovative

aspects:

1. This chapter marks the initial development of a generalised ontological semantic model tailored for HRC D environments. The methodology introduced here is broadly applicable and versatile. Leveraging the HRC D ontology, it allows for the semantic representation of any mechanical product or disassembly scenario through structured language. This approach is distinguished by its flexibility and efficiency, enhanced by the incorporation of product-specific information.
2. This chapter advances the categorisation of product components, building on existing methodologies that typically distinguish between functional parts and fasteners. Such traditional classifications aid in establishing disassembly priority constraints derived from product topology but often prove too broad, complicating the retrieval of specific component information. In response to the nuances of HRC D in remanufacturing contexts, this study introduces a refined three-tier division: functional parts, accessory parts, and fasteners. While this more detailed classification increases the complexity of constructing product topology and defining disassembly priority constraints, it significantly enhances the accessibility of component-specific information and supports informed decision-making in subsequent remanufacturing processes.
3. Contrary to conventional heuristic optimisation algorithms, this chap-

ter employs semantically constructed disassembly rules to infer and establish the optimal sequence and scheme for HRCd. These rules are expressible through SWRL/SQWRL, facilitating interaction between computers and robots. Effective reasoning with these rules generates viable disassembly sequences, ensuring the creation of high-quality, executable disassembly plans suitable for complex mechanical devices. Furthermore, the development of rules grounded in semantic principles enhances both the flexibility and efficiency of the disassembly process.

The effectiveness of the proposed method is confirmed through a case study and comparative experiments. In comparison with six fundamental optimisation algorithms, this method registers the minimal process time of 308 units and the least number of directional changes, totalling three. Additionally, this approach promotes the integration, dissemination, and augmentation of disassembly knowledge, thereby providing a versatile methodology for formulating disassembly solutions for diverse EoL products.

By standardising and modularising the modelling and management of EoL products, the impact of inherent uncertainty can be mitigated. Furthermore, the contributions of this chapter have the potential to significantly enhance the efficiency and performance of the disassembly process within the CPRS at the individual-level.

6

Large-language model for Human-Robot Collaborative Disassembly Sequence Planning and Analysis in CPRS

6.1 Introduction

Remanufacturing represents a critical approach within the proposed smart manufacturing frameworks, marking a shift toward sustainable and circular economic practices [15]. This process encompasses various manufacturing stages that rejuvenate EoL products to a functional state equivalent to, or

better than, new items [188]. By amalgamating used and new components, remanufactured products not only prolong their service life but also diminish the need for raw materials [189]. Furthermore, remanufacturing enhances the lifespan of EoL products, aiding in the conservation of resources, reduction of manufacturing expenses, and mitigation of environmental impacts.

The initial and vital step in the remanufacturing process is disassembly, which involves separating a product into its individual components [190]. This stage is essential for the effective remanufacturing of products, as it facilitates the recovery and refurbishment of parts that possess remaining utility and significant residual value. In contrast to the disassembly methods used in routine maintenance or recycling, remanufacturing requires non-destructive techniques that maintain the integrity and value of each component [191]. Non-destructive disassembly prevents damage to high-value parts. Additionally, by dismantling products into separate units for thorough inspection and assessment, remanufacturing ensures the enhanced performance of the final remanufactured product, serving as a critical quality control measure within the process.

Disassembly, a divergent process, involves numerous potential sequences for dismantling EoL products into their constituent parts [192]. Complex and larger EoL products often present a multitude of optional disassembly sequences, posing challenges in planning and identifying the most effective approach. Traditionally, the planning and sequencing of disassembly tasks were predominantly guided by the expertise and intuition of engineers [193],

a method that, despite its reliance on skilled professionals, could fall short in consistently achieving the most effective outcomes. With advancements in technology, heuristic optimisation algorithms have become a leading strategy in orchestrating disassembly tasks. Although these algorithms provide significant flexibility and are widely applicable, they often lack transparency, and their results may not always be optimal [194]. To address these limitations, knowledge-based models have been developed. These models utilise explicit rules and heuristics derived from expert insights to guide the disassembly process [195]. While more systematic and reliable than intuition-based methods, these models might not possess the necessary flexibility or adaptability to handle complex or unexpected scenarios effectively.

Disassembly of EoL products inherently involves unpredictability and uncertainty due to their variable conditions [196]. Engineers often encounter unfamiliar equipment and EoL products, which necessitates a thorough understanding of its structure and the determination of optimal disassembly techniques. Although their prior experience is invaluable, it may not consistently provide reliable guidance due to the unique and complex nature of each task. In such situations, engineers typically search for advice or references to aid their decision-making processes. However, finding and locating reliable sources can prove challenging. Conventional knowledge databases and manuals may not cover specific or unusual scenarios, and peers or experts are not always available for consultation [197]. Moreover, the relevance of the available advice might vary with the specific circumstances and conditions

at hand. This uncertainty and the scarcity of dependable information underscore the need for more advanced and flexible tools in disassembly planning.

The emergence of Large Language Models (LLMs) has attracted significant attention worldwide [198]. These models hold potential for enhancing disassembly planning due to the rich semantic content inherent in disassembly sequences. Utilising LLMs to field queries about these sequences can offer diverse insights, though the responses may sometimes embody uncertainty [199]. The principal challenge involves effectively utilising the deep knowledge within LLMs to facilitate the planning of disassembly sequences, a problem that has yet to be fully resolved.

In response to these challenges, this paper proposes the development of an LLM-based Bayesian Network designed to produce a robust human-robot collaborative disassembly sequence planning (HRCDSP) with accompanying explanations and qualifications of uncertainty. This approach entails a dynamic interaction between the Bayesian Network and the LLM, orchestrated through a Generative Adversarial Network (GAN). The primary contributions of this initiative are outlined as follows:

1. A disassembly constraint graph-based Dirichlet Bayesian Network (DiBN) was developed for HRC sequence planning. This method represents the HRC process as a graph and quantifies uncertainties using posterior probability distributions. The Dirichlet distribution is particularly apt due to its capacity to effectively depict the logical event space inherent in HRC processes.

2. A novel evaluation method for HRC D sequences was developed using a LLM that has been fine-tuned with domain-specific knowledge in HRC D. To maintain the consistency of the outputs from the LLM and reduce potential biases, a customised prompt strategy is employed. This approach enhances the robustness of the responses generated by the LLM.
3. A GAN framework was adapted to facilitate the synergistic integration of DiBN and LLM. Within this framework, the responses from the LLM are utilised to update the DiBN based on defined criteria. This integration allows the DiBN, which is a reliable planner for HRC D, to effectively assimilate and incorporate valuable knowledge from the LLM's output, leveraging open-source information.

6.2 Methodology

6.2.1 Problem Statement

This chapter aims to develop a robust and effective disassembly sequence for handling unfamiliar tasks, as depicted in Figure 6.1. Initially, a disassembly graph is constructed, serving as the foundational guideline for the disassembly task. This graph, however, presents multiple potential sequences. Selecting and determining the optimal sequence becomes a subsequent challenge. As the graph represents an ontological structure of the disassembly constraint graph (DCG), it is convertible into the DiBN for quantitative

analysis. In this conversion, a starting node based on the DCG structure is incorporated into the DiBN. Sampling efforts initiate from this starting node, progressing to the base of the DiBN before restarting, with a mechanism to mark nodes post-sampling to avoid repetition. Given the limited availability of validated sequence labels, the probability estimates remain uncertain yet necessary. To address this, a reinforcement learning strategy using a GAN is proposed. This method leverages a LLM to predict subsequent disassembly steps based on the current state, while feedback or rewards from the system adjust the prompts and probabilities in the Bayesian network. This integrated approach allows engineers, using a given DCG, to deduce the optimal disassembly sequence through reasoning facilitated by an LLM-enhanced Bayesian Network.

Given that the disassembly graph embodies an ontological structure, it can be converted into a Bayesian network for quantitative analysis. However, the calculation of independent probabilities remains uncertain and unreliable due to the limited availability of validated ground truth data. To address this challenge, a reinforcement learning (RL) approach is introduced. This method utilizes a LLM to predict the subsequent part to disassemble based on the current state of assembly. Concurrently, feedback or rewards from the environment are used to adjust the prompts and probabilities within the Bayesian network. Employing this process, engineers can use the disassembly graph to estimate the optimal disassembly sequence by querying the LLM with specifically tailored prompts.

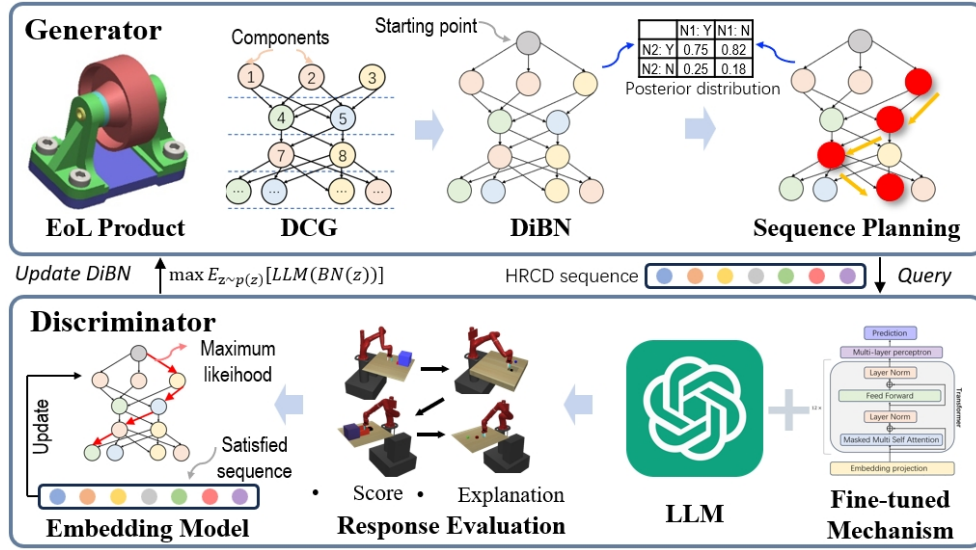


Figure 6.1: Workflow of the Proposed LLM-based DiBN Model.

6.2.2 Generated Disassembly Graph

The proposed method entails developing a disassembly graph that visualises the disassembly process. This graph encapsulates the hierarchical organisation of components, delineates their interrelationships, and sequences the operations involved [200]. The notations employed are described as follows:

Nodes N : These denote the components within the assembly, with each node being allocated a level (L) reflective of its hierarchical positioning

Edges E : These illustrate the interconnections between components, differentiated into two categories:

Solid edges E_s : Indicate contact relationships among components.

Dashed edges E_d : Signify non-contact relationships between components.

Hierarchical Structure of Components

In the proposed graph model $G(N, E)$, components N are arranged hierarchically. Each component is assigned a level L that reflects its dependencies. Components at higher levels, which require the prior disassembly of those at lower levels, are positioned higher within the hierarchy. This hierarchical organisation governs the precedence sequence of the disassembly process.

Relationships of Components

The graph also delineates both contact and non-contact relationships among components of EoL products via edges E . Contact relationships, denoted by solid edges E_s , indicate a physical linkage between components, requiring that a component connected by a solid edge be removed before or concurrently with its adjacent component. Non-contact relationships, depicted by dashed edges E_d , represent logical associations among components that do not engage physically but are interconnected through the sequence of disassembly operations. Recognising these non-contact relationships is crucial for identifying concealed dependencies and potential bottlenecks within the disassembly process.

AND/OR Precedence of Components

The established graph model integrates both AND/OR precedence relationships among components of EoL products. AND precedence occurs when multiple components are capable of being disassembled simultaneously, illustrated by parallel edges emanating from a single node within the graph.

OR precedence is presented through alternative paths emanating from one node to others, indicating a variety of viable sequences for disassembling components. This versatility proves beneficial under different conditions or constraints.

Figure 6.2 provides an illustrative example of component relationship of a satellite, whose disassembly process can be modelled in this format. Such a disassembly graph lays the groundwork for subsequent graph embedding training.

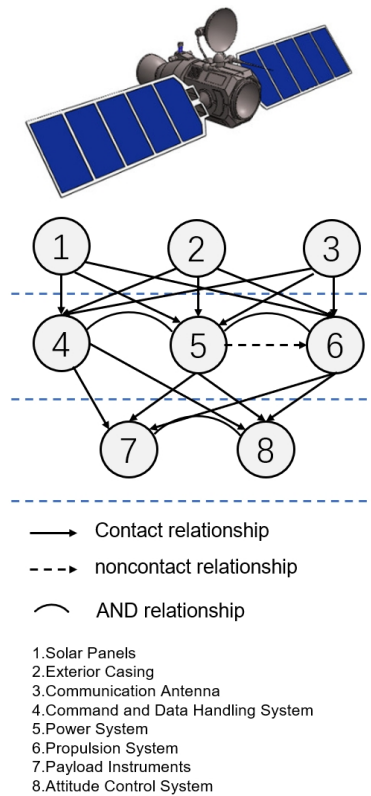


Figure 6.2: Disassembly graph of the satellite.

6.2.3 Disassembly Graph-Based Bayesian Network

The disassembly graph, while comprehensive, might not encompass all possible current scenarios and could present multiple choices within a specific configuration. Consequently, a quantitative analysis method is essential. A Bayesian network is suggested to model the probabilities of various outcomes, with its structure derived from the disassembly graph. The probability estimates within the Bayesian network can be approximated using outputs from a LLM. Therefore, a Bayesian network based on the disassembly graph is proposed, with its parameters determined by sampling from a specified Dirichlet distribution.

The disassembly graph-based Bayesian network is denoted as $B(V, E)$, where V represents the set of node set, while E denoted the edge set.

Based on Bayes' theorem, the calculation of conditional probability can be expressed using the following equation:

$$P(A|B) = \frac{P_j(A, B)}{P(A)}, \quad (6.1)$$

where P_j is the joint probability, $P(A|B)$ represents the dependent probability. It can also represent as $P(A|B, C...Z) = \frac{P_j(A, B, \dots, Z)}{P(B, \dots, Z)}$ if this equation involves more than two nodes for its inference. To minimise uncertainty, each conditional probability is modelled using a Dirichlet distribution, the parameters of which are influenced by the sample data:

$$P(A = x_i | B_j, C_k \dots Z_l) = \text{Dirichlet}(x; \alpha), \quad (6.2)$$

where $x = (x_1, x_2, \dots, x_m)$, m is the number of X 's condition. B_j , C_k , and Z_l denotes the specific condition of B , C and Z , respectively.

Within the sequential environment, feedback in the form of a reward is provided to the Bayesian network to facilitate parameter updates. Specifically, if a reward surpasses a predefined threshold—indicative of a satisfactory sequence—then a maximum likelihood approach is employed to update the parameter.

$$L(\theta | X) = \prod_{i=1}^n P(x^i | \theta), \quad (6.3)$$

In this context, X represents a set of observed data points x^1, x^2, \dots, x^N , where each x^i denotes the specific condition of event x .

Upon finalising the graph structure, accurately determining the dependent probability becomes challenging. The LLM can be utilised to approximate both dependent and independent probabilities. Additionally, the reward score provided by the environment serves to update these probabilities.

6.2.4 LLM-based sequence planning

Given the current state, the LLM can estimate the probability of the next action using a customised prompt. In the context of remanufacturing disassembly, this action must be evaluated concerning various factors, including

environmental impact, cost, and time duration. As illustrated in Fig. 6.3, an engineer will engage with the LLM by submitting the disassembled object and a proposed sequence, anticipating both an evaluation score and an explanatory output from the LLM.

To prevent and reduce the occurrence of illogical comments and unstable scores, a Prompt Rephraser and random trials are implemented to create comparable prompts that query the LLM for evaluating the HRCD sequence, as depicted in Fig. 6.3. After numerous iterations, the system compiles and reviews the evaluated results, assessing score stability (targeting a variance less than 5). Should the scores demonstrate stability, the system randomly selects one record to represent the final output. This approach strengthens the system's robustness and applies constraints informed by the domain knowledge encapsulated within the DiBN.

6.2.5 GAN Based HRCD Sequence Planning

The aforementioned modules can be synthesized into the GAN framework, wherein the Bayesian Network (BN) functions as the Generator and the LLM acts as the Discriminator. Within this framework, the BN is capable of generating a potential sequence through the described process, while the LLM assesses this sequence from various viewpoints.

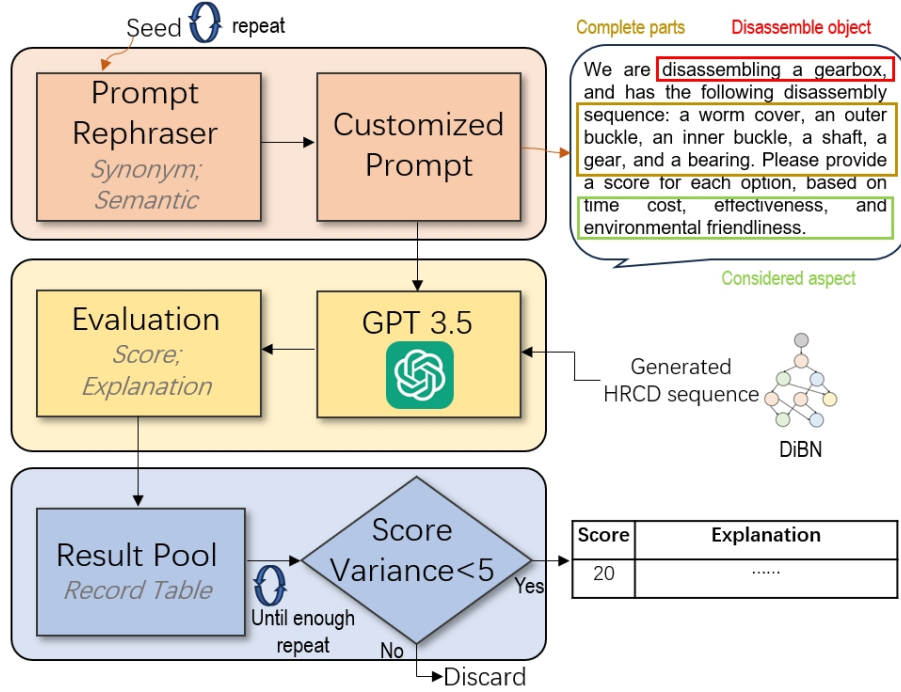


Figure 6.3: The querying process of the LLM.

$$\min_{DiBN} \max_{LLM} = \mathbb{E}_{s \sim p_s(s)} [\text{Log} LLM(s)] + \mathbb{E}_{z \sim p_z(z)} [\text{Log}(1 - LLM(DiBN(z)))], \quad (6.4)$$

Where z represents the random noise sample drawn from a prior distribution $p_z(z)$, s denotes the feasible sequence generated by the DiBN, and p_s signifies the effective sequence space. Additionally, $DiBN(z)$ is the sequence generated by the Bayesian network from the noise sample z , and $LLM(DiBN(z))$ is the evaluation score assigned by the fixed discriminator

to the generated sequence.

During the training phase, a batch of sequences $S = s_1, s_2, \dots, s_n$ is generated by the DiBN and evaluated by the LLM, which assigns scores to each sequence, denoted as $D(s_i)$ for the score of sequence s_i . From the batch S , sequences $S_{high} \in S$ that exceed a predefined score threshold or are among the top-k highest scoring are selected. These sequences are deemed most informative for the generator’s learning process, representing the most promising HRCD sequences according to the LLM’s evaluation. The selected sequences S_{high} are subsequently used to refine the DiBN, enhancing its probability distributions to more effectively generate realistic and efficient disassembly sequences. This iterative process continues until a satisfactory level of performance is reached. Algorithm 2 outlines a unified pipeline summarising the key steps of this methodology.

Algorithm 2 Unified Pipeline of LLM-based HRCD sequence generation

Input: DCG : Disassembly constraint graph; $Prompt$: Tailored prompt;

Output: $HRCDsequence$: HRCD sequence from well-trained DiBN

```
1: Transfer  $DCG$  into  $DiBN$ ;
2: Score_list = [0,0,0,0,0];
3: while Average (Score_list[:-5]) < 90 do
4:   HRCD sequence=Sampling ( $DiBN$ )
5:   Text = LLM Query (HRCD sequence)
6:   Score, Explanation = Extract (Text)
7:   Score_list.extend (Score)
8:   if Score > Threshold then
9:     Update  $DiBN \leftarrow$  HRCD sequence
10:  end if
11: end while
12: Final HRCD sequence = Sampling n( $DiBN$ )
```

6.3 Case Study

6.3.1 Case Study I: belt roller

The initial case study examines the disassembly process of a belt roller within the HRCDF framework. A detailed breakdown of the disassembly components is provided in Table 6.1, where DM denotes the disassembly method. This method may involve a human (H), robot (R), or a combined human-robot effort (HR). The disassembly planner, based on their expertise, assigns each disassembly task to an appropriate agent, as represented by the various colours in the DCG depicted in Fig. 6.4. Furthermore, an illustration of the DCG for the belt roller, which reflects both the structural composition and prior disassembly experiences, is positioned in the lower right corner of the referenced figure.

Table 6.1: Component list of the belt roller.

ID	Name	DM	ID	Name	DM
1	Bolts	H/R	5	Left Bush	R
2	Left Bracket	H/R	6	Right Bush	H/R
3	Right Bracket	H/R	7	Shaft	H
4	Base	R	8	Roller	HR

The DiBN is constructed using the DCG tailored to the precedence constraints of the belt roller. This BN initially creates potential and optional disassembly sequences through graph navigation, though these initial sequences may be sub-optimal. These sequences undergo evaluation by a LLM using the specified prompt. The feedback from the LLM is then employed to en-

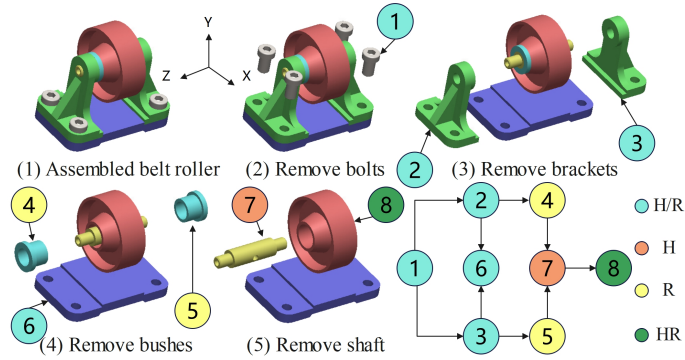


Figure 6.4: Structure and precedence constraints of the belt roller.

hance the DiBN model iteratively, with each cycle of feedback considered a distinct step in the refinement process. Figure 6.5 illustrates this process: the blue curve represents the sequence generation by the DiBN prior to LLM integration, following the default probabilistic pathways. Conversely, the orange curve displays the sequence outcomes post LLM integration, showing initial similarity but diverging significantly after continued refinement. After ten steps of incorporating high-scoring sequences, the DiBN demonstrates a marked improvement in sequence quality. This divergence becomes particularly pronounced in the latter five steps, underscoring the impact of LLM-based refinement on the DiBN’s performance.

The efficacy of the training regimen and the enhancements made by the newly proposed DiBN are demonstrated through a comparative analysis with the original BN. This analysis is visually represented by the loss curves of both models as depicted in Fig. 6.6. The loss curves reveal that the DiBN

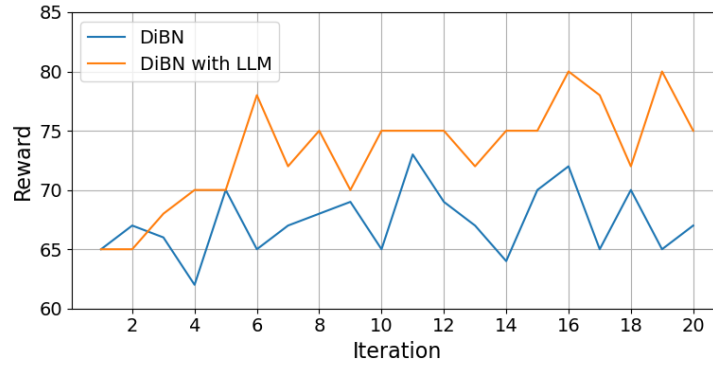


Figure 6.5: Reward comparison between DiBN with and without LLM in belt roller HRCDSP.

not only converges more rapidly but also attains a lower overall loss, albeit with some fluctuations. Such a visual comparison distinctly underscores the improvements in both training efficiency and model accuracy facilitated by the modifications implemented in the DiBN.

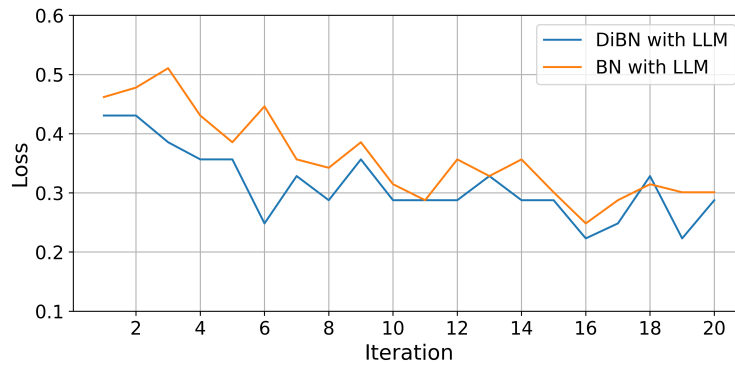


Figure 6.6: Training Loss comparison in belt roller HRCDSP.

To address the uncertainties associated with the LLM, the DiBN incorporates a latent space, as outlined in the preceding section. A sampling method is employed to assess this latent space, and Fig. 6.7 displays several repre-

representative conditional probabilities within the BN. The X-axis represents the directional flow of these probabilities. For example, the notation ‘N1→N2’ indicates the probability of proceeding with ‘N2’ when the witnessed evidence is ‘N1’. As illustrated in Fig. 6.7, the conditional probability of ‘N1→N2’, whether to disassemble ‘N2’ or not, shows minimal variance (0.52 vs. 0.48). This reflects practical scenarios where, following the disassembly of ‘N1’ (bolts), the subsequent removal of either the left or right bracket is equally feasible. Conversely, the conditional probability for ‘N7→N8’ is significantly higher, which is logical given that the shaft is positioned inside the roller, making sequential disassembly a practical approach. These probabilities help to quantify and mitigate the uncertainty associated with each decision in the disassembly process.

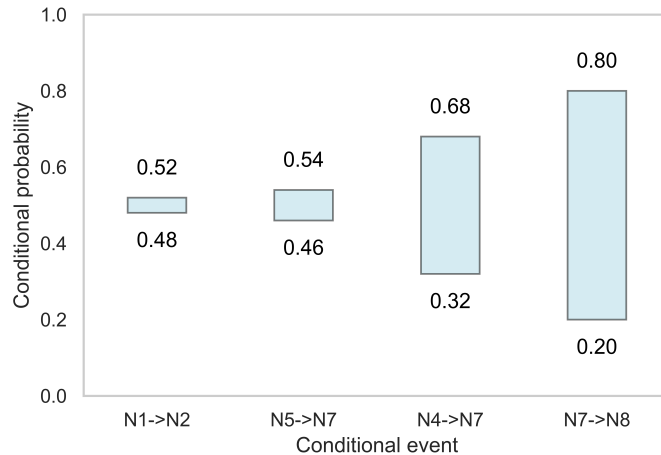


Figure 6.7: Conditional probability of disassembly events in belt roller.

The established HRCDD planning method does not necessitate the inclu-

sion of additional attributes within the DCG, such as time expenditure or economic costs, which are circumvented by the use of a LLM. To assess the efficacy of this method, it is benchmarked against various advanced models, including Topological Sorting [201], Greedy Search [202], Depth-first Search (DFS) [203], and Breadth-first Search (BFS) [204]. Given that the focus of this comparison is the HRC sequence, the Kendall Rank Correlation Coefficient [205] and Spearman's Rank Correlation [206] are utilised to gauge the performance of each model, providing a statistical measure of their relative effectiveness.

Figure 6.8 illustrates that the LLM-DiBN method outperforms others in terms of the Kendall and Spearman correlation metrics, achieving scores close to 1. This indicates that the proposed method is capable of generating HRC sequence plans that closely match the optimal ground truth plans. Nevertheless, the performance differential between the methods is not substantial. A plausible explanation for this minor discrepancy is the relatively simple structure of the belt roller, characterised by a limited number of EoL components and parts.

6.3.2 Case Study II: gearbox

In the second case study, the disassembly of a gearbox is examined, as depicted in Figure 5.8 (Chapter 5, Section 5.4). This gearbox consists of 23 components that require disassembly, details of which are summarised in Table 8.3 (Appendix 8.2).

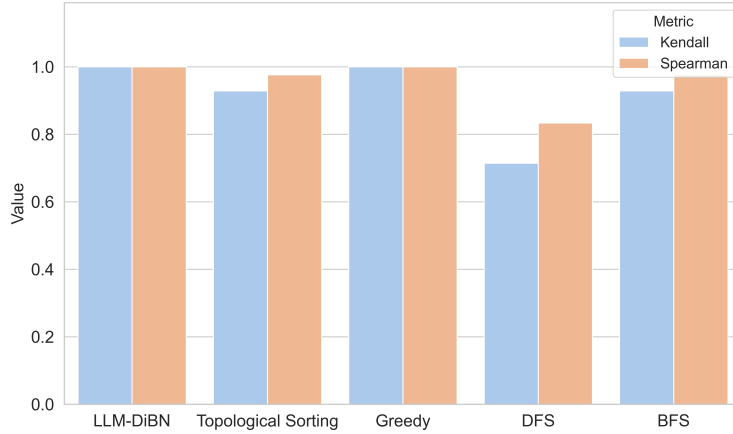


Figure 6.8: Cutting-edges methods comparison for belt roller HRCDSP.

The DCG for the gearbox is redefined and updated based on the mechanical structure and precedence disassembly constraints, as illustrated in Fig.6.9. Utilising a similar approach as in the first case study, the DiBN is refined with high-scoring sequences following evaluation by a LLM. Figure6.10 displays the variability in rewards, where the traditional DiBN, initiated randomly, shows fluctuating results without notable improvement. Conversely, the DiBN that incorporates feedback from the LLM exhibits a consistent upward trend. In later stages, this LLM-enhanced DiBN significantly surpasses the performance of the original model. This outcome suggests that incorporating an LLM as a discriminator enhances the logical structuring of the disassembly sequences. Notably, the disparity in performance during later iterations is more pronounced than observed in Fig. 6.5. This is likely due to the gearbox’s complexity, which consists of 23 components, creating a larger HRCDSpace compared to the six components in the belt roller from the first

case study.

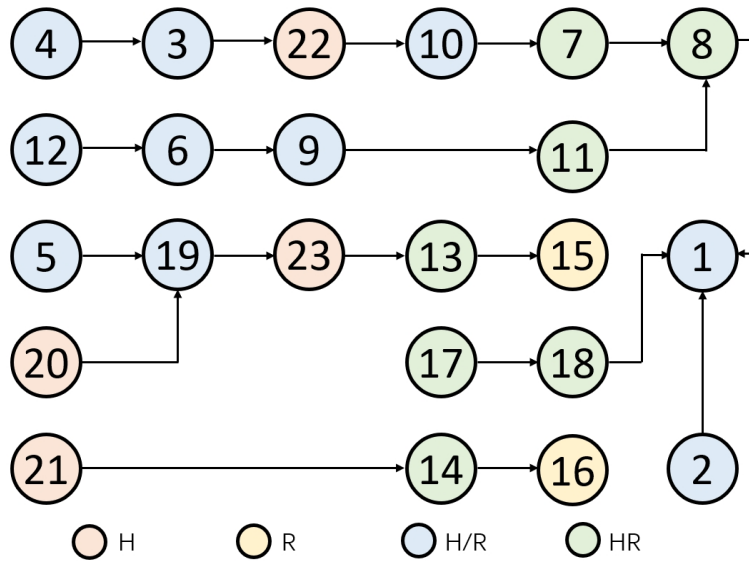


Figure 6.9: Precedence constraints graph of the gearbox.

Statistical sampling is employed to assess the latent space for uncertainty quantification within the DiBN of a gearbox. Figure 6.11 presents various typical conditional probabilities. For instance, the conditional probability of transitioning from ‘N4→N3’ shows minimal variation between the options of disassembling ‘N4’ or not (0.65 vs. 0.35). This scenario mirrors practical conditions where, subsequent to the removal of ‘N4’, a screw, the disassembly of other external components such as ‘N12’ and ‘N21’ is feasible. In contrast, the conditional probability of ‘N9→N11’ is markedly higher, reflecting the proximity of the inner buckle to the bearing, which can be disassembled without the need for additional tools or extensive effort.

The conditional probability of disassembling a specific component cor-

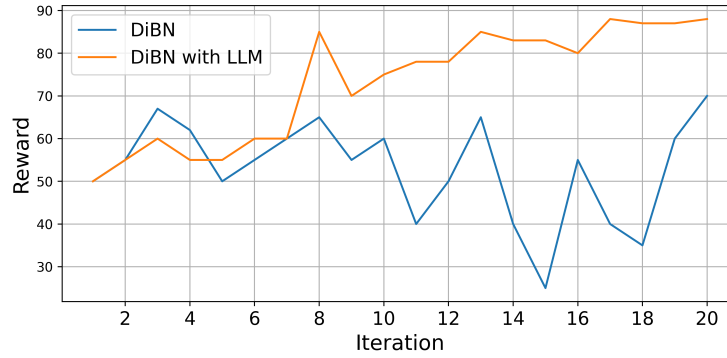


Figure 6.10: Reward comparison between DiBN with and without LLM in gearbox HRCDSP.

relates positively with the accumulation of observed evidence. Figure 6.12 delineates the conditional probabilities for various disassembly nodes, highlighting three particular components (Node 3, Node 6, and Node 14) for detailed examination. The X-axis denotes the count of evidence observed for each node. For example, one piece of evidence for Node 3 implies observation of its parent node (N4), whereas two pieces of evidence might indicate that two other nodes, such as Node 5 or Node 20, have been disassembled. An averaging approach is utilised to calculate the conditional probability of Node 3 given two pieces of evidence, and similar calculations apply to other nodes. As depicted in Fig. 6.12, there is a discernible upward trend in the conditional probabilities as the evidence increases. This pattern is consistent with established disassembly practices where, for instance, Node 3 is a potential candidate for removal following the disassembly of Node 4, but its immediate removal is not obligatory as alternatives like Nodes 12, 5, and 20

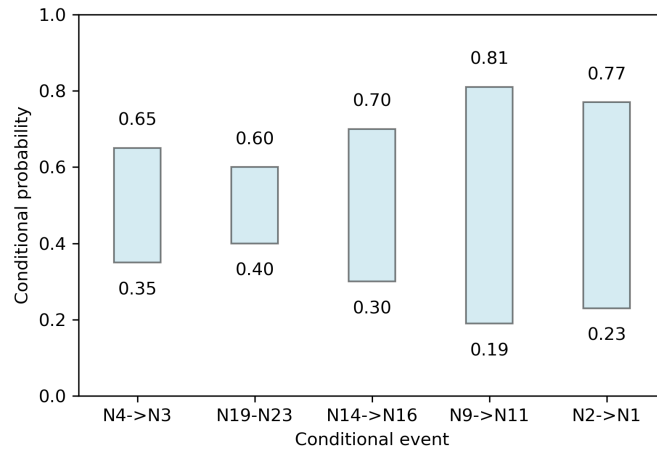


Figure 6.11: Conditional probability of disassembly events in gearbox.

are also viable subsequent steps.

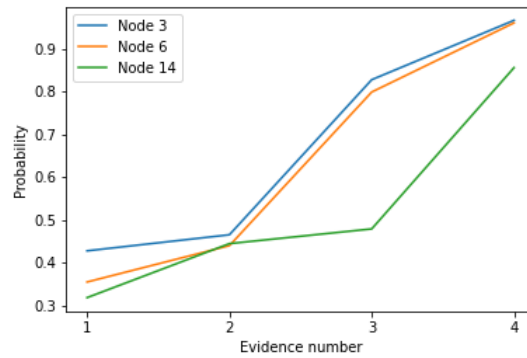


Figure 6.12: Condition probability with increase evidence in gearbox.

As Case Study I, the performance of the DiBN is benchmarked against the original BN model by analysing their respective loss curves during the training phase. Figure 6.13 illustrates comparable outcomes, with the DiBN demonstrating quicker convergence and achieving a lower loss. Both models

show a pronounced downward trend in loss, more significant than in Case Study I, which underscores the improvements in training efficiency and model accuracy achieved with the DiBN implementation.

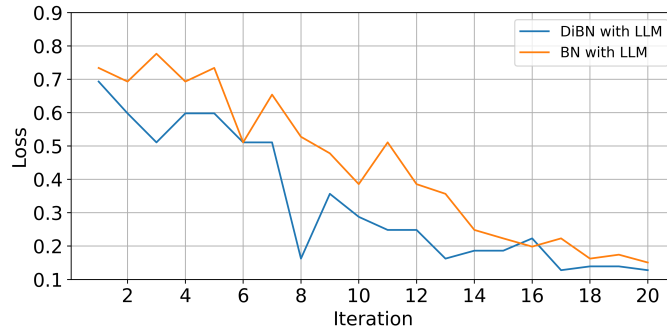


Figure 6.13: Training Loss comparison in gearbox HRCDSP.

To demonstrate the efficiency of the proposed method, it is evaluated against other advanced methods, employing a similar approach as in Case Study I. Figure 6.14 shows that the proposed LLM-DiBN method outperforms the others, achieving the highest scores in both Kendall and Spearman metrics, approximately 0.7.

In contrast to Case Study I, there is a notable performance discrepancy between the proposed method and its counterparts. This difference can be attributed to the gearbox’s complex structure, which comprises 23 components and parts, resulting in a more intricate search space for disassembly planning. This substantial performance gap underscores the efficiency and robustness of the proposed method in handling complex scenarios.

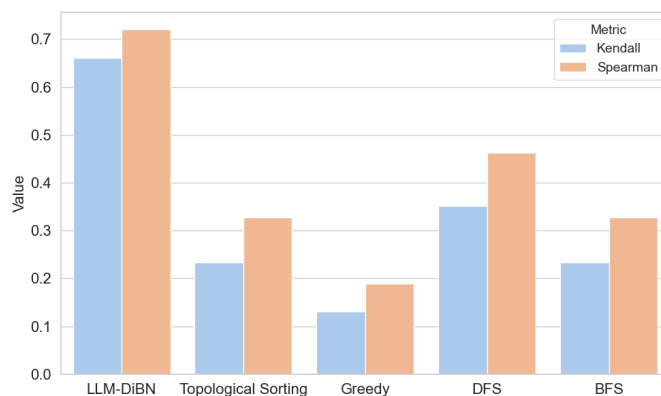


Figure 6.14: Cutting-edges methods comparison for gearbox HRCDSP.

6.4 Chapter Summary

This chapter explores the pioneering integration of LLMs into HRC D within the realm of smart remanufacturing. Initially, the chapter presents an introduction that highlights the importance of integrating advanced AI technologies, such as LLMs, to elevate the efficiency and sophistication of disassembly processes in remanufacturing environments. It emphasises the role of these technologies in bridging communication divides between humans and robots, thus enabling smoother and more intuitive collaborative efforts. In the methodology section, a detailed framework for embedding LLMs into HRC D is delineated, beginning with a problem statement that prepares the groundwork for further developments. This includes the creation of a disassembly graph that lays the groundwork for a Bayesian network. This network models the probabilistic interdependencies among various disassembly tasks. The discussion progresses to the utilisation of LLMs for sequence planning

and introduces the application of GANs in optimising disassembly sequences. This section showcases advanced strategies that utilise the predictive strength of LLMs to manage intricate disassembly tasks effectively.

This chapter also presents two case studies to demonstrate the practical application of the methodologies discussed, illustrating the use of the LLM-embedded HRCD approach in real-world remanufacturing scenarios. These case studies highlight how integrating LLMs and GANs into the disassembly process not only increases the efficiency and flexibility of the disassembly sequences but also enhances the interaction between human operators and robotic systems. The chapter concludes with a reflection on the implications of these research findings, emphasising the transformative impact of incorporating LLMs into HRCD systems on the future of smart remanufacturing. It points out that these technological advancements could foster more sustainable manufacturing practices by enhancing the efficiency of material reuse and recycling through improved disassembly processes, thereby contributing to the circular economy.

7

Conclusions and Future Work

7.1 Recap of The Research

In recapitulating the research outlined across the discussed chapters, this section synthesises the progressive exploration and innovative methodologies developed for enhancing human-robot collaborative disassembly in the context of smart remanufacturing.

Chapter 2 laid the foundational knowledge and state-of-the-art research on Cyber-Physical Production Systems (CPPS), Disassembly Line Balanc-

ing Problem (DLBP), human-robot collaborative disassembly (HRCD) and Large Language Models (LLMs) in HRCD, dissecting their integral role in modern smart remanufacturing. Moreover, the research gaps and challenges and other advanced computational techniques are also discussed and analysed in this chapter.

Moving forward, Chapter 3 detailed proposed a conceptual framework for Cyber-Physical Remanufacturing Systems (CPRS), emphasising the seamless integration of cyber systems with physical manufacturing processes. It mainly focuses on the system level remanufacturing processes management. The discussion on current challenges and future perspectives shed light on the critical areas of EoL product modelling, process planning, and data communication essential for the realisation of efficient CPRS. It mainly focuses on the system level remanufacturing processes management. However, the overall framework of the CPRS is too large which is beyond the research scope of this research. Therefore, the disassembly process, as one of the most important processes in remanufacturing, is focused and determined in following research.

Chapter 4 innovated upon this foundation by proposing a novel simulated annealing-based hyper-heuristic algorithm specifically designed to tackle the stochastic parallel disassembly line balancing problem which is mainly focus on the workshop level, showcasing its effectiveness through comprehensive computational experiments and a practical case study.

Chapter 5 further refined the approach to disassembly planning by in-

roducing an ontology and rule-based method, aimed at facilitating precise and efficient human-robot collaboration in disassembly tasks which is the individual level. Through detailed case studies, this chapter demonstrated the practical application and effectiveness of the proposed methodology in real-world scenarios.

Lastly, Chapter 6 expanded the horizon of human-robot collaborative disassembly (HRCd) by embedding Large-Language Models (LLM) into the disassembly planning process. This chapter explored the establishment of disassembly graphs, the application of Bayesian networks, and innovative sequence planning through generative adversarial networks, culminating in a case study that highlights the transformative potential of LLMs in smart remanufacturing.

Together, these chapters articulate a cohesive and comprehensive research journey, from the foundational understanding of CPPS to the cutting-edge application of LLMs in disassembly planning. This recap underscores the evolution of methodologies and technologies aimed at revolutionising smart remanufacturing through enhanced human-robot collaboration, offering insights into future research directions and the continuous pursuit of sustainability and efficiency in manufacturing processes.

7.2 Research Contributions

The research contributions derived from this thesis are manifold, reflecting significant advancements in the domain of human-robot collaborative dis-

assembly (HRCd) and smart remanufacturing. These contributions can be summarised as follows:

- Established a Conceptual Framework of Cyber-Physical Remanufacturing Systems (CPRS): The development of a conceptual framework for CPRS, as delineated in Chapter 3, contributes to integrating cyber-physical systems and related advanced 'Industry 4.0' technologies within the remanufacturing domain. This framework establishes a practical foundation for subsequent research in smart remanufacturing systems, underscoring the prospective contributions of cloud services and edge computing to augment the efficiency and sustainability of remanufacturing processes.
- Advancements in Optimisation Algorithms for DLBP: Chapter 4 introduces a proposed optimisation algorithm based on simulated annealing hyper-heuristics to address the stochastic parallel disassembly line balancing problem, significantly enhancing the optimisation of disassembly processes. This methodology effectively mitigates the inherent uncertainties associated with disassembly tasks and improves line efficiency, thereby establishing a new benchmark for algorithmic approaches in remanufacturing systems.
- Proposed Ontology Model and Rule-Based Method for HRCd Sequence Planning: The methodology presented in Chapter 5 employs ontology and rule-based reasoning to structure disassembly sequence planning,

offering a systematic and efficient approach to managing complex disassembly tasks. This contribution enhances human-robot collaboration in disassembly processes by providing a transparent and systematic framework for knowledge representation and decision-making, thus improving operational efficiencies.

- **Integration of Large Language Models in HRCD:** As explored in Chapter 6, the LLM is embedded in HRCD to support the evaluation of disassembly sequences. This approach leverages the power of LLMs for sequence planning and decision-making in disassembly tasks, marking a significant stride towards the intelligent automation of HRCD sequence planning. The use of disassembly graphs and Bayesian networks further exemplifies the innovative integration of AI and machine learning techniques in disassembly.
- **Practical Application and Validation Through Case Studies:** Across the chapters, the application of these novel methodologies and algorithms is validated through detailed case studies, particularly in the disassembly of complex products like gearboxes. These practical applications not only demonstrate the effectiveness of the proposed solutions but also provide valuable insights into their real-world implications and potential for industry adoption.

Together, these research contributions from this thesis represent a significant achievement in the field of smart remanufacturing and human-robot col-

laborative disassembly, offering new directions for research and development. By addressing critical challenges in disassembly line balancing, enhancing the precision and efficiency of human-robot collaboration, and applying advanced AI technologies in remanufacturing, this thesis paves the way for more sustainable, efficient, and smart remanufacturing practices.

7.3 Limitations and Future Research Directions

7.3.1 Disassembly Line Balancing Problem

In future research, the mathematical model of disassembly line could be further improved to better model actual conditions of disassembly in remanufacturing. The collaborative human robot disassembly line in a workstation will provide more alternative choices in disassembly task allocation, which makes it a more complex scenario. Moreover, the emerging deep learning and reinforcement learning optimisation algorithms may have more advantages for multi-objective optimisation problems. Deep learning-based algorithms have great ability on solving nonlinear fitting, while reinforcement learning based algorithms are suitable for decision-making learning [207]. Nowadays, the deep reinforcement learning method is generated and combined the advantages of those two methods, which has great ability to solve more complex optimisation problems in real-world scenarios [208]. Due to the highly versatile of the proposed HH algorithm, it is possible to combine hyper-heuristic

algorithms with those intelligence algorithms to further enhance the performance of optimisation problems. Additionally, the optimisation of DLBP in remanufacturing can be considered and pursued for larger-scale and more complex actual products.

7.3.2 Human-Robot Collaborative Disassembly

For future research, the following three primary aspects should be considered:

This research is the first to introduce an ontology model and a rule-based reasoning method for human-robot collaborative disassembly sequence planning. Therefore, this research focuses on proposing the upper-layer framework of the ontology model and the reasoning rules in human-robot collaborative disassembly. Practical factors such as uncertainty and failure are not considered in this research. The ontology model can be further expanded through integrating these factors to reflect a more practical industrial scenario. Moreover, the generative pre-trained transformer (GPT) models offer a potential solution to generate, learn and update the ontology model automatically.

In this research, the generated disassembly strategies consider only a complete and damage-free disassembly mode. Feasible and optimal disassembly schemes are determined based on the overall process time and the number of disassembly direction changes. However, due to the various constraints and uncertainties associated with product components in real-world disassembly, as well as potential failures during the disassembly process, the complexity

evaluation of each disassembly task should be enhanced by considering economic and technical factors. Subsequently, the selection of disassembly methods and the optimisation of human-robot collaborative disassembly schemes will ensure greater practical significance and value.

The proposed ontology model and disassembly-related rules can be further adapted and expanded to encompass the entire remanufacturing process [209]. The full life-cycle of EoL products can be incorporated into the EoL product ontology knowledge base, which can also aid in establishing the digital twin model of EoL products. Furthermore, the SWRL rules have the potential to support and enhance planning and optimisation within the entire remanufacturing process. Consequently, a smart remanufacturing system embedded with the ontology model and rule-based reasoning mechanism can be established.

7.3.3 Large-Language Model for HRCD

The exploration of Large-Language Models (LLM) for human-robot collaborative disassembly, while groundbreaking, brings to light several limitations that pave the way for future research directions. One of the primary limitations lies in the current capability of LLMs to fully understand and interpret the complex, technical language specific to disassembly processes and manufacturing schematics. Despite their remarkable progress in natural language understanding, LLMs occasionally struggle with the precise interpretation of technical jargon and the application of this knowledge in practical, physi-

cal tasks. Additionally, the integration of LLMs into physical disassembly systems poses significant challenges, particularly in ensuring seamless communication between the cyber and physical components of collaborative disassembly operations. The latency in response times and the potential for misinterpretation of commands can hinder the efficiency and effectiveness of human-robot collaboration, necessitating further refinement of these models to better accommodate the nuances of technical language and real-world manufacturing contexts.

Future research directions should focus on enhancing the contextual understanding of LLMs, particularly in interpreting and acting upon complex disassembly instructions within varied manufacturing environments. This entails the development of specialised LLMs trained explicitly on technical datasets, incorporating industry-specific knowledge that can bridge the current gaps in language comprehension. Another promising avenue is the improvement of integration techniques for LLMs within cyber-physical systems, aiming to reduce latency and increase the reliability of human-robot interactions. Exploring advanced communication protocols and real-time data processing frameworks could significantly enhance the synchronisation between humans, robots, and LLMs. Additionally, addressing the ethical and safety considerations inherent in human-robot collaboration is paramount, ensuring that advancements in LLM technology do not compromise worker safety or job security. Through targeted research and development efforts, the potential of LLMs to revolutionise smart remanufacturing and collabo-

rative disassembly processes can be fully realised, pushing the boundaries of current manufacturing capabilities towards more efficient, sustainable, and intelligent production systems.

7.4 Chapter Summary

This chapter serves as a culminating summary of the research conducted, alongside an articulation of its scientific contributions and a forward-looking perspective on limitations and future directions. The chapter begins with a concise recap of the research, emphasising the novel integration of cyber-physical systems, advanced heuristic algorithms, ontology and rule-based methods, and large language models within the realm of human-robot collaborative disassembly in smart remanufacturing. This synthesis not only encapsulates the journey taken but also highlights the nuanced understanding and innovations developed to tackle the complexities of disassembly processes, optimising them for efficiency, accuracy, and sustainability.

In discussing scientific contributions, the chapter proudly outlines the strides made in addressing the Disassembly Line Balancing Problem (DLBP), enhancing Human-Robot Collaborative Disassembly (HRCD), and pioneering the use of Large-Language Models (LLMs) for HRCD. These contributions represent significant advancements in the field, offering methodologies and frameworks that could be applied across a range of disassembly scenarios in smart remanufacturing contexts. However, the narrative also acknowledges inherent limitations, particularly in the scalability of solutions to DLBP, the

integration depth of human-robot interactions in HRCD, and the domain-specific performance of LLMs. Future research directions are thoughtfully proposed, suggesting a deeper exploration into adaptive algorithms that can more dynamically respond to the unpredictable nature of disassembly tasks, the development of more intuitive interfaces and protocols for human-robot collaboration, and the refinement of LLMs to better handle the specific linguistic and procedural nuances of disassembly tasks. These pathways not only aim to address the current gaps but also envision a future where smart remanufacturing is more efficient, adaptable, and collaborative.

8

Appendix

8.1 Bill of Materials of Splitter Gearboxes

Table 8.1: Bill of materials of splitter gearboxes series 85000.

No.	Description (Parts)	Quality (Q)	Mean Process Time (t)	Deviation (D)	Revenue (r)
1	Housing	1	8.2	2.1	25.3
2	Cover	1	10.4	3.5	43.5
3	Bearing 6010	1	5.6	1.2	12.6
4	Pinion gear	2	3.4	1.4	6.6
5	Sealing ring 45×65×8	2	7.6	2.2	4.8
6	Oil plug 3/8"	2	4.8	2.0	2.2
7	Oil drain plug 3/8"	1	5.2	1.6	1.4
8	Key 12*25	1	2.6	0.8	0.7
9	Snap ring UNI 7435-50	2	6.4	4.2	4.7
10	Oil dipstick with vent	1	7.3	1.4	2.6
11	Male P.T.O. shaft 1"3/8 Z6	1	8.4	3.4	23.4
12	Ring gear	1	18.7	5.2	4.3
13	Bearing 6009	4	5.4	1.3	11.2
14	Sealing ring 50*65*8	1	4.7	1.4	2.5
15	Cap DIN 470 D.38	5	10.5	4.5	1.5
16	Bearing 6210	1	10.2	3.5	15.6
17	Gasket	4	4.8	1.6	60.4
18	Washer Grower d.8	12	15.6	1.2	67.9
19	Nut M8	12	25.2	2.4	7.2
20	Peg UNI 8751 6*24	8	10.4	1.6	0.8
21	Socket cap screw M8*45	12	27.6	3.6	42.2
22	Gasket	1	8.5	1.4	14.3
23	Snap ring UNI 7435-48	1	3.4	1.2	2.3
24	Ring	1	4.7	2.1	3.7
25	Spring	1	2.6	1.4	2.3
26	Spring ring	1	8.6	2.4	4.2
27	Ball	3	4.2	0.9	12.7
28	Female P.T.O. shaft—1"3/8" Z6	1	4.6	1.6	16.6
29	Female P.T.O. shaft short 1"3/8	1	5.2	1.4	20.7
30	Female P.T.O. shaft long 1"3/8	1	3.4	0.8	23.4

Table 8.2: Bill of materials of splitter gearboxes series 90000.

No.	Description (Parts)	Quality(Q)	Mean Process Time (t)	Deviation (D)	Revenue (r)
1	Socket cap screw M6*20	4	9.2	1.2	14.2
2	Oil level plug	1	2.4	1.1	1.4
3	Gasket	1	1.2	0.4	0.6
4	Gasket	1	6.5	2.4	1.4
5	Socket cap screw	10	23.1	6.4	31.2
6	Peg ϕ 6	2	2.6	0.6	0.2
7	Snap ring ϕ 58	3	9.6	3.2	5.4
8	Bearing type 6010	5	28	6	63
9	Cap DIN 470	2	4.2	1.8	0.6
10	Pinion Gear	2	3.4	1.4	6.6
11	Sealing ring ϕ	3	11.4	2.1	7.2
12	Oil dipstick with vent	1	7.3	1.4	2.6
13	Gasket	3	3.6	1.2	45.3
14	O-Ring	2	8.2	2.2	0.6
15	Corteco Ring	2	10.4	3.8	6.4
16	Gasket	2	16.4	6.4	23.6
17	Flange SAE B	1	12.7	4.2	16.6
18	Socket cap screw	6	13.8	1.8	21.1
19	Flange SAE A	1	14.2	4.1	23.5
20	Oil drain plug 3/8"	1	5.2	1.6	1.4
21	Housing	1	8.4	2.2	25.4
22	Gasket	1	8.5	1.4	14.3
23	Ring gear	1	18.7	5.2	4.3
24	Male P.T.O. shaft 1" 3/8	1	4.6	1.6	16.4
25	Bearing type 6210	1	10.2	3.5	15.6
26	Ball	3	4.2	0.9	12.7
27	Spring	1	2.6	1.4	2.3
28	Female P.T.O. shaft 1" 3/8 long	1	3.4	0.8	23.4
29	Cap DIN 470	3	6.3	2.7	0.9
30	Female P.T.O. shaft 1-3/8"	1	7.3	2.4	18.4
31	Spring ring	1	8.6	2.4	4.1
32	Female P.T.O. shaft 1" 3/8 short	1	5.2	1.4	20.7
33	Cover	1	10.8	2.4	24.8
34	Cap	1	8.6	2.2	8.2
35	Ring	1	4.8	1.8	3.8

8.2 Disassembly-Related Information of The Gearbox

The BOM and related information of the gearbox are presented in Table 8.3.

Table 8.3: Disassembly-related information of the gearbox.

ID	Name	Instance in Protégé	Category	Quantity	DA	DTI	DM	ProcessTime
1	House	house	<i>fp</i>	1	-	-	-	-
2	Ventilator	ventilator	<i>fp</i>	1	Rotate	Wrench	H/R	10/8
3	Flange	flange	<i>fp</i>	1	Unscrew	-	H/R	15/10
4	Screw-1	screw-1	<i>f</i>	6	Unscrew	Screwdriver	H/R	5/2
5	Screw-2	screw-2	<i>f</i>	6	Unscrew	Screwdriver	H/R	5/2
6	Outer Buckle-52	outer_buckle_52	<i>ap</i>	1	Unplug	Circlip pliers	H/R	8/6
7	Bearing-32205	bearing_32205	<i>fp</i>	1	Place, Grasp, Move, Unplug	Puller, Separators, Circlip pliers	HR	30
8	Worm Shaft	worm_shaft	<i>fp</i>	1	Grasp, Move, Slide, Rotate	Puller, Separators, Circlip pliers	HR	26
9	Inner Buckle	inner_buckle	<i>ap</i>	1	Unplug	Circlip pliers	H/R	17/10
10	Outer Buckle-68	outer_buckle_68	<i>ap</i>	1	Unplug	Circlip pliers	H/R	12/9
11	Bearing-32008	bearing_32008	<i>fp</i>	1	Place, Grasp, Move, Unplug	Puller, Separators, Circlip pliers	HR	30
12	Worm Cover	worm_cover	<i>ap</i>	1	Unplug	Circlip pliers	H/R	14/10
13	Bearing-32010-1	bearing_32010_1	<i>fp</i>	1	Place, Grasp, Move, Unplug	Puller, Separators, Circlip pliers	HR	25
14	Bearing-32010-2	bearing_32010_2	<i>fp</i>	1	Place, Grasp, Move, Unplug	Puller, Separators, Circlip pliers	HR	25
15	Gear spacer-1	gear_spacer_1	<i>fp</i>	1	Grasp, Unplug	Circlip pliers	R	14
16	Gear spacer-2	gear_spacer_2	<i>ap</i>	1	Grasp, Unplug	Circlip pliers	R	14
17	Gear shaft	gear_shaft	<i>fp</i>	1	Grasp, Move, Slide, Rotate	Puller, Separators, Circlip pliers	HR	23
18	Gear	gear	<i>fp</i>	1	Slide, Move, Grasp	Puller, Separators, Circlip pliers	HR	45
19	Gear Cover	gear_cover	<i>ap</i>	1	Move	Rubber Mallet	H/R	20/12
20	Gear retentor-1	gear_retentor_1	<i>ap</i>	1	Grasp, Unplug	Puller, Circlip plier	H	15
21	Gear retentor-2	gear_retentor_2	<i>ap</i>	1	Grasp, Unplug	Puller, Circlip plier	H	15
22	Worm retentor	worm_retentor	<i>ap</i>	1	Grasp, Unplug	Puller, Circlip plier	H	22
23	Cover retentor	cover_retentor	<i>ap</i>	1	Grasp, Unplug	Puller, Circlip plier	H	18

8.3 Link for The Illustrative Example and The Case Study

Open source:

1. <https://www.statista.com/statistics/490764/energy-consumption-from-renewable-and-waste-sources-in-manufacturing-uk>
2. <https://www.ellenmacarthurfoundation.org/circulate-products-and-materials>
3. https://www.youtube.com/watch?v=b6h_ZiGoLY0
4. <https://grabcad.com/library/worm-gear-reducer-13>
5. <https://grabcad.com/library/belt-roller-support-assembly-in-solidworks-1>
6. <https://github.com/thieu1995/mealpy>

References

- [1] B. Esmailian, S. Behdad, and B. Wang. The evolution and future of manufacturing: A review. *Journal of Manufacturing Systems*, 39:79–100, 2016.
- [2] S. Cannella, M. Bruccoleri, and J. M. Framinan. Closed-loop supply chains: What reverse logistics factors influence performance? *International Journal of Production Economics*, 175:35–49, 2016.
- [3] Walter Cardoso Satyro, Mauro de Mesquita Spinola, Cecília MVB de Almeida, Biagio F Giannetti, José Benedito Sacomano, Jose Celso Contador, and Jose Luiz Contador. Sustainable industries: Production planning and control as an ally to implement strategy. *Journal of Cleaner Production*, 281:124781, 2021.
- [4] H. J. Ngu, M. D. Lee, and M. S. Bin Osman. Review on current challenges and future opportunities in malaysia sustainable manufacturing: Remanufacturing industries. *Journal of Cleaner Production*, 273, 2020.

- [5] Barack Obama. *Strategy for American innovation: Driving towards sustainable growth and quality jobs*. DIANE Publishing, 2011.
- [6] Heiner Lasi, Peter Fettke, Hans-Georg Kemper, Thomas Feld, and Michael Hoffmann. Industry 4.0. *Business & information systems engineering*, 6(4):239–242, 2014.
- [7] Harry Sminia, Aylin Ates, Steve Paton, and Marisa Smith. High value manufacturing: Capability, appropriation, and governance. *European Management Journal*, 37(4):516–528, 2019.
- [8] JAPAN MINISTRY, OF ECONOMY TRADE INDUSTRY, 2018.
- [9] Ling Li. China’s manufacturing locus in 2025: With a comparison of “made-in-china 2025” and “industry 4.0”. *Technological Forecasting and Social Change*, 135:66–74, 2018.
- [10] Yuqian Lu, Hao Zheng, Saahil Chand, Wanqing Xia, Zengkun Liu, Xun Xu, Lihui Wang, Zhaojun Qin, and Jinsong Bao. Outlook on human-centric manufacturing towards industry 5.0. *Journal of Manufacturing Systems*, 62:612–627, 2022.
- [11] X. G. Zhang, M. Y. Zhang, H. Zhang, Z. G. Jiang, C. H. Liu, and W. Cai. A review on energy, environment and economic assessment in remanufacturing based on life cycle assessment method. *Journal of Cleaner Production*, 255, 2020.

- [12] I. Masudin, F. R. Jannah, D. M. Utama, and D. P. Restuputri. Capacitated remanufacturing inventory model considering backorder: A case study of Indonesian reverse logistics. *Ieee Access*, 7:143046–143057, 2019.
- [13] X. F. Zhang, S. Y. Zhang, L. C. Zhang, J. F. Xue, R. Sa, and H. Liu. Identification of product’s design characteristics for remanufacturing using failure modes feedback and quality function deployment. *Journal of Cleaner Production*, 239, 2019.
- [14] S. Turki, C. Sauvey, and N. Rezg. Modelling and optimization of a manufacturing/remanufacturing system with storage facility under carbon cap and trade policy. *Journal of Cleaner Production*, 193:441–458, 2018.
- [15] M. Kerin and D. T. Pham. Smart remanufacturing: a review and research framework. *Journal of Manufacturing Technology Management*, 2020.
- [16] Evandro Leonardo Silva Teixeira, Benny Tjahjono, Macarena Beltran, and Jorge Julião. Demystifying the digital transition of remanufacturing: A systematic review of literature. *Computers in Industry*, 134:103567, 2022.
- [17] Okechukwu Okorie, Fiona Charnley, Augustine Ehiagwina, Divya Tiwari, and Konstantinos Salonitis. Towards a simulation-based under-

- standing of smart remanufacturing operations: a comparative analysis. *Journal of Remanufacturing*, pages 1–24, 2020.
- [18] Yuyao Guo, Lei Wang, Zelin Zhang, Jianhua Cao, Xuhui Xia, and Ying Liu. Integrated modeling for retired mechanical product genes in remanufacturing: A knowledge graph-based approach. *Advanced Engineering Informatics*, 59:102254, 2024.
- [19] M. Kerin and D. T. Pham. A review of emerging industry 4.0 technologies in remanufacturing. *Journal of Cleaner Production*, 237, 2019.
- [20] R. Subramoniam, D. Huisingh, and R. B. Chinnam. Remanufacturing for the automotive aftermarket-strategic factors: literature review and future research needs. *Journal of Cleaner Production*, 17(13):1163–1174, 2009.
- [21] V. Hashemi, M. Y. Chen, and L. P. Fang. Modeling and analysis of aerospace remanufacturing systems with scenario analysis. *International Journal of Advanced Manufacturing Technology*, 87(5-8):2135–2151, 2016.
- [22] Wenjie Wang, Guangdong Tian, Mengqi Luo, Honghao Zhang, Gang Yuan, and Kejia Niu. More mixed-integer linear programming models for solving three-stage remanufacturing system scheduling problem. *Computers & Industrial Engineering*, 194:110379, 2024.

- [23] Anjar Priyono, Winifred Ijomah, and Umit S Bititci. Disassembly for remanufacturing: A systematic literature review, new model development and future research needs. *Journal of Industrial Engineering and Management (JIEM)*, 9(4):899–932, 2016.
- [24] K. D. Dingec and A. Korugan. A stochastic analysis of asynchronous demand in disassembly processes of remanufacturing systems. *European Journal of Industrial Engineering*, 7(2):175–205, 2013.
- [25] Yixiong Feng, Kaiyue Cui, Zhaoxi Hong, Zhiwu Li, Weiyu Yan, and Jianrong Tan. Disassembly sequence planning of product structure with an improved qica considering expert consensus for remanufacturing. *IEEE Transactions on Industrial Informatics*, 2022.
- [26] Yujie Ma, Gang Du, and Roger J Jiao. Design for product upgradability considering remanufacturing outsourcing: A three-level joint optimization approach. *International Journal of Production Economics*, 272:109233, 2024.
- [27] B. Liu, W. J. Xu, J. Y. Liu, B. T. Yao, Z. D. Zhou, and D. T. Pham. Human-robot collaboration for disassembly line balancing problem in remanufacturing. *Proceedings of the Asme 14th International Manufacturing Science and Engineering Conference, 2019, Vol 1*, 2019.
- [28] Zhigan JIANG, Bin XIE, Shuo ZHU, Hua ZHANG, Wei YAN, and Mingren DAI. Dynamic data flow-driven knowledge graph construction

- method for remanufacturing disassembly process. *Computer Integrated Manufacturing System*, 30(3):879, 2024.
- [29] Edward A Lee. The past, present and future of cyber-physical systems: A focus on models. *Sensors*, 15(3):4837–4869, 2015.
- [30] Edward A Lee. Cyber physical systems: Design challenges. In *2008 11th IEEE international symposium on object and component-oriented real-time distributed computing (ISORC)*, pages 363–369. IEEE, 2008.
- [31] László Monostori, Botond Kádár, Thomas Bauernhansl, Shinsuke Kondoh, Soundar Kumara, Gunther Reinhart, Olaf Sauer, Gunther Schuh, Wilfried Sihn, and Kenichi Ueda. Cyber-physical systems in manufacturing. *Cirp Annals*, 65(2):621–641, 2016.
- [32] Bo-Hu Li, Lin Zhang, Shi-Long Wang, Fei Tao, Jun Wei Cao, Xiao Dan Jiang, Xiao Song, and Xu Dong Chai. Cloud manufacturing: a new service-oriented networked manufacturing model. *Computer integrated manufacturing systems*, 16(1):1–7, 2010.
- [33] Xun Xu. From cloud computing to cloud manufacturing. *Robotics and computer-integrated manufacturing*, 28(1):75–86, 2012.
- [34] Dazhong Wu, David W Rosen, Lihui Wang, and Dirk Schaefer. Cloud-based design and manufacturing: A new paradigm in digital manufacturing and design innovation. *Computer-aided design*, 59:1–14, 2015.

- [35] Olivier Cardin. Classification of cyber-physical production systems applications: Proposition of an analysis framework. *Computers in Industry*, 104:11–21, 2019.
- [36] Askiner Gungor and Surenda M Gupta. A solution approach to the disassembly line balancing problem in the presence of task failures. *International journal of production research*, 39(7):1427–1467, 2001.
- [37] Kaipu Wang, Xinyu Li, and Liang Gao. Modeling and optimization of multi-objective partial disassembly line balancing problem considering hazard and profit. *Journal of Cleaner Production*, 211:115–133, 2019.
- [38] Zeynel Abidin Cil, Suleyman Mete, and Faruk Serin. Robotic disassembly line balancing problem: A mathematical model and ant colony optimization approach. *Applied Mathematical Modelling*, 2020.
- [39] S Agrawal and MK Tiwari. A collaborative ant colony algorithm to stochastic mixed-model u-shaped disassembly line balancing and sequencing problem. *International journal of production research*, 46(6):1405–1429, 2008.
- [40] Kaipu Wang, Liang Gao, and Xinyu Li. A multi-objective algorithm for u-shaped disassembly line balancing with partial destructive mode. *Neural Computing and Applications*, pages 1–22, 2020.
- [41] Kaipu Wang, Xinyu Li, and Liang Gao. A multi-objective discrete flower pollination algorithm for stochastic two-sided partial disassem-

- bly line balancing problem. *Computers & Industrial Engineering*, 130:634–649, 2019.
- [42] Ibrahim Kucukkoc. Balancing of two-sided disassembly lines: Problem definition, milp model and genetic algorithm approach. *Computers & Operations Research*, 124:105064, 2020.
- [43] Abdolreza Roshani, Parviz Fattahi, Abdolhassan Roshani, Mohsen Salehi, and Arezoo Roshani. Cost-oriented two-sided assembly line balancing problem: A simulated annealing approach. *International Journal of Computer Integrated Manufacturing*, 25(8):689–715, 2012.
- [44] Ayyuce Aydemir-Karadag and Orhan Turkbey. Multi-objective optimization of stochastic disassembly line balancing with station parallelizing. *Computers & Industrial Engineering*, 65(3):413–425, 2013.
- [45] Kaipu Wang, Xinyu Li, Liang Gao, Peigen Li, and Surendra M Gupta. A genetic simulated annealing algorithm for parallel partial disassembly line balancing problem. *Applied Soft Computing*, 107:107404, 2021.
- [46] Wei Liang, Zeqiang Zhang, Tao Yin, Yanqing Zeng, and Yu Zhang. Multi-parallel disassembly line balancing problem and improved ant lion optimizer for mixed-waste electrical and electronic equipment. *International Journal of Precision Engineering and Manufacturing-Green Technology*, 11(1):243–258, 2024.

- [47] Seamus M McGovern and Surendra M Gupta. Ant colony optimization for disassembly sequencing with multiple objectives. *The International Journal of Advanced Manufacturing Technology*, 30(5-6):481–496, 2006.
- [48] Fatma Tevhide Altekin, Levent Kandiller, and Nur Evin Ozdemirel. Disassembly line balancing with limited supply and subassembly availability. In *Environmentally conscious manufacturing iii*, volume 5262, pages 59–70. International Society for Optics and Photonics, 2004.
- [49] F Tevhide Altekin, Levent Kandiller, and Nur Evin Ozdemirel. Profit-oriented disassembly-line balancing. *International Journal of Production Research*, 46(10):2675–2693, 2008.
- [50] Kento Igarashi, Tetsuo Yamada, Surendra M Gupta, Masato Inoue, and Norihiro Itsubo. Disassembly system modeling and design with parts selection for cost, recycling and co2 saving rates using multi criteria optimization. *Journal of Manufacturing Systems*, 38:151–164, 2016.
- [51] Eren Ozceylan and Turan Paksoy. Interactive fuzzy programming approaches to the strategic and tactical planning of a closed-loop supply chain under uncertainty. *International Journal of Production Research*, 52(8):2363–2387, 2014.
- [52] Seamus M McGovern and Surendra M Gupta. Greedy algorithm for disassembly line scheduling. In *SMC'03 Conference Proceedings. 2003 IEEE International Conference on Systems, Man and Cyber-*

- netics. Conference Theme-System Security and Assurance (Cat. No. 03CH37483)*, volume 2, pages 1737–1744. IEEE, 2003.
- [53] Seamus M McGovern and Surendra M Gupta. Combinatorial optimization methods for disassembly line balancing. In *Environmentally Conscious Manufacturing IV*, volume 5583, pages 53–66. International Society for Optics and Photonics, 2004.
- [54] Can B Kalayci and Surendra M Gupta. Simulated annealing algorithm for solving sequence-dependent disassembly line balancing problem. *IFAC Proceedings Volumes*, 46(9):93–98, 2013.
- [55] Can B Kalayci and Surendra M Gupta. Ant colony optimization for sequence-dependent disassembly line balancing problem. *Journal of Manufacturing Technology Management*, 2013.
- [56] Can B Kalayci, Olcay Polat, and Surendra M Gupta. A hybrid genetic algorithm for sequence-dependent disassembly line balancing problem. *Annals of Operations Research*, 242(2):321–354, 2016.
- [57] Ullah Saif, Zailin Guan, Li Zhang, Jahanzeb Mirza, and Yue Lei. Hybrid pareto artificial bee colony algorithm for assembly line balancing with task time variations. *International Journal of Computer Integrated Manufacturing*, 30(2-3):255–270, 2017.
- [58] Can B Kalayci and Surendra M Gupta. Artificial bee colony algo-

- rithm for solving sequence-dependent disassembly line balancing problem. *Expert Systems with Applications*, 40(18):7231–7241, 2013.
- [59] Can B Kalayci and Surendra M Gupta. A tabu search algorithm for balancing a sequence-dependent disassembly line. *Production Planning & Control*, 25(2):149–160, 2014.
- [60] Zeqiang Zhang, Kaipu Wang, Lixia Zhu, and Yi Wang. A pareto improved artificial fish swarm algorithm for solving a multi-objective fuzzy disassembly line balancing problem. *Expert Systems with Applications*, 86:165–176, 2017.
- [61] Lixia Zhu, Zeqiang Zhang, and Yi Wang. A pareto firefly algorithm for multi-objective disassembly line balancing problems with hazard evaluation. *International Journal of Production Research*, 56(24):7354–7374, 2018.
- [62] Iwona Paprocka and Bożena Skołod. A predictive approach for disassembly line balancing problems. *Sensors*, 22(10):3920, 2022.
- [63] S. M. Mcgovern and S. M. Gupta. Combinatorial optimization analysis of the unary np-complete disassembly line balancing problem. *International Journal of Production Research*, 45(18-19):4485–4511, 2007.
- [64] Eren Ozceylan, Can B Kalayci, Aşkıner Güngör, and Surendra M Gupta. Disassembly line balancing problem: a review of the state

- of the art and future directions. *International Journal of Production Research*, 57(15-16):4805–4827, 2019.
- [65] Shwetank Avikal, Rajeev Jain, Harish Yadav, and PK Mishra. A new heuristic for disassembly line balancing problems with and/or precedence relations. In *Proceedings of the Second International Conference on Soft Computing for Problem Solving (SocProS 2012), December 28-30, 2012*, pages 519–525. Springer, 2014.
- [66] Shanli Xiao, Yujia Wang, Hui Yu, and Shankun Nie. An entropy-based adaptive hybrid particle swarm optimization for disassembly line balancing problems. *Entropy*, 19(11):596, 2017.
- [67] Can B Kalayci, Arif Hancilar, Askiner Gungor, and Surendra M Gupta. Multi-objective fuzzy disassembly line balancing using a hybrid discrete artificial bee colony algorithm. *Journal of Manufacturing Systems*, 37:672–682, 2015.
- [68] Francesco Pistolesi, Beatrice Lazzerini, Michela Dalle Mura, and Gino Dini. Emoga: A hybrid genetic algorithm with extremal optimization core for multiobjective disassembly line balancing. *IEEE Transactions on Industrial Informatics*, 14(3):1089–1098, 2017.
- [69] Yinsheng Yang, Gang Yuan, Qianwei Zhuang, and Guangdong Tian. Multi-objective low-carbon disassembly line balancing for agricultural

- machinery using mdfoa and fuzzy ahp. *Journal of Cleaner Production*, 233:1465–1474, 2019.
- [70] Jianhua Cao, Xuhui Xia, Lei Wang, Zelin Zhang, and Xiang Liu. A novel multi-efficiency optimization method for disassembly line balancing problem. *Sustainability*, 11(24):6969, 2019.
- [71] Riccardo Maderna, Maria Pozzi, Andrea Maria Zanchettin, Paolo Rocco, and Domenico Prattichizzo. Flexible scheduling and tactile communication for human–robot collaboration. *Robotics and Computer-Integrated Manufacturing*, 73:102233, 2022.
- [72] Timon Hoebert, Stephan Seibel, Manuel Amersdorfer, Markus Vincze, Wilfried Lepuschitz, and Munir Merdan. A framework for enhanced human–robot collaboration during disassembly using digital twin and virtual reality. *Robotics*, 13(7):104, 2024.
- [73] Chong Chen, Chao Liu, Tao Wang, Ao Zhang, Wenhao Wu, and Lian-glun Cheng. Compound fault diagnosis for industrial robots based on dual-transformer networks. *Journal of Manufacturing Systems*, 66:163–178, 2023.
- [74] Ziqi Huang, Marcel Fey, Chao Liu, Ege Beysel, Xun Xu, and Christian Brecher. Hybrid learning-based digital twin for manufacturing process: Modeling framework and implementation. *Robotics and Computer-Integrated Manufacturing*, 82:102545, 2023.

- [75] Chao Liu, Pai Zheng, and Xun Xu. Digitalisation and servitisation of machine tools in the era of industry 4.0: a review. *International journal of production research*, pages 1–33, 2021.
- [76] Quan Liu, Zhihao Liu, Wenjun Xu, Quan Tang, Zude Zhou, and Duc Truong Pham. Human-robot collaboration in disassembly for sustainable manufacturing. *International Journal of Production Research*, 57(12):4027–4044, 2019.
- [77] Jun Huang, Duc Truong Pham, Yongjing Wang, Mo Qu, Chunqian Ji, Shizhong Su, Wenjun Xu, Quan Liu, and Zude Zhou. A case study in human–robot collaboration in the disassembly of press-fitted components. *Proceedings of the Institution of Mechanical Engineers, Part B: Journal of Engineering Manufacture*, 234(3):654–664, 2020.
- [78] Jun Huang, Duc Truong Pham, Ruiya Li, Mo Qu, Yongjing Wang, Mairi Kerin, Shizhong Su, Chunqian Ji, Omar Mahomed, Riham Khalil, David Stockton, Wenjun Xu, Quan Liu, and Zude Zhou. An experimental human-robot collaborative disassembly cell. *Computers & Industrial Engineering*, 155:107189, 2021.
- [79] Meng-Lun Lee, Sara Behdad, Xiao Liang, and Minghui Zheng. Task allocation and planning for product disassembly with human–robot collaboration. *Robotics and Computer-Integrated Manufacturing*, 76:102306, 2022.

- [80] Wenjun Xu, Quan Tang, Jiayi Liu, Zhihao Liu, Zude Zhou, and Duc Truong Pham. Disassembly sequence planning using discrete bees algorithm for human-robot collaboration in remanufacturing. *Robotics and Computer-Integrated Manufacturing*, 62:101860, 2020.
- [81] Soran Parsa and Mozafar Saadat. Human-robot collaboration disassembly planning for end-of-life product disassembly process. *Robotics and Computer-Integrated Manufacturing*, 71:102170, 2021.
- [82] Íñigo Elguea-Aguinaco, Antonio Serrano-Muñoz, Dimitrios Chrysostomou, Ibai Inziarte-Hidalgo, Simon Bøgh, and Nestor Arana-Arexolaleiba. Goal-conditioned reinforcement learning within a human-robot disassembly environment. *Applied Sciences*, 12(22):11610, 2022.
- [83] Mengling Chu and Weida Chen. Human-robot collaboration disassembly planning for end-of-life power batteries. *Journal of Manufacturing Systems*, 69:271–291, 2023.
- [84] Lei Guo, Zeqiang Zhang, and Xiufen Zhang. Human-robot collaborative partial destruction disassembly sequence planning method for end-of-life product driven by multi-failures. *Advanced Engineering Informatics*, 55:101821, 2023.
- [85] Jiayi Liu, Zude Zhou, Duc Truong Pham, Wenjun Xu, Chunqian Ji, and Quan Liu. Robotic disassembly sequence planning using enhanced

- discrete bees algorithm in remanufacturing. *International Journal of Production Research*, 56(9):3134–3151, 2018.
- [86] Claudio Sassanelli, Paolo Rosa, and Sergio Terzi. Supporting disassembly processes through simulation tools: A systematic literature review with a focus on printed circuit boards. *Journal of Manufacturing Systems*, 60:429–448, 2021.
- [87] Bin Zhou, Xingwang Shen, Yuqian Lu, Xinyu Li, Bao Hua, Tianyuan Liu, and Jinsong Bao. Semantic-aware event link reasoning over industrial knowledge graph embedding time series data. *International Journal of Production Research*, 61(12):4117–4134, 2023.
- [88] Andrea Rega, Marino Castrese Di, Agnese Pasquariello, Ferdinando Vitolo, Stanislao Patalano, Alessandro Zanella, and Antonio Lanzotti. Collaborative workplace design: A knowledge-based approach to promote human–robot collaboration and multi-objective layout optimization. *Applied Sciences*, 11(24):12147, 2021.
- [89] Soh-Khim Ong, Miko May Lee Chang, and Andrew YC Nee. Product disassembly sequence planning: state-of-the-art, challenges, opportunities and future directions. *International Journal of Production Research*, 59(11):3493–3508, 2021.
- [90] Bin Zhou, Jinsong Bao, Jie Li, Yuqian Lu, Tianyuan Liu, and Qiwan Zhang. A novel knowledge graph-based optimization approach for re-

- source allocation in discrete manufacturing workshops. *Robotics and Computer-Integrated Manufacturing*, 71:102160, 2021.
- [91] Yuqian Lu, Qun Shao, Chirpreet Singh, Xun Xu, and Xinfeng Ye. Ontology for manufacturing resources in a cloud environment. *International Journal of Manufacturing Research*, 9(4):448–469, 2014.
- [92] Alessandro Umbrico, Andrea Orlandini, and Amedeo Cesta. An ontology for human-robot collaboration. *Procedia CIRP*, 93:1097–1102, 2020.
- [93] Lihong Qiao, Yifan Qie, Zuowei Zhu, Yixin Zhu, and Nabil Anwer. An ontology-based modelling and reasoning framework for assembly sequence planning. *The International Journal of Advanced Manufacturing Technology*, 94(9):4187–4197, 2018.
- [94] Yanru Zhong, Chaohao Jiang, Yuchu Qin, Guoyu Yang, Meifa Huang, and Xiaonan Luo. Automatically generating assembly sequences with an ontology-based approach. *Assembly Automation*, 2019.
- [95] Hanqing Gong, Lingling Shi, Xiang Zhai, Yimin Du, and Zhijing Zhang. Assembly process case matching based on a multilevel assembly ontology method. *Assembly Automation*, 2021.
- [96] Bicheng Zhu and Utpal Roy. Ontology-based disassembly information system for enhancing disassembly planning and design. *The Inter-*

- national Journal of Advanced Manufacturing Technology*, 78(9):1595–1608, 2015.
- [97] Bicheng Zhu and Utpal Roy. Modeling and validation of a web ontology language based disassembly planning information model. *Journal of Computing and Information Science in Engineering*, 18(2), 2018.
- [98] Gwendolyn Foo, Sami Kara, and Maurice Pagnucco. An ontology-based method for semi-automatic disassembly of lcd monitors and unexpected product types. *International Journal of Automation Technology*, 15(2):168–181, 2021.
- [99] Gwendolyn Foo, Sami Kara, and Maurice Pagnucco. Artificial learning for part identification in robotic disassembly through automatic rule generation in an ontology. *IEEE Transactions on Automation Science and Engineering*, 2022.
- [100] Janus S. Liang. The methodology of knowledge acquisition and modeling for troubleshooting in automotive braking system. *Robotics and Computer-Integrated Manufacturing*, 28(1):24–34, 2012.
- [101] Liu Jiang, Jianyong Shi, and Chaoyu Wang. Multi-ontology fusion and rule development to facilitate automated code compliance checking using bim and rule-based reasoning. *Advanced Engineering Informatics*, 51:101449, 2022.

- [102] Pitipong Veerakamolmal and Surendra M Gupta. A case-based reasoning approach for automating disassembly process planning. *Journal of Intelligent Manufacturing*, 13:47–60, 2002.
- [103] Fabio Giudice. Disassembly depth distribution for ease of service: a rule-based approach. *Journal of Engineering Design*, 21(4):375–411, 2010.
- [104] Shaoli Chen, Jianjun Yi, Hui Jiang, and Xiaomin Zhu. Ontology and cbr based automated decision-making method for the disassembly of mechanical products. *Advanced Engineering Informatics*, 30(3):564–584, 2016.
- [105] Jianping Yu, Hua Zhang, Zhigang Jiang, Wei Yan, Yan Wang, and Qi Zhou. Disassembly task planning for end-of-life automotive traction batteries based on ontology and partial destructive rules. *Journal of Manufacturing Systems*, 62:347–366, 2022.
- [106] SB Tor, GA Britton, WY Zhang, and Y-M Deng. Guiding functional design of mechanical products through rule-based causal behavioural reasoning. *International Journal of Production Research*, 40(3):667–682, 2002.
- [107] Chen Zheng, Yushu An, Zhanxi Wang, Xiansheng Qin, Benoît Eynard, Matthieu Bricogne, Julien Le Duigou, and Yicha Zhang. Knowledge-based engineering approach for defining robotic manufacturing sys-

- tem architectures. *International Journal of Production Research*, 61(5):1436–1454, 2023.
- [108] Yuqian Lu and Xun Xu. A semantic web-based framework for service composition in a cloud manufacturing environment. *Journal of manufacturing systems*, 42:69–81, 2017.
- [109] Bharath Reddy and Richard Fields. From past to present: a comprehensive technical review of rule-based expert systems from 1980–2021. In *Proceedings of the 2022 ACM Southeast Conference*, pages 167–172, 2022.
- [110] Chen Li, Xiaochun Zhang, Dimitrios Chrysostomou, and Hongji Yang. Tod4ir: A humanised task-oriented dialogue system for industrial robots. *IEEE Access*, 10:91631–91649, 2022.
- [111] Shuang Li, Xavier Puig, Chris Paxton, Yilun Du, Clinton Wang, Linxi Fan, Tao Chen, De-An Huang, Ekin Akyürek, and Anima Anandkumar. Pre-trained language models for interactive decision-making. *Advances in Neural Information Processing Systems*, 35:31199–31212, 2022.
- [112] Bilel Benjdira, Anis Koubaa, and Anas M Ali. Rosgpt_vision: Commanding robots using only language models’ prompts. *arXiv preprint arXiv:2308.11236*, 2023.

- [113] Anthony Brohan, Yevgen Chebotar, Chelsea Finn, Karol Hausman, Alexander Herzog, Daniel Ho, Julian Ibarz, Alex Irpan, Eric Jang, and Ryan Julian. Do as i can, not as i say: Grounding language in robotic affordances. In *Conference on Robot Learning*, pages 287–318. PMLR, 2023.
- [114] Shirui Pan, Linhao Luo, Yufei Wang, Chen Chen, Jiapu Wang, and Xindong Wu. Unifying large language models and knowledge graphs: A roadmap. *IEEE Transactions on Knowledge and Data Engineering*, 2024.
- [115] Sai Vemprala, Rogerio Bonatti, Arthur Bucker, and Ashish Kapoor. Chatgpt for robotics: Design principles and model abilities. *Microsoft Auton. Syst. Robot. Res*, 2:20, 2023.
- [116] Yaqi Xie, Chen Yu, Tongyao Zhu, Jinbin Bai, Ze Gong, and Harold Soh. Translating natural language to planning goals with large-language models. *arXiv preprint arXiv:2302.05128*, 2023.
- [117] Derong Xu, Wei Chen, Wenjun Peng, Chao Zhang, Tong Xu, Xiangyu Zhao, Xian Wu, Yefeng Zheng, and Enhong Chen. Large language models for generative information extraction: A survey. *arXiv preprint arXiv:2312.17617*, 2023.
- [118] Sherry Yang, Ofir Nachum, Yilun Du, Jason Wei, Pieter Abbeel, and

- Dale Schuurmans. Foundation models for decision making: Problems, methods, and opportunities. *arXiv preprint arXiv:2303.04129*, 2023.
- [119] Ceng Zhang, Junxin Chen, Jiatong Li, Yanhong Peng, and Zebing Mao. Large language models for human-robot interaction: A review. *Biomimetic Intelligence and Robotics*, page 100131, 2023.
- [120] Zirui Zhao, Wee Sun Lee, and David Hsu. Large language models as commonsense knowledge for large-scale task planning. *arXiv preprint arXiv:2305.14078*, 2023.
- [121] Zhujun Zhang, Gaoliang Peng, Weitian Wang, Yi Chen, Yunyi Jia, and Shaohui Liu. Prediction-based human-robot collaboration in assembly tasks using a learning from demonstration model. *Sensors*, 22(11):4279, 2022.
- [122] Jingqing Ruan, Yihong Chen, Bin Zhang, Zhiwei Xu, Tianpeng Bao, Guoqing Du, Shiwei Shi, Hangyu Mao, Xingyu Zeng, and Rui Zhao. Tptu: Task planning and tool usage of large language model-based ai agents. *arXiv preprint arXiv:2308.03427*, 2023.
- [123] Kolby Nottingham, Yasaman Razeghi, Kyungmin Kim, JB Lanier, Pierre Baldi, Roy Fox, and Sameer Singh. Selective perception: Optimizing state descriptions with reinforcement learning for language model actors, 2023.

- [124] Yash Shukla, Wenchang Gao, Vasanth Sarathy, Alvaro Velasquez, Robert Wright, and Jivko Sinapov. Lgts: Dynamic task sampling using llm-generated sub-goals for reinforcement learning agents. *arXiv preprint arXiv:2310.09454*, 2023.
- [125] Ishika Singh, Valts Blukis, Arsalan Mousavian, Ankit Goyal, Danfei Xu, Jonathan Tremblay, Dieter Fox, Jesse Thomason, and Animesh Garg. Progprompt: program generation for situated robot task planning using large language models. *Autonomous Robots*, 47(8):999–1012, 2023.
- [126] Gautier Dagan, Frank Keller, and Alex Lascarides. Dynamic planning with a llm. *arXiv preprint arXiv:2308.06391*, 2023.
- [127] Chan Hee Song, Jiaman Wu, Clayton Washington, Brian M Sadler, Wei-Lun Chao, and Yu Su. Llm-planner: Few-shot grounded planning for embodied agents with large language models. In *Proceedings of the IEEE/CVF International Conference on Computer Vision*, pages 2998–3009, 2023.
- [128] Vladimir Polotski, Jean-Pierre Kenné, and Ali Gharbi. Estimation-based production control of manufacturing–remanufacturing systems with uncertain seasonal return and imprecise demand and inventory. *International Journal of Production Research*, 62(13):4595–4622, 2024.
- [129] Richard G Sharpe, Paul A Goodall, Aaron D Neal, Paul P Conway, and

- Andrew A West. Cyber-physical systems in the re-use, refurbishment and recycling of used electrical and electronic equipment. *Journal of cleaner production*, 170:351–361, 2018.
- [130] Nehika Mathur, Noah Last, and KC Morris. A process model representation of the end-of-life phase of a product in a circular economy to identify standards needs. *Frontiers in Manufacturing Technology*, 3:988073, 2023.
- [131] Yuanjun Laili, Yulin Li, Yilin Fang, Duc Truong Pham, and Lin Zhang. Model review and algorithm comparison on multi-objective disassembly line balancing. *Journal of Manufacturing Systems*, 56:484–500, 2020.
- [132] S. Sitcharangsie, W. Ijomah, and T. C. Wong. Decision makings in key remanufacturing activities to optimise remanufacturing outcomes: A review. *Journal of Cleaner Production*, 232:1465–1481, 2019.
- [133] Meng-Lun Lee, Xiao Liang, Boyi Hu, Gulcan Onel, Sara Behdad, and Minghui Zheng. A review of prospects and opportunities in disassembly with human–robot collaboration. *Journal of Manufacturing Science and Engineering*, 146(2), 2024.
- [134] D. Singhal, S. Tripathy, and S. K. Jena. Remanufacturing for the circular economy: Study and evaluation of critical factors. *Resources Conservation and Recycling*, 156, 2020.

- [135] Yankai Wang, Shilong Wang, Bo Yang, Lingzi Zhu, and Feng Liu. Big data driven hierarchical digital twin predictive remanufacturing paradigm: Architecture, control mechanism, application scenario and benefits. *Journal of Cleaner Production*, 248:119299, 2020.
- [136] Benjamin T Hazen, Diane A Mollenkopf, and Yacan Wang. Remanufacturing for the circular economy: An examination of consumer switching behavior. *Business Strategy and the Environment*, 26(4):451–464, 2017.
- [137] C. K. Chen and M. Akmalul’Ulya. Analyses of the reward-penalty mechanism in green closed-loop supply chains with product remanufacturing. *International Journal of Production Economics*, 210:211–223, 2019.
- [138] Jinhua Xiao, Weidong Li, Yaqiong Lv, and Guangchao Du. Disassembly information interoperability for electric vehicle battery in remanufacturing based on step standards. *Procedia CIRP*, 104:1873–1877, 2021.
- [139] Saverio Ferraro, Francesco Baffa, Alessandra Cantini, Leonardo Leoni, Filippo De Carlo, and Gianni Campatelli. Exploring remanufacturing conveniency: An economic and energetic assessment for a closed-loop supply chain of a mechanical component. *Journal of Cleaner Production*, 458:142504, 2024.
- [140] N. K. Dev, R. Shankar, and F. H. Qaiser. Industry 4.0 and circular

- economy: Operational excellence for sustainable reverse supply chain performance. *Resources Conservation and Recycling*, 153, 2020.
- [141] X. V. Wang, L. H. Wang, and L. Gao. From cloud manufacturing to cloud remanufacturing: a cloud-based approach for weee. *2013 Ieee 10th International Conference on E-Business Engineering (Icebe)*, pages 399–406, 2013.
- [142] Fei Tao, Qinglin Qi, Lihui Wang, and AYC Nee. Digital twins and cyber–physical systems toward smart manufacturing and industry 4.0: Correlation and comparison. *Engineering*, 5(4):653–661, 2019.
- [143] Lin Zhang, Yongliang Luo, Fei Tao, Bo Hu Li, Lei Ren, Xuesong Zhang, Hua Guo, Ying Cheng, Anrui Hu, and Yongkui Liu. Cloud manufacturing: a new manufacturing paradigm. *Enterprise Information Systems*, 8(2):167–187, 2014.
- [144] Johan Vogt Duberg, Erik Sundin, and Ou Tang. Assessing the profitability of remanufacturing initiation: a literature review. *Journal of Remanufacturing*, 14(1):69–92, 2024.
- [145] Mairi Kerin and Duc Truong Pham. Smart remanufacturing: a review and research framework. *Journal of Manufacturing Technology Management*, 31(6):1205–1235, 2020.
- [146] Parviz Kahhal, Yeong-Kwan Jo, and Sang-Hu Park. Recent progress in remanufacturing technologies using metal additive manufacturing pro-

- cesses and surface treatment. *International Journal of Precision Engineering and Manufacturing-Green Technology*, 11(2):625–658, 2024.
- [147] Wenjie Wang, Guangdong Tian, Honghao Zhang, Kangkang Xu, and Zheng Miao. Modeling and scheduling for remanufacturing systems with disassembly, reprocessing, and reassembly considering total energy consumption. *Environmental Science and Pollution Research*, pages 1–17, 2021.
- [148] Qinxin Xiao, Xiuping Guo, and Dong Li. Partial disassembly line balancing under uncertainty: robust optimisation models and an improved migrating birds optimisation algorithm. *International Journal of Production Research*, pages 1–19, 2020.
- [149] Xi Vincent Wang and Lihui Wang. Digital twin-based weee recycling, recovery and remanufacturing in the background of industry 4.0. *International Journal of Production Research*, 57(12):3892–3902, 2019.
- [150] J. P. Jensen, S. M. Prendeville, N. M. P. Bocken, and D. Peck. Creating sustainable value through remanufacturing: Three industry cases. *Journal of Cleaner Production*, 218:304–314, 2019.
- [151] C. H. Liu, Q. H. Zhu, F. F. Wei, W. Z. Rao, J. J. Liu, J. Hu, and W. Cai. A review on remanufacturing assembly management and technology. *International Journal of Advanced Manufacturing Technology*, 105(11):4797–4808, 2019.

- [152] Chao Liu and Xun Xu. Cyber-physical machine tool—the era of machine tool 4.0. *Procedia Cirp*, 63:70–75, 2017.
- [153] Philipp Middendorf, Richard Blümel, Lennart Hinz, Annika Raatz, Markus Kästner, and Eduard Reithmeier. Pose estimation and damage characterization of turbine blades during inspection cycles and component-protective disassembly processes. *Sensors*, 22(14):5191, 2022.
- [154] Süleyman Mete, Zeynel Abidin Cil, Eren Ozceylan, and Kürşad Ağpak. Resource constrained disassembly line balancing problem. *IFAC-PapersOnLine*, 49(12):921–925, 2016.
- [155] M. I. Rizova, T. C. Wong, and W. Ijomah. A systematic review of decision-making in remanufacturing. *Computers & Industrial Engineering*, 147, 2020.
- [156] Paul Vanegas Pena, Jef Peeters, Dirk Cattrysse, Joost Duflou, Paolo Tecchio, Fabrice Mathieux, and Fulvio Ardente. Study for a method to assess the ease of disassembly of electrical and electronic equipment. method development and application to a flat panel display case study. *Joint Research Centre (JRC) Technical Reports*, 2016.
- [157] Saralees Nadarajah and Samuel Kotz. The cycle time distribution. *International Journal of Production Research*, 2008.

- [158] Uğur Özcan. Balancing stochastic parallel assembly lines. *Computers & Operations Research*, 99:109–122, 2018.
- [159] Antonio Benitez-Hidalgo, Antonio J Nebro, Jose Garcia-Nieto, Izaskun Oregi, and Javier Del Ser. jmetalpy: A python framework for multi-objective optimization with metaheuristics. *Swarm and Evolutionary Computation*, 51:100598, 2019.
- [160] Hadi Gökçen, Kürşad Ağpak, and Recep Benzer. Balancing of parallel assembly lines. *International Journal of Production Economics*, 103(2):600–609, 2006.
- [161] Mohand Lounes Bentaha, Olga Battaïa, and Alexandre Dolgui. Disassembly line balancing problem with fixed number of workstations under uncertainty. *IFAC Proceedings Volumes*, 47(3):3522–3526, 2014.
- [162] Edmund K Burke, Michel Gendreau, Matthew Hyde, Graham Kendall, Gabriela Ochoa, Ender Özcan, and Rong Qu. Hyper-heuristics: A survey of the state of the art. *Journal of the Operational Research Society*, 64(12):1695–1724, 2013.
- [163] Edmund K Burke, Matthew R Hyde, Graham Kendall, Gabriela Ochoa, Ender Özcan, and John R Woodward. *A classification of hyper-heuristic approaches: Revisited*, pages 453–477. Springer, 2019.
- [164] Kalyanmoy Deb, Amrit Pratap, Sameer Agarwal, and TAMT Meyari-

- van. A fast and elitist multiobjective genetic algorithm: Nsga-ii. *IEEE transactions on evolutionary computation*, 6(2):182–197, 2002.
- [165] Eckart Zitzler, Marco Laumanns, and Lothar Thiele. Spea2: Improving the strength pareto evolutionary algorithm. *TIK-report*, 103, 2001.
- [166] Qingfu Zhang and Hui Li. Moea/d: A multiobjective evolutionary algorithm based on decomposition. *IEEE Transactions on evolutionary computation*, 11(6):712–731, 2007.
- [167] John H Drake, Ahmed Kheiri, Ender Ozcan, and Edmund K Burke. Recent advances in selection hyper-heuristics. *European Journal of Operational Research*, 285(2):405–428, 2020.
- [168] L. Wang, Y. Y. Guo, Z. L. Zhang, X. H. Xia, and J. H. Cao. Generalized growth decision based on cascaded failure information: Maximizing the value of retired mechanical products. *Journal of Cleaner Production*, 269, 2020.
- [169] Martina Marruganti and Leonardo Frizziero. Maintainability of a gear-box using design for disassembly and augmented reality. *Machines*, 8(4):87, 2020.
- [170] C. H. Feng and S. Huang. The analysis of key technologies for sustainable machine tools design. *Applied Sciences-Basel*, 10(3), 2020.
- [171] Eugenia Mincă, Adrian Filipescu, Daniela Cernega, Răzvan Şolea, Adriana Filipescu, Dan Ionescu, and Georgian Simion. Digital twin for

a multifunctional technology of flexible assembly on a mechatronics line with integrated robotic systems and mobile visual sensor—challenges towards industry 5.0. *Sensors*, 22(21):8153, 2022.

- [172] Marina Indri, Luca Lachello, Ivan Lazzero, Fiorella Sibona, and Stefano Trapani. Smart sensors applications for a new paradigm of a production line. *Sensors*, 19(3):650, 2019.
- [173] Soumaya El Kadiri and Dimitris Kiritsis. Ontologies in the context of product lifecycle management: state of the art literature review. *International Journal of Production Research*, 53(18):5657–5668, 2015.
- [174] Anil Kumar Inkulu, M. V. A. Raju Bahubalendruni, Dara Ashok, and K. SankaranarayanaSamy. Challenges and opportunities in human robot collaboration context of industry 4.0 - a state of the art review. *The Industrial Robot*, 49(2):226–239, 2022.
- [175] KL Keung, CKM Lee, XIA Liqiao, LIU Chao, LIU Bufan, and P Ji. A cyber-physical robotic mobile fulfillment system in smart manufacturing: The simulation aspect. *Robotics and Computer-Integrated Manufacturing*, 83:102578, 2023.
- [176] J. Huang, D. T. Pham, Y. J. Wang, C. Q. Ji, W. J. Xu, Q. Liu, and Z. D. Zhou. A strategy for human-robot collaboration in taking products apart for remanufacture. *Fme Transactions*, 47(4):731–738, 2019.

- [177] Hao Wang, Jiaqi Tao, Tao Peng, Alexandra Brintrup, Edward Elson Kosasih, Yuqian Lu, Renzhong Tang, and Luoke Hu. Dynamic inventory replenishment strategy for aerospace manufacturing supply chain: combining reinforcement learning and multi-agent simulation. *International Journal of Production Research*, 60(13):4117–4136, 2022.
- [178] Zhihao Liu, Quan Liu, Wenjun Xu, Lihui Wang, and Zude Zhou. Robot learning towards smart robotic manufacturing: A review. *Robotics and Computer-Integrated Manufacturing*, 77:102360, 2022.
- [179] Debasmita Mukherjee, Kashish Gupta, Li Hsin Chang, and Homaoun Najjaran. A survey of robot learning strategies for human-robot collaboration in industrial settings. *Robotics and Computer-Integrated Manufacturing*, 73:102231, 2022.
- [180] Raffaello Lepratti. Advanced human-machine system for intelligent manufacturing: Some issues in employing ontologies for natural language processing. *Journal of Intelligent Manufacturing*, 17(6):653–666, 2006.
- [181] Xingwang Shen, Xinyu Li, Bin Zhou, Yanan Jiang, and Jinsong Bao. Dynamic knowledge modeling and fusion method for custom apparel production process based on knowledge graph. *Advanced Engineering Informatics*, 55:101880, 2023.
- [182] Antonio Giovannini, Alexis Aubry, Hervé Panetto, Michele Dassisti,

- and Hind El Haouzi. Ontology-based system for supporting manufacturing sustainability. *Annual Reviews in Control*, 36(2):309–317, 2012.
- [183] Helena Sofia Pinto and João P Martins. Ontologies: How can they be built? *Knowledge and information systems*, 6:441–464, 2004.
- [184] Deborah L McGuinness and Frank Van Harmelen. Owl web ontology language overview. *W3C recommendation*, 10(10):2004, 2004.
- [185] Asunción Gómez-Pérez and Oscar Corcho. Ontology languages for the semantic web. *IEEE Intelligent systems*, 17(1):54–60, 2002.
- [186] Francesco De Fazio, Conny Bakker, Bas Flipsen, and Ruud Balkenende. The disassembly map: A new method to enhance design for product repairability. *Journal of Cleaner Production*, 320:128552, 2021.
- [187] Regina Kyung-Jin Lee, Hao Zheng, and Yuqian Lu. Human-robot shared assembly taxonomy: A step toward seamless human-robot knowledge transfer. *Robotics and Computer-Integrated Manufacturing*, 86:102686, 2024.
- [188] Atalay Atasu, Miklos Sarvary, and Luk N Van Wassenhove. Remanufacturing as a marketing strategy. *Management science*, 54(10):1731–1746, 2008.
- [189] SS Yang, N Nasr, SK Ong, and Andrew YC Nee. Designing automotive products for remanufacturing from material selection perspective. *Journal of Cleaner Production*, 153:570–579, 2017.

- [190] F Javier Ramírez, Juan A Aledo, Jose A Gamez, and Duc T Pham. Economic modelling of robotic disassembly in end-of-life product recovery for remanufacturing. *Computers & Industrial Engineering*, 142:106339, 2020.
- [191] Youxi Hu, Chao Liu, Ming Zhang, Yu Jia, and Yuchun Xu. A novel simulated annealing-based hyper-heuristic algorithm for stochastic parallel disassembly line balancing in smart remanufacturing. *Sensors*, 23(3):1652, 2023.
- [192] Xiwang Guo, Shixin Liu, MengChu Zhou, and Guangdong Tian. Disassembly sequence optimization for large-scale products with multiresource constraints using scatter search and petri nets. *IEEE transactions on cybernetics*, 46(11):2435–2446, 2015.
- [193] Kirsi Laitala, Ingun Grimstad Klepp, Vilde Haugrønning, Harald Throne-Holst, and Pål Strandbakken. Increasing repair of household appliances, mobile phones and clothing: Experiences from consumers and the repair industry. *Journal of Cleaner Production*, 282:125349, 2021.
- [194] Zude Zhou, Jiayi Liu, Duc Truong Pham, Wenjun Xu, F Javier Ramirez, Chunqian Ji, and Quan Liu. Disassembly sequence planning: Recent developments and future trends. *Proceedings of the Institution of Mechanical Engineers, Part B: Journal of Engineering Manufacture*, 233(5):1450–1471, 2019.

- [195] Shana Smith, Li-Yen Hsu, and Gregory C Smith. Partial disassembly sequence planning based on cost-benefit analysis. *Journal of cleaner production*, 139:729–739, 2016.
- [196] Yicong Gao, Shanhe Lou, Hao Zheng, and Jianrong Tan. A data-driven method of selective disassembly planning at end-of-life under uncertainty. *Journal of Intelligent Manufacturing*, pages 1–21, 2023.
- [197] Xiwang Guo, MengChu Zhou, Abdullah Abusorrah, Fahad Alsokhry, and Khaled Sedraoui. Disassembly sequence planning: a survey. *IEEE/CAA Journal of Automatica Sinica*, 8(7):1308–1324, 2020.
- [198] Enkelejda Kasneci, Kathrin Seßler, Stefan Küchemann, Maria Bannert, Daryna Dementieva, Frank Fischer, Urs Gasser, Georg Groh, Stephan Günnemann, and Eyke Hüllermeier. Chatgpt for good? on opportunities and challenges of large language models for education. *Learning and individual differences*, 103:102274, 2023.
- [199] Michihiro Yasunaga, Jure Leskovec, and Percy Liang. Lm-critic: Language models for unsupervised grammatical error correction. *arXiv preprint arXiv:2109.06822*, 2021.
- [200] Xikun Zhao, Congbo Li, Ying Tang, and Jiabin Cui. Reinforcement learning-based selective disassembly sequence planning for the end-of-life products with structure uncertainty. *IEEE Robotics and Automation Letters*, 6(4):7807–7814, 2021.

- [201] Deepak Ajwani, Adan Cosgaya-Lozano, and Norbert Zeh. A topological sorting algorithm for large graphs. *Journal of Experimental Algorithmics (JEA)*, 17:3–1, 2012.
- [202] Wouter Jan Klerk, Wim Kanning, Matthijs Kok, and Rogier Wolfert. Optimal planning of flood defence system reinforcements using a greedy search algorithm. *Reliability Engineering & System Safety*, 207:107344, 2021.
- [203] Jie Wang, Yongfang Xie, Shiwen Xie, and Xiaofang Chen. Cooperative particle swarm optimizer with depth first search strategy for global optimization of multimodal functions. *Applied Intelligence*, pages 1–20, 2022.
- [204] Lei Hao, Ying Wang, Yuanqi Bai, and Qiongyang Zhou. Energy management strategy on a parallel mild hybrid electric vehicle based on breadth first search algorithm. *Energy Conversion and Management*, 243:114408, 2021.
- [205] Hervé Abdi. The kendall rank correlation coefficient. *Encyclopedia of measurement and statistics*, 2:508–510, 2007.
- [206] Philip Sedgwick. Spearman’s rank correlation coefficient. *Bmj*, 349, 2014.
- [207] Pedro P Garcia, Telmo G Santos, Miguel A Machado, and Nuno

- Mendes. Deep learning framework for controlling work sequence in collaborative human–robot assembly processes. *Sensors*, 23(1):553, 2023.
- [208] Yang Liu, Fanyou Wu, Cheng Lyu, Shen Li, Jieping Ye, and Xiaobo Qu. Deep dispatching: A deep reinforcement learning approach for vehicle dispatching on online ride-hailing platform. *Transportation Research Part E: Logistics and Transportation Review*, 161:102694, 2022.
- [209] Youxi Hu, Chao Liu, Ming Zhang, Yu Jia, and Yuchun Xu. A conceptual framework of cyber-physical remanufacturing system. In *2022 8th International Conference on Nanomanufacturing & 4th AET Symposium on ACSM and Digital Manufacturing (Nanoman-AETS)*, pages 1–6. IEEE, 2022.